ADSORPTION AND QUANTUM CHEMICAL STUDIES ON SOME DYES AS CORROSION INHIBITORS ON MILD STEEL IN ACIDIC MEDIUM

Thabo Peme

ADSORPTION AND QUANTUM CHEMICAL STUDIES ON SOME DYES AS CORROSION INHIBITORS ON MILD STEEL IN ACIDIC MEDIUM

Thabo Peme

B.Sc (NWU), B.Sc (Hons) (NWU)

A thesis submitted in fulfilment of the requirements for the degree of

Master of Science (Physical Chemistry)

in the

Department of Chemistry

Faculty of Agriculture, Science and Technology,

North-West University (Mafikeng Campus)

Supervisor: Prof Eno. E. Ebenso

Co-Supervisor: Dr M.M Kabanda

May 2014

DECLARATION

I declare that this project which is submitted in fulfilment of the requirements for the degree of Master of Science in Chemistry (M.Sc) at North-West University, Mafikeng Campus has not been previously submitted for a degree at this university or any other university. The following research was compiled, collated and written by me. All the quotations are indicated by appropriate punctuation marks. Sources of my information are acknowledged in the reference pages.

T. Peme

.....

Thabo Peme

ACKNOWLEDGEMENTS

I would like to express my enormous gratitude to my Lord and saviour **Jesus Christ** for the divine strength and wisdom. I thank you Lord for giving me the gift of life, the feeling to breathe in oxygen then release carbon dioxide, respectively. I give all glory to you O' Lord for the divine ability you granted me through this entire work, without you I would have not completed this work, in Jesus Name, Amen.

If I was to search in deeper places to find words to precise my earnest appreciation to my supervisor and mentor, Prof Eno E. Ebenso; you have done a wonderful work, equipping and guiding me through the entire project. Thank you for making me fall in love with research world and the making me the scientist I am today. I'm forever thankful.

I'm gratefully taking this opportunity to acknowledge Dr Mwadham M. Kabanda, for all the encouragements and motivations he has given me throughout my work, the professional work he has done as far as the quantum chemical work is regarded. Your help not only with all quantum calculations but also in compiling and editing of this project is highly appreciated..

Without the assistance of Mr Chester Murulana and Dr Sudhish K. Shukla, this work would have taken a different path. I am so much thankful for both of you, the assistance you have given me with regard to the gravimetric/ experimental analysis.

I would have not known how to perform experiments in Auto lab- Potentiometric analysis if it wasn't for the help I got from Mr Obadele Tunde. Thank you Tunde for all the hard work and your patience in making me a guru in running the Autolab and thanks Dr Olubambo for allowing us to perform our electrochemical analysis at the Tshwane University of Technology(TUT).

I also want to take this opportunity to humbly acknowledge SASOL INZALO foundation for the support that they offered me to assist in completing this research work, without any financial burden. I'm grateful for the support you offered me through this entire project; I had no stress concerning any financial problems.

The life at graduate institute is sometimes never wonderful. For instance, coping with pressures that involves social or spiritual matters and other study related challenges. Nevertheless, I thank God for having blessed me with wonderful friends who inspirit and encourages me to stand strong and overcomes these difficulties. These friends are Pastor Labious Morobela, Masego Dibetsoe, Zweli Ndlovu and Owen Malete. Special thanks to Miss Ntombizanele Qompi for her enormous love, support and courage in my life and through this entire work, thank you Zanele.

I would like to express my endless thanks to my Mom and Dad; I would not be where I am today if it wasn't because of the love you have given me, the care, the support and the courage and also for believing in me. You brought me up as child through thin and thick, but you showed me tender care and support. Thank you Mommy and Papa for the financial support and encouragement throughout my life, without your support, it would have not been possible. My siblings, Dineo Peme, Kefilwe Peme, Phemelo Peme and the little sweet girl Tlamelo Peme, it is previllege and an honour to be your older brother. I love you all.

To the Chemistry department of North West University (Mafikeng campus), I salute you and thank you for the support.

ABSTRACT

The corrosion inhibition of some selected dyes namely Sunset yellow (SS), Amaranth (AM), Allura red (AR), Tartrazine(TZ) and Fast green (FG) on mild steel in 0.5M HCl was studied at 30-60°C using weight loss, electrochemical and quantum chemical methods. Quantum calculation based on the density functional theory (DFT) was used to investigate the reactivities and selectivities of four (4) of the studied dyes. The effects of inhibitor concentration on the inhibition efficiency have been studied. Inhibition efficiency increased with increase in concentration of the all the studied dyes within the concentration range 25–150 ppm. The results obtained showed that the experimental inhibition efficiency follows the order: Fast green (FG) > Allura red (AR) > Amaranth (AM) > Tartrazine (TZ). The potentiodynamic studies revealed that all the inhibitors are of mix-type. The adsorption of the studied dyes obeyed the Langmuir adsorption isotherm. Some thermodynamic parameters such as the heat of adsorption, entropy of adsorption and free energy of adsorption have been calculated. Apparent activation energy has been calculated and discussed. Synergism parameter evaluated was found to be greater than unity for all the concentration of the dyes used suggesting that the increase in the inhibition efficiency of the dyes by the addition of KI is only due to the synergism. Density Functional Theory method was used utilized on the quantum chemical calculation performed both in *vacuo* and in solution using both the protonated and non-protonated species. The quantum chemical descriptors e.g. E_{HOMO}, E_{LUMO} and Fukui indices have been discussed and compared with the trend in experimental inhibition efficiencies.

.

LIST OF ABBREVIATIONS

SSC	Stress Corrosion Cracking
HE	Hydrogen Embrittlement
PPM	Part Per Million
HCl	Hydrochloric acid
KI	Potassium iodide
IE	Inhibition Efficiency
AM	Amaranth
AR	Allura red
SS	Sunset yellow
TZ	Tartrazine
FG	Fast green
GNP	Gross National product
ICCP	Impressed Current Cathodic Protection
SACP	Sacrificial Anode and Cathodic Protection
DFT	Density functional theory
MD	Methyl-Blue
EFM	Electrochemical Frequency modulation
HOMO	Highest Occupied Molecular Orbital
LUMO	Lowest Unoccupied Molecular Orbital
EA	Electron Affinity
IP	Ionization Potential
PDP	Potentiodynamic Polarization
CE	Counter Electrode
OCP	Open Circuit Electrode
RE	Reference Electrode
WE	Working Electrode
SSE	Silver/Silver Electrode
HSAB	Hard and Soft Acids and Bases

LIST OF FIGURES

LIST OF TABLES

TABLE OF CONTENTS

Chapter 1

INTRODUCTION

1.1 Definition of corrosion

Corrosion is the breaking down of the material due to the reaction with its environment, where the material (metal) reacts in the presence of water and oxygen [1]. Corrosion can either be chemical or electrochemical in nature. The distinction between chemical and electrochemical depends upon the corrosion causing mechanism. Chemical corrosion is the direct result of exposure of material (e.g. with dry air or oxygen) and is controlled by the kinetics of chemical, whereas the electrochemical corrosion occurs in the presence of an electrolyte and it is said to be the dissolution of a metal through the oxidation process [2, 3]. Therefore with metallic materials and aqueous solution, the reactions are normally electrochemical in nature. Corrosion is said to be a thermodynamically feasible process because it involves negative change of Gibbs free energy [4]. Therefore corrosion is a reaction that involves the transfer of metal ions into the solution at active area (anode), passage of electron from the metal to an acceptor at less active area (cathode), an ionic current in the solution and an electronic current in the metal [5, 6].

Corrosion does not only occur in metals and their alloys, but it can also occur in all types of natural and man-made materials including biomaterials and nanomaterials. However, amongst many metals, corrosion is mostly experienced in iron and steel [7, 8]. The terms corrosion and rusting are often utilized interchangeably; the word "rusting" normally applies to ferrous material, iron and steel and the word "corrosion is commonly used because it is inclusive of non-ferrous metal as well [8]. Corrosion can be classified as either dry or wet corrosion. In most practical occasions the liquid can also contain aggressive ions such as Cl^-, SO_4^{2-}, I^- etc, which are responsible for accelerating the rate of corrosion. In the case of dry corrosion, the environment is normally gaseous and high temperatures and reactive gases are often evolved [4]. In wet corrosion (also known as "electro-chemical corrosion") the electrochemical reaction which causes corrosion is: e.g. Iron;

$$Fe_{lattice} \longrightarrow Fe_{aq}^{++} + 2e^- \qquad (1)$$

Atmospheric corrosion can be regarded as special type of wet corrosion due to the fact that the corrosion processes evolve in a wet film on the metal surface formed by condensation from the atmosphere. In the case of dry corrosion (also known as "chemical corrosion "or high temperature oxidation) the corrosion reaction is e.g. Iron [9, 10].

$$Fe_{lattice} \longrightarrow Fe_{oxyde}^{++} + 2e^- \qquad (2)$$

The corrosion process normally involves two simultaneous changes, namely, the anodic change where oxidation takes place, and four various factors influence the electrochemical reaction namely;

i. Cathode
ii. Electrolyte
iii. Anode
iv. Electronic circuit

In the presence of moisture, iron reacts with oxygen to form Iron oxide (rust) with the formula $Fe_2O_{3x}H_2O$, where x represent the amount of water that is present in rust which also determines the color of that rust.

In this reaction iron undergoes oxidation, and it loses electrons according to the following reaction;

$$Fe \longrightarrow Fe^{2+} + 2e^{-} \quad (3)$$

Iron then reacts with oxygen to form iron hydroxide according to the reaction below;

$$Fe^{2+}(aq) + 2OH^{-}(aq) \longrightarrow Fe(OH)_2(s) \quad (4)$$

Iron (+2) hydroxide is further oxidized by oxygen to iron (+3), according to reaction3;

$$Fe(OH)_2 + \text{dissolved oxygen} \longrightarrow \text{rust } (Fe_2O_3) \quad (5)$$

Reduction reaction occurs when the electrons that are released from the process are taken up by hydrogen atoms into water where a gas is produced as in reaction 4;

$$2H^{+}(aq) + 2e^{-} \longrightarrow H_2(aq) \quad (6)$$

Rusting will then occur due to the water drop on iron surface and this is possible because of more oxygen being dissolved from the air near the edges of the drop [4, 10]. Figure 1.1 shows example of rusting of an iron ore.

Figure 1.1: Iron oxide (rust)

1.2 Types of corrosion

Corrosion occurs in various widely differing forms. The classification is normally based upon one of the three factors;

- *Mechanism of corrosion*: It involves either electrochemical or direct chemical reactions.
- *Appearance of the corroded metal*: Corrosion can either be uniform and the metal can corrode at the same rate over the entire surface.
- *Nature of corrodent*: Corrosion can either be classified as wet or dry. Dry corrosion normally involves reaction with high temperature gases. And wet corrosion normally takes place in environment where the relative humidity exceeds 60% [8, 11, 12].

However, there are various forms of corrosion categorized according to different criteria, such as type of attack, mechanical stress, its shape and size, its specific functions, atmospheric conditions and the corrosion producing agent present [8, 11].

1. Group 1: Can be identified by visual perception (i.e. by naked eye) namely:

i. **Crevice corrosion**: It takes place at localized areas of contact with the metal with the other or metal with a non-metal. It is typically encountered with metals and alloys which are depended on the surface oxide film for corrosion protection. For crevice corrosion to take place, a certain induction period is needed to create local corrosion cell between the inside and the outside crevice [1, 4, 12].

ii. **Uniform corrosion**: This is characterized by direct attack on the surface of the material, and it often occurs on the environment where there is essentially low corrosion rate or correctly maintained. It is the most common form of corrosion experienced with majority of metal, and the common one being the rusting of common [1, 9, 12].

iii. **Petting corrosion:** This is a form of localized attack that causes small holes to form in the metal. It is known as a white or grey powdery similar to dust, which blemishes at the surface. Petting corrosion is said to be stimulated by low-velocity, stagnant-type conditions where concentrated "bubbles "of corrosives could form. It cake up to months or years before its effects can be seen [1, 9].

iv. **Filiform corrosion**: This type of corrosion normally occurs in painted surfaces. It is often seen by a thin threadlike attack continuing along the surface beneath a surface layer. Filiform corrosion is a special form of crevice corrosion where the chemistry build up takes place under a protection film that has been breached [1, 4, 8].

v. **Galvanic corrosion**: Also known as bimetallic corrosion, it occurs when two or more dissimilar conducting materials are connected electrically and are exposed to an electrolyte. The forming of galvanic corrosion results in one of the metal in the couple being the anode and corrodes faster than it would all by itself, while the one being the cathode and corrodes slower than it would [1, 4, 8–9].

vi. **Lamellar corrosion**: It is a form of corrosion that normally start from sites of initiation along parallel planes to the surface, generally at grain boundaries, forming corrosion product that force metal way from the body of the material , thus giving it a layer appearance. [1, 4, 9].

1. **Group 2:** Can be identified by means of examination (velocity related intergranular, dealloying corrosion) namely;
   i. **Erosion corrosion**: Is an increase rate of corrosion attack on the metal as result of a relative movement of corrosive fluid and the metal surface. It can be incited by faulty workmanship. Erosion corrosion is often the result of the wearing away of a protection scale or coating on the metal surface [1, 9, 12].
   ii. **Cavitation corrosion**: A special form of corrosion that is enhanced through the formation and collapse of a gas or vapor at or near the metal surface. In this form of corrosion, pits are normally localized close to each other or grown together along smaller or large areas, making a rough, spongy surface. It is said to take place at high flow velocities and fluid dynamic conditions which results in large pressure variations, mostly in the case water turbines, propellers and pump rooters [1, 8].
   iii. **Dealloying corrosion**: Also known as selective leaching, occurs when the alloy losses its element and retains its resistance component. It can also take place by redeposition of the noble component of the alloy on the metal surface [8, 9, 12].
   iv. **Intergranular corrosion:** Also referred to as "intercrystalline corrosion "or interdendritic corrosion, it is a localized attack in on or adjacent to the grain boundaries of the metal or alloy. The attack is normally associated with the segregation of a specific element or the formation of a compound in the compound [4, 8, 12].
   v. **Fretting corrosion**: This refers to corrosion resulting from the damage of two metal surfaces rubbing together at a point. This damage is induced under load and in the presence of repeated relative surface motion, as induced for example by vibration. The damage can also take place at the interface of two highly loaded surfaces which are not designed to move against each other [8, 9].
2. **Group 3:** Can only be identified with the aid of a microscope namely;
   i. **Environmental cracking** : It is caused by many conditions that usually result in the following form of corrosion damage;

- **Stress Corrosion Cracking (SCC)**: This type of corrosion forms a crack under mechanical stress in the presence of corrosion media. The stress is caused by applied load, residual stress from the manufacturing process. It may also occur in combination with hydrogen embrittlement [1, 4, 8, 9].
- **Corrosion fatigue**: This special type of corrosion occurs as result of the combined action of an alternating or cycling stress and a corrosive environment [1, 7].

- **Hydrogen embrittlement (HE)**: This is a process that results from in a decrease of the toughness or ductility of metal due to the presence of atomic hydrogen [1, 4, 9].

1.3 Rate of corrosion

Corrosion process involves the degradation of materials due to environmental factors such as water, air and temperature; thus a material loses its original value and weight loss is encountered during that process. It is very essential to know the corrosion rate of a certain material in order to affectively use metals in outdoors structures. The rate of corrosion of metals can be expressed as mpy or mmpy and is usually measured either by gravimetric methods or by electrochemical methods. In this current study the rate of corrosion is measured by gravimetric method, normally expressed as the loss per unit time [13, 3], and it is given by the equation;

$$C_{(R)} = \frac{W_b - W_a}{At} \tag{7}$$

Where W_b and W_a are specimen weight losses before and after immersion in the tested solution in grams (g), A is the area of mild steel (cm^2) and t is the exposure time in (hrs) [14]. Corrosion rate is strongly dependent upon the material being corroded. The known electrochemical technique that has qualitative ability concerning corrosion rate is called the polarization resistance, this is a laboratory based technique which relies on the application of a small electrical perturbation to the metal. The way in which corrosion rate is predicted is based upon the given sufficient qualitative information about the electrochemical reaction taking place [13, 15].

Like most chemical reactions to take place, there must be change caused by the surrounding conditions or reaction within the substance itself. There are several factors that stimulate the rate of corrosion namely;

I. **Material**: This depends on the chemical composition of an alloy (i.e. the chemical elements within a particular metal). As in the case of a metal, the metal with lower electrode potential is more reactive susceptible for corrosion and the metal that has high electrode potential are less reactive and less susceptible for corrosion. It also depends on the crystal structure and grain boundary composition. One of the most elements for this factor is the surface conditions, because corrosion rate is strongly depended upon the surface [10, 11, 12].

II. **Temperature**: At high temperatures most chemical reactions speed up, and therefore the rate of corrosion increases. This is due to the fact that the temperature and pressure of corrosive material regulate the solubilities of certain species in the fluid such as oxygen (O), and carbon dioxide (CO_2) [4, 8, 12].

III. **Water velocity**: This is also one of the factors that affect the rate of corrosion. Water (H_2O) is a molecule which contains particles which are in motion, and so at extremely high velocities those particles tend to remove the protective oxide layer and thus expose the metal to corrosion [1, 8, 9].

IV. **Environmental**: This is dependent upon the chemistry type like; the hydrogen-ion concentration, the influence of oxygen in solution adjacent to the metal [1, 4, 12].

V. **Anodic or Cathodic area:** The relative sizes of cathode and anode mostly affect the rate of corrosion. Metals having smaller anodic area and the larger cathodic area exposed to corrosive atmosphere are said to have more intense and faster corrosion occurring at the anodic area due to the oxidation taking place at the anode causing electron liberation [4, 8, 12].

VI. **Hydrogen ion concentration of the solution:** As the concentration of the hydrogen ions is increased in a given environment (when the pH of the medium is decreased), the rate of corrosion increases [16]. The corrosion rates are normally slow in alkaline environment. Acidic environment are often aggressive than the environments which have low concentrations of hydrogen and high pH values [16, 17].

VII. **Galvanic thickness/thinness:** Different metals which are joined together in the construction of the cooling system and also exposed to water, forms galvanic corrosion. This normally results in one of the metal in the couple being the anode and corrodes faster than it would by itself, while on the hand; the other is cathode and corrodes slower than it would. Galvanic series is based on measuring the potentials of metals as compared to a reference electrode [4, 8].

1.4 Effects of corrosion

Corrosion is considered to be a major problem experienced in industries and in our everyday life, and. Corrosion is therefore a potent force, affecting lives, jobs and the economy in our everyday life. Below are some effects of corrosion; [1, 12, 18].

i. **Economic effects**: Useful manufacturing equipment most of which are made from metals are degraded by corrosion, for an example in petroleum industries where they use metals for their fluid carrying pipes and tanks. Now these industries usually find themselves losing great amount of money in trying to reduce this corrosion process. Because of corrosion, industries do lose huge amounts of money in maintaining and repairing of equipments, replacing corroded equipments, and overdesigning of material [1, 4, 9, 12].

ii. **Safety effects**: There are various uses of metals in construction industries like in the construction of bridges and huge buildings, that when corroded can result in failure or breakdown and thus causing harm or injuries to human beings. Corrosion also affects our traveling from home to work or anywhere, this is due to the fact that we use vehicle (including cars, planes, train and ships) which are made from metal and, so any damage

due corrosion of this metals can cause accidents leading to injuries and deaths. Some failures in corrosion can result in explosions, fire, collapsing of structures [1, 4, 9].

iii. **Health effects**: The water we use may be contaminated as a result of escaping contents from the corroded structures such as plumbing system, and thus resulting in the malfunctioning of our body system i.e. causing the diseases. Other effects arise from continuous use of metallic plates and cups, and when these are affected by corrosion they can put human health at risk causing diseases [4, 8, 12].

iv. **Cultural effects**: The statues of our heroes (e.g. political or social heroes, musical legends and many more) are made from metallic products. And these statues are considered to be very important by many nations since they pride themselves about those heroes. Since those statues are made from metal, they can be attacked by corrosion and therefore impacting the cultural beliefs of that nation [12].

v. **Technological effects**: Most of the economic effects also affect technology, this is because most of the technological gadgets are made from metallic products (these include mechanical or electronic device). When these materials are exposed to corrosive environment such high temperatures or high pressure, technological problems are experienced [8].

1.5 Kinetics and thermodynamics of corrosion

1.5.1 Kinetics of corrosion

The kinetics of corrosion gives information on how fast or slow corrosion can occur at a given time and environment. The reactions involved during corrosion process normally produce and consume electrons. Enough information on the electrochemical behavior of metallic material in aggressive media can be obtained through the influence of temperature on process of corrosion. The Arrhenius law provides the relationship between the dependence of the rate constant of chemical reaction on the temperature [19].

$$k = Ae^{-E_a / RT} \tag{8}$$

where: k= the Arrhenius pre-exponential rate constant

A= the pre-exponential factor or the pre-factor

R= Molar gas constant

E_a= the apparent activation corrosion energy

T= the absolute temperature.

From equation 8, corrosion rate increases when the temperature increases and E_a and A may vary with temperature.

The rate of corrosion can be measured differently depending on the method of analysis used. Corrosion rate can be expressed as follows using the gravimetric method;

$$\rho = \left(\frac{\Delta w}{St} \right) \tag{9}$$

ρ = the corrosion rate

W = the average weight loss of the material

S = the total area of the of the material

t = the immersion time

1.5.2 Thermodynamic of Corrosion

The term corrosion can be best explained in terms of the stability of chemical species and reactions associated therein. The thermodynamics control concept plays a vital role in understanding the corrosion process of a system. Nonetheless, corrosion rates are not predicted through the thermodynamics calculations. Corrosion processes are normally spontaneous processes nature. The theory of spontaneous and non-spontaneous reaction is very vital in understanding the study of corrosion processes. In spontaneous reaction, the free energy of a certain reaction must have a negative value [19]. As already mentioned above that the process of corrosion involves the oxidation and reduction half reaction, the overall free energy for the redox is negative. Under standard conditions, the standard free energy of the cell reaction ΔG^0 can be calculated using the following equation:

$$\Delta G^\circ = -nF\Delta E^\circ \tag{10}$$

where ΔG° is the standard free energy change, n is the number of electrons exchanged, F is the Faraday constant and ΔE° is the standard energy change in the reaction. Literature has shown that values for the free energy, ΔG° around -20 kJmol^{-1} or lower suggest the electrostatic interaction between the charged molecules and the charged metal (physisorption) and those around -40 kJmol^{-1} or higher involve charge sharing or transfer from organic molecules to the metal surface to form a coordinate type of bond (chemisorption) [19–20]. Physisorption is a process that involves the electrostatic forces between ionic charges or dipole on the adsorbed species and the electric charge at metal/solution interface. Normally the heat of adsorption is low and therefore is stable only at relatively low temperatures. In chemisorption the electron transfer is typical for transition metals having vacant low-energy electron orbital. It is also characterized by a much stronger adsorption energy than physical adsorption [20–22].

Other thermodynamic quantities such as the adsorptive enthalpy, ΔH^0_{ads} can also be determined. The Van't Hoff equation is used to find such parameters;

$$\ln K = -\frac{\Delta H^\circ_{ads}}{RT} + \text{Constant} \tag{11}$$

where K is the adsorption equilibrium constant, R is the molar gas constant, T is the temperature. Gibbs-Helmholtz can also be used to estimate ΔH^{0}_{ads} obtained from equation (12) and expressed as follows,

$$\left[\frac{\partial\left(\Delta G^{0}_{ads}/T\right)}{\partial T}\right]_{P} = -\frac{\Delta H^{0}_{ads}}{T^{2}} \qquad (12)$$

The equation 13 can be arranged in the following equation:

$$\frac{\Delta G^{\circ}}{T} = \frac{\Delta H^{\circ}ads}{T} + \mathrm{k} \qquad (13)$$

The standard enthalpy of adsorption (ΔS°) can also be obtained using the thermodynamic basic equation:

$$\Delta G^{\circ}_{ads} = \Delta H^{\circ}_{ads} + T\Delta S^{\circ} \qquad (14)$$

1.6. Mechanism of metal corrosion

Most structural metals are obtained from their ore or naturally-occurring compounds by the consumption of large amount of energy. These metals are taken to be in metastable state and will tend to lose their energy by reverting to compounds more or less similar to the original states. The environmental factors such as soil, water, air plays an important role in corrosion mechanism. Corrosion reactions are normally electrochemical in nature, at anodic sites on the surface the iron goes into solution as ferrous ions, this constituting the anodic reaction [23, 24.] Normally for a corrosion process to take place, there are some conditions that must exist such as; a chemical potential difference between adjacent sites on a metal surface (or between alloy) of different composition, an electrolyte ought to be available in order to allow solution conductivity and as a source of material to be reduced at the cathode and lastly an electrical path through the metal or between metal must be present so as to permit electron flows [23, 24]. The electrolytic corrosion (an electrochemical reaction made of both anodic and cathodic reaction) is composed of two half–cell processes occurring at the anode (anodic half–cell reaction) and the cathode (cathodic half–cell reaction). The combined two half–reactions are known as redox reaction [23]. The cathodic half reaction involves the reduction reaction where the ions at the interface between the metal and the solution accepting the electrons from the metal, whereas the anodic half reaction cell is the oxidation reaction involving the metal releasing electron. A typical example of electrochemical corrosion of metal in contact with water is illustrated below. In this process, a metal goes under oxidation process and losses the electron in the equation below.

$$M \rightarrow M^{++} + 2e- \qquad (15)$$

A metal ion in contact with water or solution forms positively charged ions. Ions moves away from the metal and further oxidation takes place. The reduction reaction which occurs at the cathode, involving the acceptance of electron from the metal by species is solution, can be in the form of hydrogen-evolution or oxygen reduction. Hydrogen ion gas under reduction process by the excess of electron at the cathode surface and there is the evolution of hydrogen gas.

$$2H^{+} + 2e^{-} \rightarrow H_{2\uparrow} \quad (16)$$

Cathodic reaction decreases when hydrogen is not removed from the surface, and this reduces the corrosion rate. This reaction in equation (2) is associated with the environment of low pH values (acidic conditions). When air is present, the reduction of oxygen it is most likely to occur, and therefore forming the following these two possible reactions;

$$O_2 + 4H^{+} + 4e^{-} \rightarrow 2H_2O \quad (17)$$

$$O_2 + 2H_2O + 4e^{-} \rightarrow 4\,(OH)^{-} \quad (18)$$

The reaction in equation (17), the hydrogen evolution, or the oxygen reduction with the formation of water in equation (18), most takes place in acidic media. In some instances, oxygen reduction with formation of hydroxyl is likely to occur in neutral or alkaline environment.

1.6.1 Mild steel

Mild steel is a type of alloy having the chemical composition of C (0,120%), Mn (0.85%), S (0.055%), P (0.05%), Si (0.09%) and the remaining 98.84% is iron (Fe) [25], consisting mainly of iron. Steels are said to be mild, medium- or high-carbon steel, according to the percentage of carbon they contain .The surface of the metal in air (except for gold) is covered with film oxide, which prevents the anodic dissolution. Mild steel has been widely employed under different conditions in chemical and allied industries in the treatment of alkaline, acid and salt solution, and therefore gets corroded when exposed to different environmental factors such as temperatures, water and air [27–29].

Iron in steel is said to be unstable under atmospheric conditions, and because of this behavior will deteriorate to a more stable state called iron oxide (Fe_2O_3). At ordinary atmospheric conditions, iron is at the lowest energy state known as an oxide, which is the type of rust. In the process, oxygen acts as catalyst facilitating the formation of iron oxide. This reaction is said to be very slow at ordinary temperatures, but tend to proceed faster when water is present. This simple process is shown in figure 1.1 below [3].

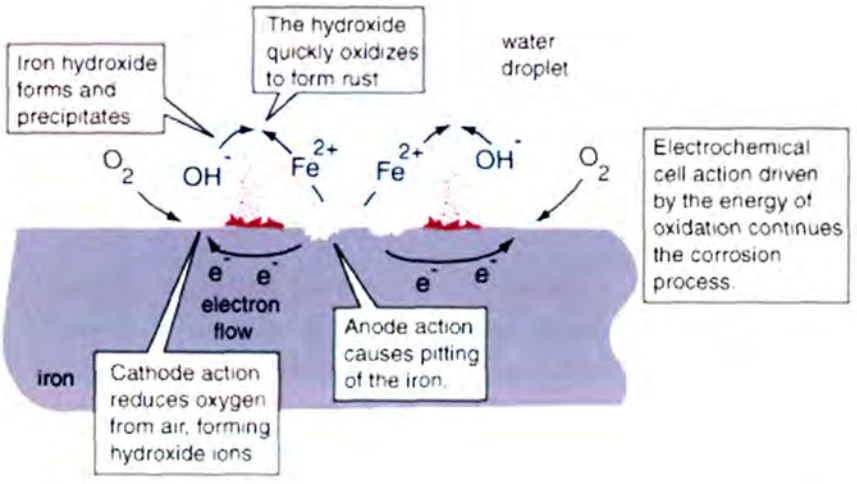

Figure 1.2 Process involved in the formation of iron oxide (rust) in the electrochemical cell.

1.7 Corrosion cost and control

The economic factor is taken to be a very important incentive for much of the current research in corrosion. The cost of corrosion is said to be partly connected with the efforts to give structures an attractive appearance, it is also partly the direct cost of replacement and maintenance and simultaneous economic loss due to production interruption, and it involves extra cost of using expensive materials [15]. The larger number of corrosion cost offers numerous opportunities to users, manufactures and suppliers. Nonetheless several opportunities exist to reduce the cost of corrosion and risk of failure, and to develop new expanded markets. The cost of corrosion differs considerably from industry to industry; however substantial savings are achievable in most industries [7, 8, 15].

The corrosion cost can either be direct or indirect. Previous studies by Battle-NBS pointed out the severe impact of the United States caused by corrosion; it estimated that in 1995 the cost of cost corrosion in the U.S alone was approximately $ 276 billion, which is 3.1 % of the Gross national product (GNP) [29–31]. Another estimation also pointed out that about 25–30 % of this total could be avoided if the currently available corrosion technology were effective [32]. In other countries including Australia, Great Britain, Japan, and many others, studies on cost of corrosion were also done. In each of the country studied, the cost of corrosion was found to be approximately 3-4% of the Gross National Product (GNP) [31, 33]. Corrosion has a very great impact on the environment and economy on virtually all facets of the world's infrastructure, from highways, bridges and buildings to oil and gas, chemical, and water and wastewater system [24].

It has been further estimated that about 20 % of this loss could have been saved through better use of existing knowledge in corrosion protection and design. This therefore, gives rise to higher

demand for applied research, education, information, transfer of knowledge and technology, and technical development. It is also necessary to have teaching, where considerable emphasis could be placed on the connection between practical problem and basic scientific principles. The damage caused by corrosion does not only generate high cost of inspection, repair and replacement, but furthermore these constitute a public risk, therefore there is a need for developing methods for corrosion control [31, 34, 35].

Corrosion is a naturally occurring process which cannot, if strict definitions are used, be eliminated. Nonetheless, if the rate of corrosion was to be decreased so that the amount of corrosion which occurs over the lifetime of a structure is negligible, then corrosion has been in practical terms, eliminated. The methods for controlling and preventing corrosion are depended upon the specific material to be protected; environmental concerns such as soil resistivity, humidity, and exposure to saltwater or industrial environment, the type of product to be processed or transported and other factors. There are different corrosion prevention techniques that are known and are discussed as follows [1, 15, 23].

- **Material selection:** It is of vital importance to understand the corrosive attack that occurs on the metal. There are no materials that are resistant to corrosion in all environments. Therefore there is a need for materials to be frequently matched to the environment that we encounter in service. The corrosion and other functional properties of the materials are depended upon the various external factors including geometry, surface conditions, environmental factors and mechanical load conditions [2, 4, 10]. These factors are to be evaluated for each of these functional factors. When materials are selected, each component has to be taken consideration with respect to the design, manufacture and its effect on the total geometry. It is also necessary that the materials are compatible. Compatibility simply means that detrimental galvanic elements are not taken into consideration. A suitable selection of material is depended upon adequate knowledge of how the actual practical conditions affect the material [5, 9–11].

- **Protective Coatings**

Protective coatings are the most commonly applied corrosion control technique. They act as sacrificial anode or release substance that inhibits corrosive attack on substrate. There are two broad groups of coatings for corrosion protection namely;

1. *Metallic coatings*: They provide a layer that alters the surface properties of the workpiece to those of the metal being applied. Corrosion protection by metallic coating is to protect unalloyed or low-alloy steel, but there are also many cases of other metals to be protected. Metallic coating can be divided into two groups, namely; Cathodic coating, which are said to be more noble than the substrate, and anodic ones, which are less noble that the substrate.

Cathodic coatings often act by barrier effect only, but in case of combinations of substrate and environment the substrate can also be anodically protected.

II. *Inorganic coatings*: This type of coating can be produced by chemical action, with or without electrical resistance. It includes porcelain, enamels, chemical-setting silicate cement lining and glass coatings [3, 12, 18, 26].

- **Cathodic Protection:** It uses electrochemical properties of metal in ensuring that the metal of interest is of the cathode of an electrolyte cell. Cathodic protection also reduces the rate of corrosion of a metallic structure by simply decreasing its corrosion potential, causing the metal to be closer to an immune state. This is an electrical means of corrosion control. Primarily it has been applied for protection of ordinary structural steel in soil and seawater, more seldom for steel exposed to fresh water. Cathodic protection consists of two types, namely; impressed current cathodic protection (ICCP) and sacrificial anode cathodic protection (SACP). Metal surface which is cathodically protected can be maintained in a corrosive environment without deterioration for an indefinite time. It can be used in practice to protect metals steel, copper, lead and brass [4, 9–11].
- **Corrosion inhibitors**: A corrosion inhibitor is a substance that when added to the environment in minute concentrations decreases the rate of corrosion on the metal [2, 8, 36]. They reduce the rate of corrosion by
  I. Adsorption of ions or molecules onto the metal surface,
  II. Increase or decrease the anodic or cathodic reaction,
  III. Decreasing the diffusion rate for reactants to the surface of the metal,
  IV. And also by decreasing the electrical resistance of the metal surface [6, 37].

  Inhibitors often work by adsorbing themselves on the metallic surface, protecting the metallic surface by forming a film. Inhibitors are also sometimes used as additives to prevent steel from flash rusting during wet abrasive blasting. Inhibitors can be classified as (1) passivators, (2) organic inhibitors which include slushing compounds and pickling compounds and (3) Vapour-phase inhibitors [11, 36–38]. Factors that contribute to the action of an inhibitor are; chain length, size of a molecule, bonding, aromatic/conjugate, strength of bonding to the substrate, cross-linking ability, solubility in the environment [6, 37]. Corrosion inhibitors are said to form barrier of one or several molecular layers against acid attack. That protective attack is normally associated with chemical and/ or physical adsorption involving a variation in the charge of the adsorbed substance and transfer of charge from one phase to the other [37].
- **Over-design**: Over-design of structures simply refers to the common use of heavier structural member of thicker plates than actually required in anticipation of corrosion losses. The design and material selection are done in connection with each other. In this process, both the individual components, interactions between them and the relation to other structures and the surroundings are taken into consideration [4, 29].

There are other corrosion protection methods which are not stated above. Therefore for this research purpose food dyes are used as corrosion inhibitors for corrosion of mild steel in acidic and basic medium. There are various types of corrosion inhibitors that are commonly used today namely, dyes and ionic liquids to name just a few [39]. A lot of the effective organic inhibitors that are applied contains atoms such N (nitrogen), O (oxygen), P (phosphorus) and multiple bond between their molecules through which adsorption takes place in their metal surface. The corrosion-resistance property of the metal can vary perceptibly due to the adsorption of the surfactant on the metallic surface [40, 41]. The purpose of addition of inhibitors is that they protect the iron and its alloys against acid attack effectively. Adsorption behaviour of organic molecules on the surface of the metal does not only depend on the characteristics of the environment in which it acts, the nature of the metal surface and electrochemical potential at the interface, but is also dependent upon the structure of the inhibitor itself, including the number of adsorption active centres in the molecule, their charge density, the molecule size, the mode of adsorption, the formation of metallic complexes and the projected area of the inhibitors on the metal surface [42, 43].

1.8 Research aim

Organic inhibitors normally possessing the heteroatoms such as N (nitrogen), O (Oxygen), S (sulphur) and P (phosphorus), are found to have basicity and electron density and thus act as corrosion inhibitor. These heteroatoms are said to be the active centres during the process of adsorption on the metal surface. Organic compounds also contain electronegative functional groups and π-electrons in triple or conjugated double bond. The molecular structures of dyes highly recommend them for investigation as possible corrosion inhibitors when compared with other reports on the organic inhibitors [37–39]. There is no adequate amount of information available on food dyes as corrosion inhibitors, therefore this research was proposed with the aim to investigate more information concerning this. The main aim of this research is to investigate the adsorption and quantum chemical studies of some food dyes (Fast green, Amaranth, Allura Red AC, Sunset Yellow FCF and Tartrazine) as corrosion inhibitors for mild steel in acidic media.

1.9 Research objectives

a) To propose the possible mechanism, type of adsorption and adsorption isotherm for the corrosion inhibition.
b) Compare the effect of various food dyes on the mild steel corrosion.
c) Apply thermodynamics, kinetics and adsorption principles in studying the inhibition potentials of some selected food dyes, their effect concentration and temperature on the corrosion rate.
d) Synergistic and /or antagonistic effect of the addition of KI to the inhibitors.

e) Use of quantum chemical/theoretical techniques e.g. density functional theory (DFT), to calculate quantum chemical parameters of the selected inhibitors and correlate them with the experimentally obtained inhibition efficiency and to determine nucleophilicity, electrophilicity, Fukui and global softness indices.

Chapter 2

LITERATURE SURVEY

2.1 Dyes

2.1.1 Description and background

Dye is any substance which when added or applied to food, drug or cosmetic or the human body, has the capability of impacting colour. Dyes are said to be coloured, ionising and aromatic organic compound which show affinity towards the substrate to which it being applied. The affinity of a dye for a fabric is depended upon the chemical structure of the dye and fabric molecules and on the interactions between them. Chemical bonding therefore plays an important role in determining the functioning of dyes [44, 45]. They are mostly applied for quite a few reasons such as; to offset color loss due to exposure to light, air, temperature extremes, to correct natural variations in colour and to enhance colours occurring naturally. Dyes are not only used on traditional product such as fibers and leather goods, but they are currently essential for the production of newspapers and magazines, books, plastics product, decorative materials, films and food [46, 47].

Dyes are originally synthesised from tar and coal and now petroleum. It is very significant to bear in mind that dyes may not necessarily be coloured substances. Hence optical brightness or whiteness which may be called white dyes may also be included in the term dye [46, 47]. Recently dyes are available in different forms such as dry powders, granules, pastes, liquids, pellet, chips concentration; the concentration form and purity of a dye is determined largely by the use for which it is intended [45-47].The first dyes used were *Turkey red* which was produced from common madder and *Indigo blue* obtained from plant belonging to the family *Indigofera* [45] .However, during the event of synthesis of dyes, synthetic (organic) dyes, mauveine, were the first dyes to be discovered by an 18 year old English chemist William Henry Perkin in 1856, when he was trying to synthesize quinine in aniline. Perkin named his colour mauveine, after the French name of non-fast colour which was obtained from natural dyes [46, 48].

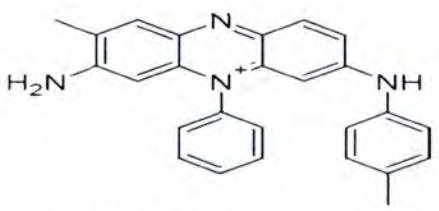

Figure 2.1 Structure of Mauveine

For synthesis purposes, benzene was nitrated to nitro-benzene and then reduced to aniline, which was further oxidized since from then, this process became the basis for the first industrial process for the production of synthetic dye. Prior to that time, all coloring materials were extracted from barks, roots, seeds, leaves and shellfish. Most of these synthetic dyes are prepared from aromatic compounds which are mostly obtained from coal tar or petroleum [46, 48, 49].

2.1.2 Classification of dyes

There are various ways of classifying dyes based on the unique chemistry, structure and particular way of bonding. Dyes can be classified as organic/inorganic, natural or synthetic. The classification of dyes is also primarily based on the presence of chromophores, i.e. chemical group which determines the dyeing power. Most food dyes that are used today are synthetic. It is reported that almost all colours that we see are synthetic, and colours are the most popular varieties of synthetic dyes [47]. There are other types of dyes that are obtained from either synthetic or natural that are commonly used, namely; direct acid or base, sulphur, azoic, the vat dyes, azo-dyes, mordant, sublimation, reactive dyes etc. However the present study focuses more on food dyes, which are mainly obtained from synthetic dyes. Synthetic dyes can be classified according to their characteristics or their applications [45, 49].

They are also named according to the chemical structure of their particular chromophoric group. For example, diphenylmethane derivatives, xanthene compounds, Azo dyes to name just a few. Out of these dyes, Azo dyes are the most popular varieties of synthetic dyes [45, 50]. Today, Azo dyes are being used up to 90% in the units, as they are versatile and easy to synthesize. Azo dyes are synthetic dyes containing azo group, N=N, as part of the structure. They account for about 60-70% of the all dyes used in food and textile manufactures. The nature of aromatic substituents on either sides of the azo group control the colours of azo compounds as well as the water solubility of the dyes and also their binding towards particular fabric [44, 47, 49]. The unit containing the nitrogen-nitrogen double bond is called azo group.

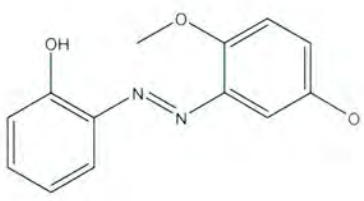

Citrus

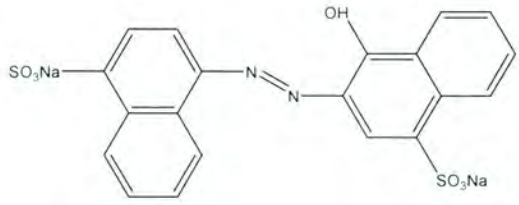

Carmoisine

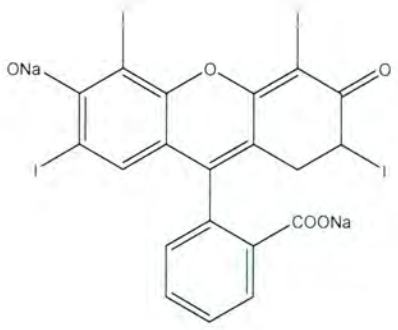

Erythrosine

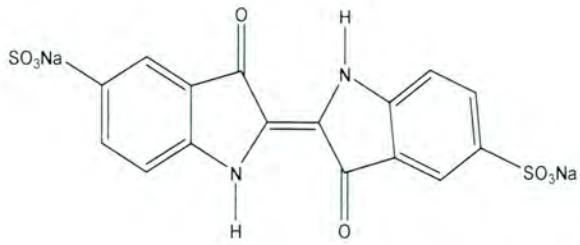

Indigo carmine

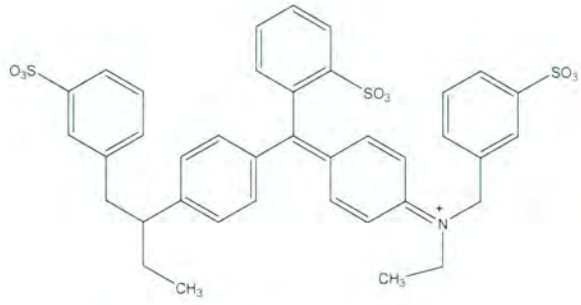

Brilliant blue

Figure 2.2 A schematic representation of some common food dyes used.

2.1.3 Properties of dyes

Azo class are chemically subdivided (according to the number of azo groups present) into mono-, dis-, tris-, tetrakis-, etc .The structure of dyes has aryl rings that have delocalized electron system, and these structures are said to be responsible for the absorption of the electromagnetic radiation that has different wavelength. However, dyes possess chromophores which are responsible for the colour in them, and enable the dyes to absorb radiation. The colour intensity of a dye molecule is depended upon how strongly it absorbs radiation in the visible regions, which extends from 400 to 700 nm [49–51]. In addition to chromophores, dyes also contain groups known as auxochromes (also known as colour helpers), e.g. sulfonic acid, amino acid and carboxyl group. Auxochromes are not really responsible for colour of dyes, because their presence can shift the colour of a colorant and so they are often used for dye solubility and cohesiveness [50, 52]. The colour of dyes can be altered by modifiers. The colour modifiers of methyl or ethyl group are responsible for any alteration in the dyes, that is, they alter the energy in the delocalized electrons [45, 52]. The presence of auxochromes in the chromogen molecule is necessary for making dye, however if present in the meta position to the chromophores, it will not affect the colour.

Dyes are water-soluble or water dispersible organic compounds having the capability of being absorbed into the substance destroying the crystal structure of the substance. The molecules of dye are chemically bonded to the surface and become a part of the material on which it is applied [49, 53]. Dyes possessing one or more azo group (i.e. azo dyes) comprise the largest family of organic dyes [52]. Colour changes in azo dyes are due to changes in extent of delocalization of electron (i.e. more delocalization shift the absorption max to longer wavelength and makes light absorbed redder, while less delocalization shift the absorption max to shorter wavelength. Almost all anionic azo dyes that possess OH or NH_2 substituents in ortho position are locked in the (E)-configuration due to intramolecular H-bonds (i.e. formation of six membered rings). The acid/base properties of aromatic azo dyes are highly relevant since pH changes due to protonations or deprotonations usually gives rise to a change in colour [52, 53].

Dyes possess wonderful advantages that make them to be of good interest to study and work on; such as wide colour range, good colour fastness and the ability to absorb light. Dyes can be synthesized cheaply because the starting materials are readily available. One of the important advantage of azo dyes is they have low impact on the environment due to the use of water as solvent in all of the reaction. Azo dyes are inexpensive compound and most of the chemistry is completed [45, 47, 49].

2.1.4 Synthesis of dyes

In the early centuries, dyes were obtained from natural sources such as plants and animals. Dyes such as Tyrian purple which were obtained from shellfish, were so rare that it could only be afforded by emperors and kings-hence the term royal purple. [46–47].Generally the synthesis of synthetic dyes, involves two-step reaction, the first step being the synthesis of aromatic diazonium ion from aniline derivative. All these substances can be obtained from coal tar, a crude material that is attained by distilling coal. The second step involves the coupling of diazonium salt with an aromatic compound [54–56].

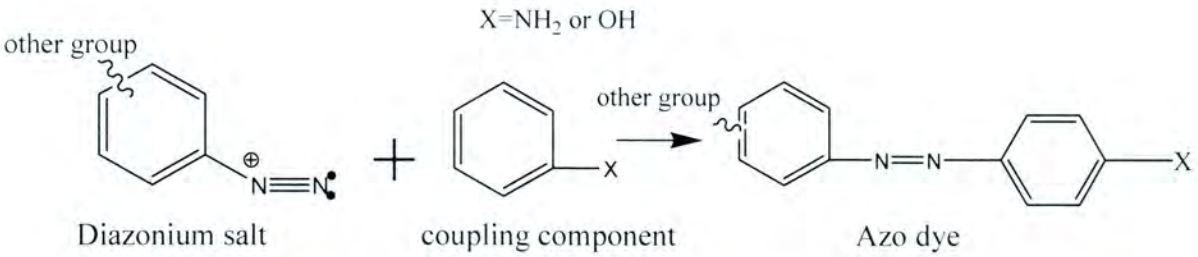

Figure 2.3 Schematic representation of an azo dye synthesis.

Azo coupling method, which is the coupling reaction between an aromatic diazo compound and coupling component, has been widely used as an important route to an azo dye preparation [45]. It normally proceeds by electrophilic aromatic substitution. In azo coupling preparation,

consideration must be taken not only in the internal equilibria of the diazo compound, but also those of the coupling. In diazo coupling, the positions where coupling will take are those which there is an increased electron density, generally at carbon atoms in the aromatic system or heterocyclic system aromatic in character, while in some cases at activated carbon atoms occurring in an aliphatic chain as in acetoacetanilide [45, 50]. The pre-equilibria of diazonium in coupling compound as a function of medium and pH strongly influence reaction rate, therefore azo coupling need to the carried out under the condition that favours not only the diazonium ions but also the more-nucleophilic coupling species (i.e. phenolate anions, unprotonated anilines, enolates) [45, 54].

Reports have shown that about 60 % of the dyes manufactured are produced by this reaction. There are other methods used in preparation of dyes which includes oxidative coupling, reaction of arylhydrazine with quinones, and oxidation of aromatic amines [45].In coupling components, primary aromatic amines are useful as coupling components not only in their own right but also as a means of introducing another azo link by diazotization and coupling with another component [50].

2.1.5 Applications of dyes

Dyes are widely used in different ways, therefore it is important to understand the application of dyes for a given substrate in order to acquire the highest fastness properties. They are used in almost every application, and possibly there would be a very few process (application), where there would be no use of dyes [45]. Dyes have become indispensable tools for a variety of industries. They are also used by industries for inks and tinting. Other industries where dyes are used in different products include paper and pulp, adhesives, art supplies, beverages, ceramics, construction, cosmetics, food, glass, paints, polymers, soap and wax biomedicine.

2.2 Dyes as corrosion inhibitors

Azo compounds are the most commonly used class of dyes due to their versatile application in various fields, including; dyeing of textile and fibres, to colouring of different materials, and high technology areas, such as electro-optical devices and ink-jet printers. They have also gained a lot of attraction due to their use as models of biological systems. Azo dyes possess molecular structures which recommend them for investigation as possible corrosion inhibitors when compared with reports on other organic inhibitors [57, 58].

Dyes possess structural features such as heteroatoms (oxygen, nitrogen and sulphur), which are capable of reducing corrosion attack on the metal [37, 58, 59]. The availability of non-bonded (lone pairs) and p-electrons in inhibitor molecules are there to facilitate electron transfer from the

inhibitor to the metal. During this process of adsorption, a coordinate covalent bond involving the transfer of electron from inhibitor to the metal surface may be formed [59].

A typical reaction indicating the adsorption process between the inhibitor and the metal adopts the following, wherein the efficiency of the Food Dye (FD) shows the ability to be adsorbed on the metal surface by displacing the water molecule from the interface which is affected by corrosion.

$$FD_{(sol)} + nH_2O_{(ads)} \rightarrow FD\ (ads) + nH_2O_{(sol)} \quad (19)$$

The adsorption of the FD (food dye) inhibitor on the metal surface during the corrosion process is influenced by the electronic structure of the inhibitor molecules and also by the steric factor, aromaticity, electron density at the donor atoms and also by the presence of the functional group –N=N–[60]. There is little information available on understanding the mechanism of interaction between food dyes and the metal surface. This information is essential in understanding the corrosion mechanism and can give information needed for the modification of food dyes so that more efficient food dyes can be synthesized.

An investigation was done using gravimetric method to study the inhibitory properties of indigo dye on the corrosion of mild steel in aerated sulphuric acid solution at 30–50°C [51]. The effect of addition of halide salts KCl, KBr, and KI was also done in this study. The corrosion rate in all system studied was found to increase with temperature rise. The study also found inhibition efficiency of indigo dye increased with concentration and synergistically increased on addition of halide salts. Studies on temperature indicated increased inhibition efficiency at higher temperature, suggesting chemisorption mechanism. The inhibitor adsorption characteristics were approximated by Frumkins isotherm and Flory-Huggins isotherm. The study revealed that the activation energy for Fe Dissolution in sulphuric acid was observed to reduce from 54.6kJmol^{-1} in the uninhibited system to 34.9kJmol^{-1} in the inhibited system.

Prabhu *et al* [61] studied the inhibition action of carmine and fast green dye on mild steel in 0.5 M HCl using mass loss, polarization and electrochemical impedance (EIS) methods at 300 K. The inhibition efficiency was found to increase with increasing concentration of the inhibitors. The inhibition efficiency of fast green (% η-98) was higher than that of carmine (% η-92) and was also found to be extreme in 1×10^{-3} M solution. The inhibitors were reported to act as mixed type with predominant cathodic effect. The inhibitors were adsorbed on the mild steel surface according to the Temkin adsorption isotherm. The surface morphology of mild steel specimen was evaluated using SEM.

Abdeli *et al* [57] investigated the inhibition behaviour of Nile Blue and Indigo Carmine organic dyes on mild steel corrosion in 1M HCl solution, using weight loss, potentiodynamic polarization, and electrochemical impedance spectroscopy techniques. The results obtained indicated that the inhibition efficiency (%IE) increased with the increasing concentration of Indigo Carmine up to 9.65×10^{-5} M (%IE ~ 98) and Nile Blue up to 1.08×10^{-4} (% IE ~75–80). A

good correlation was found between the results obtained from the different techniques used. The inhibition of both inhibitors was of a mixed anodic-cathodic nature reflected by polarization curves, and Langmuir isotherm was found to be an accurate isotherm describing the adsorption behavior. The results also indicated that the inhibition mechanism of the inhibitors involves chemisorption interaction between the inhibitor and the mild steel. The inhibition efficiency for both inhibitors showed a decrease with the rise in temperature in the range 25-55, and the results proved the chemisorption behavior of both inhibitors.

Corrosion inhibition of mild steel in hydrochloric acid solution by methyl-blue (MB) was investigated by Oguzie [62], by gravimetric techniques at 30^0 C and 60^0 C as well thermometric technique. MB was shown to be an inhibitor in the acidic corrodent. Inhibition efficiency increased with MB concentration but decreased with rise in temperature, with maximum value 94–95% obtained for 5.0 mM MB at 30° C. Corrosion inhibition obtained was attributed to the adsorption of MB on the mild steel surface via a physical adsorption mechanism. The results were further corroborated by kinetic and activation parameters for corrosion and adsorption evaluated from experimental data.

The corrosion inhibition of mild steel in 2 M H_2SO_4 using Alizarin yellow GG (AYGG) (an azo dye) in the presence of iodide ions, was investigated by Ebenso *et al* [58] at 30-60°C using weight loss and hydrogen evolution method. Results obtained showed that the inhibition efficiency increased with an increase in concentration of AYGG and decreased with increase in temperature. The inhibition efficiency of AYGG synergistically increased on addition of KI (Potassium iodide). The adsorption of AYGG alone and in combination with iodide ions on the metal surface was found to obey Temkin adsorption isotherm at all temperatures studied. Phenomenon of physical adsorption was proposed from the values of E_a and $\Delta G°_{ads}$ obtained Synergism parameter evaluated was found to be greater than unity for all concentrations of AYGG indicating that the enhanced inhibition efficiency of AYGG caused by addition of iodide ions is only due to synergism. The results obtained also indicated that the adsorption of AYGG and AYGG+KI onto mild steel surface is spontaneous.

Ashassi-Sorkhabi *et al* [63] studied the inhibition performance of Basic yellow 13 dye on mild steel corrosion in hydrochloric acid solution at 25°C using weight loss and electrochemical techniques. The effect of inhibitor concentration on the inhibition efficiency was also studied. The inhibition efficiency increased with an increase of Basic yellow 13 concentration. The results also showed that this inhibitor has good corrosion inhibition even at low concentrations (95 % for 0.005 M Basic yellow 13) and its adsorption of mild steel surface obeyed Langmuir adsorption isotherm. $\Delta G°_{ads}$ was calculated and its negative value indicated spontaneous adsorption of the Basic yellow 13 molecules on the mild steel surface and strong interaction between inhibitor molecules and metal surface. The value of $\Delta G°_{ads}$ obtained was less than the value 40 $kJmol^{-1}$, indicating the electrostatic interaction between the charged inhibitor molecules and the charged surface, i.e. physical adsorption.

Studies on the inhibition of mild steel corrosion in sulphuric acid using dyes and synergistic halide additives was done by Oguzie *et al* [64]. In this investigation, gravimetric method was used to study inhibitory properties of Indigo dye during corrosion aerated sulphuric acid solution at 30-50°C. Addition of halide salts KBr (potassium bromide), KCl (potassium chloride), and KI (potassium iodide). Results also showed that the corrosion rates in all system studied increased with an increase in temperature. There was an increase in inhibition efficiency of indigo dye with concentration and synergistically increase on addition of halide salts. The temperature studies showed an increase in inhibition efficiency at higher temperature, which indicated a chemisorption mechanism. The inhibitor adsorption characteristics were approximated by Frumkins isotherm and Flory-Huggins isotherm. Activation energy for Fe dissolution was seen to decrease from 54.6 $KJmol^{-1}$ in uninhibited system to 34.9 $KJmol^{-1}$ in the inhibition system.

Abboud *et al* [65] studied the novel azo-dye, 8-quinolinol-5-azoantipyridine as corrosion inhibitor for mild steel in acidic media. Results of weight loss and Tafel polarization measurement showed that the compound has fairly good inhibiting properties for mild steel corrosion in acidic bath, with efficiency around 96 % at a concentration of 10^{-3} M. The inhibitor was of a mixed anodic-cathodic nature. Langmuir adsorption isotherm was also found to provide an accurate description of the adsorption behaviour of the investigated azo compound. Some thermodynamic parameters such as the heat of adsorption, entropy of adsorption and free energy of adsorption were calculated using thermodynamic equations. Kinetic parameters such as the apparent activation energy and pre-exponential factor were calculate and discussed.

El-haddad *et al* [66] studied on inhibition of carbon steel corrosion in 2M hydrochloric acid (HCl) solution by thiophene azo dye derivative using weight loss, electrochemical frequency modulation (EFM), and atomic absorption technique. In their investigation, the inhibition efficiency increased with an increase in inhibitor concentration in pressure of 10^{3} μM potassium iodide (KI) according to experimental data obtained. This was due to synergistic effect. Therefore, according to the experimental results, this suggested that the presence of these anions in the solution stabilize the adsorption of inhibitors molecule in the surface and improve the inhibition efficiency. The results obtained from EFM experiments are a spectrum of current response as a function of frequency. Corrosion rate and Tafel parameter were obtained with measurement by analysing the harmonic frequencies. The results obtained also showed that the adsorption of the inhibitors on the metal surface obeyed Langmuir adsorption isotherm. The surface of metal examined using Fourier transform infrared and ultraviolet spectroscopy. The quantum chemical calculations were also carried out and relations between computed parameter and experimental inhibition efficiency were also discussed.

The study was conducted to evaluate the toxic effect of Tartrazine and Carmoisine on renal, hepatic function, lipid profile, blood glucose, body-weight gain and biomarkers of oxidative stress in tissue by Amine *et al* [67]. In this investigation, Tartrazine and carmoisine were administered orally in two doses, one low and the other high dose for 30 days followed by serum and tissue sample collection for determination of ALT, AST, ALP, urea, creatinine, total protein,

albumin, lipid profile, fasting blood glucose in serum and estimation of GSH, catalase SOD and MDA in liver tissue in male albino rat. The obtained data showed a significant increase in ALT, AST, ALP, urea, creatinine total protein and albumin in serum of rats dosed with Tartrazine and carmosine compared to control rats and these significant change were found to be more apparent in high dose that low, GSH, SOD and catalase were decrease and MDA increase in tissue homogenate in rats consumed in high Tartrazine and both dosed of carmosine. The conclusion was made in this study that Tartrazine and carmoisine affect adversely and alter biochemical markers in vital organs e.g. liver and kidney not only at higher doses but also at low doses.

Alexandro *et al* [68], investigated on the adsorption of food dyes, Acid yellow 6, (AY-6), Acid yellow 23 (AY-23), and Acid red 18 (AR-18) onto activated carbon obtained from flamboyant pods (Delonix regia) under optimized condition (AC_{op}) was performed in the study. According to the pH study, the three dyes were said to best adsorbed in acidic solution (pH=2). Ten isotherm models, four kinetic models, and the intraparticle diffusion models were also utilized to fit the experimental data. The Vieth–Sladek isotherm explained the adsorption of the three dyes very well, and the maximum adsorption amounts (Q_m) found for AY–6, AY–23, and AR–18 were 673.687, 643.041 and 551.779mg g^{-1}, respectively. The pseudo-second order model gave the best experimental data fit, although its K_2 parameter revealed that other mechanism were involved in the adsorption of AY-6 and AY-23. Similarly, the intraparticle diffusion model indicated that the adsorption was governed by several mechanisms. In this study, it was found that AC_{op} was revealed to be a fast and effective adsorbent for the removal of AY-6, AY-23, and AR-18 from aqueous solution.

Chapter 3

EXPERIMENTAL SECTION

3.1 Materials

The mild steel sheets used were be of composition 0.02 % Phosphorus (P), 0.37 % Manganese (Mn), 0.03 % Sulphur (S), 0.01 % Molybdenum (Mo), 0.039 % Nickel (Ni), 0.21 % Carbon C and the remaining part being iron (Fe).

3.2 Reagents

Hydrochloric acid (HCL) and potassium iodide (KI) used in this study were commercially obtained from MERCK CHEMICALS.

3.3 Inhibitors

Inhibitors used in this experiment were obtained from SIGMA-ALDRICH CHEMICALS. The names of inhibitors investigated in this study are;

a) Allura red AC
b) Sunset Yellow FCF
c) Tartrazine
d) Amaranth
e) Fast green

The structures of the dyes are given in figure 3.1

1. ALLURA RED AC	2. SUNSET YELLOW FCF
IUPAC NAME: Disodium 6-hydroxy-5-((2-methoxy-5-methyl-4-sulfophenyl)azo)-2-naphthalenesulfonate Molecular formula: $C_{18}H_{14}N_2Na_2O_8S_2$, MW : 496.42 $gmol^{-1}$	IUPAC Name : Disodium 6-hydroxy-5-[(4-sulfophenyl)azo]-2- naphthalenesulfonate Molecular formula: $C_{16}H_{10}N_2Na_2O_7S_2$, MW :452.37 $gmol^{-1}$

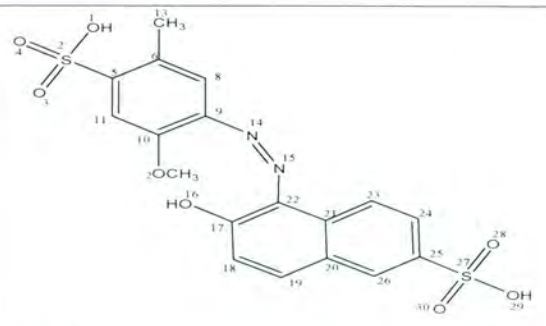

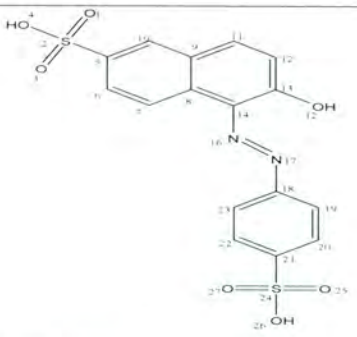

3. TARTRAZINE

IUPAC Name :Trisodium (4E)-5-oxo-1-(4-sulfonatophenyl)-4-[(4-sulfonatophenyl)hydrazono]-3-pyrazolecarboxylate

Molecular formula: : $C_{16}H_9N_4Na_3O_9S_2$, MW : 534.3 $gmol^{-1}$

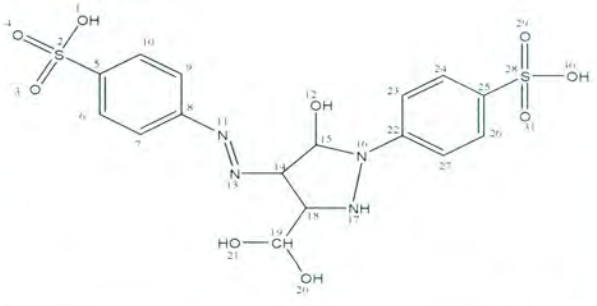

4. AMARANTH

IUPAC Name : Trisodium (4E)-3-oxo-4-[(4-sulfonato-1- naphthyl)hydrazono]naphthalene-2,7-disulfonate

Molecular formula :$C_{20}H_{11}N_2Na_3O_{10}S_3$, MW :604.47305$gmol^{-1}$

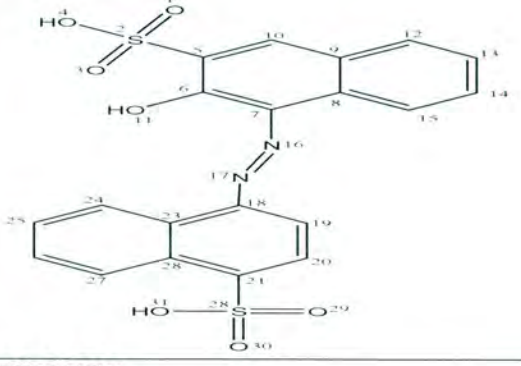

5. FAST GREEN FCF

- IUPAC NAME : Disodium 2-[(E)-{4-[ethyl(3-sulfonatobenzyl)amino]phenyl}{(4E)-4-[ethyl(3-sulfonatobenzyl)iminio]-2,5-cyclohexadien-1-ylidene}methyl]-5-hydroxybenzenesulfonate

Molecular formula : $C_{37}H_{34}N_2Na_2O_{10}S_3$, MW : 808.8 $gmol^{-1}$

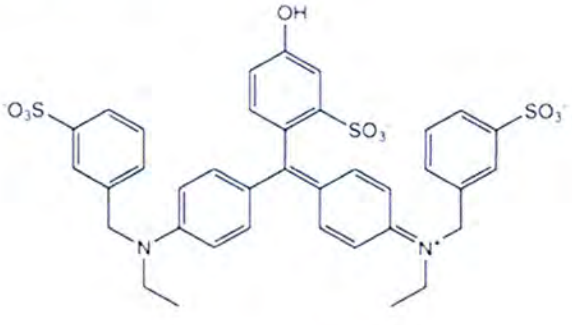

Figure 3.1: Molecular structure of the studied food dyes utilized in this study

3.4. Gravimetric methods

The gravimetric method (weight loss method) is the most important and widely used method in the area of monitoring corrosion. The method is widely applied because of its simplicity to carry out and in addition to that, it requires less expensive equipments. Despite the simplicity and inexpensiveness of this method, it does provide reliable and accurate results [69, 16].

With the inhibitor Without the inhibitor

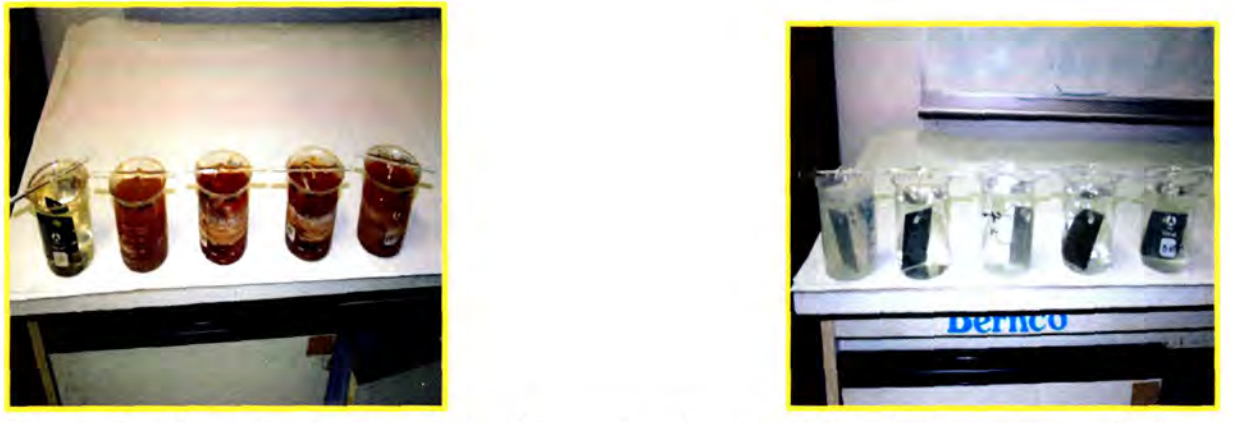

Figure 3.2: Experimental setup for the gravimetric procedure showing the metal sheets immersed in the solution with and without the inhibitor.

In this research, the weight loss measurements were carried out by totally immersing metal sheets in solution. The first experiment set was done on the acidic solution in the absence of the dyes and the second experiment set was performed by immersing the metal sheets completely in the solution containing the dye (corrosion inhibitor) in different concentrations and KI (potassium iodide) (Fig 3.2). The beakers of 250 ml in capacity were used to carry a 200 ml solution which covered the whole area of the metal sheet so as to ensure that no part of the metal was left exposed to air. The solution, were kept and maintained at different temperatures of 30 °C, 40 °C, 50 °C and 60 °C with the help of the thermostated water bath. The mild steel coupon was accurately weighed using Shimadzu AY220 sensitive analytical balance and were hooked and suspended inside the solutions with the help of a glass hook and glass rod. After 12 hours, the metal coupons were removed from the solution and cleaned with a bristle brush, rinsed severally with deionized water, and dried in acetone and re-weighed.

The following flow diagram illustrates the major steps in the experimental procedure for gravimetric method without and with the food dyes.

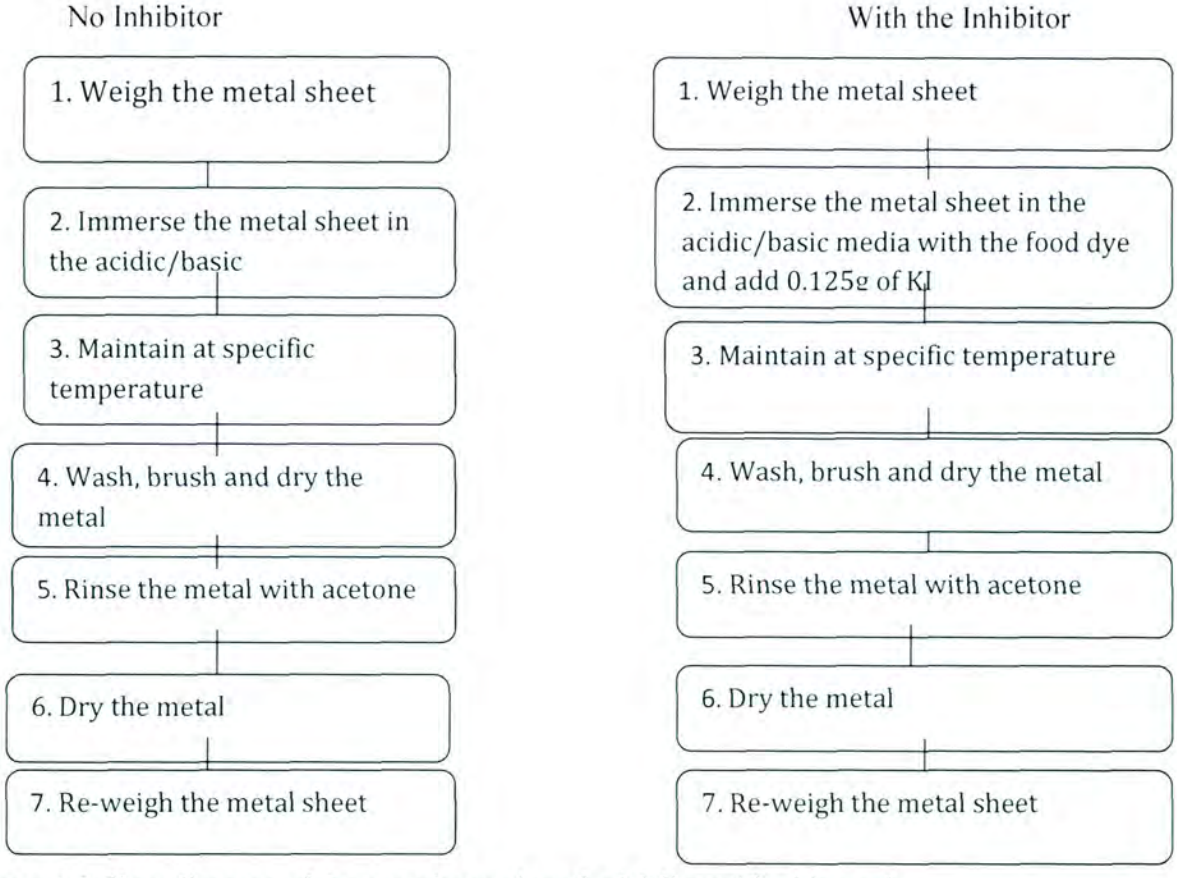

Figure 3.3 Flow diagram of the experimental method followed in this work

From the weight loss, some parameters are calculated. These include the corrosion rate, percent inhibition efficiency (% IE) and surface coverage (θ).

The corrosion rate for the mild steel in acidic environment was calculated using the equation below [40].

$$\rho = (\Delta W/St) \qquad (20)$$

where ρ= the corrosion rate density

W= the average weight loss of mild steel (in grams, g)

S= the total surface area of the mild steel (cm^2)

t= the immersion time (in hours, h)

The corrosion rate is given (in this case) in the units of $g.cm^{-2}.h^{-1}$.

From the values of the corrosion rate, the inhibition efficiency (%IE) and the degree of surface coverage (θ) for the mild steel were calculated. The equation for inhibition efficiency is given by [40];

$$\%IE = (\rho_1 - \rho_2 / \rho_2) \times 100 \quad (21)$$

where IE= the inhibition efficiency

ρ_1= the corrosion rate of the metals sheet in the absence of the inhibitor

ρ_2= the corrosion rate of the metal sheet in the presence of the inhibitor

The equation for the degree of surface coverage is given by;

$$\theta = (\rho_1 - \rho_2 / \rho_2) \quad (22)$$

Where: θ =the degree of surface coverage

ρ_1= the corrosion rate of the metals sheet in the absence of the inhibitor

ρ_2= the corrosion rate of the metal sheet in the presence of the inhibitor.

3.5 Electrochemical techniques

Specimens for electrochemical study were prepared to 10 X 10 mm. These samples were prepared by attaching an insulated copper wire to one of their faces using an aluminium conducting tape, and cold mounted in epoxy resin. The specimens were abraded through 1000-grit silicon carbide metallurgical paper in accordance to ASTM-G59-97, degreased in acetone, and washed with distilled water. Electrochemical measurements were conducted using the potentiodynamic polarization technique according to ASTM G 3-89 and ASTM 5-94. The conventional three electrode electrochemical cell system was used. The electrochemical cell was made of a 200 ml covered Pyrex glass conical flask suitable for the conventional three-electrode system; reference electrode (RE), working electrode (WE) and counter electrode (CE). The as-received mild steel was used as the working electrode, platinum rods as the counter electrodes and a silver/silver chloride 3 M KCl electrode as the reference electrode (SSE) [27, 40]

The corrosion behavior of the specimen was studied in 0.5 M HCl solution using the linear potentiodynamic electrochemical measurement technique. All electrochemical measurements were carried out at room temperature (25 ± 1 ^{o}C) using an Autolab potentiostat (PGSTAT30 computer controlled) with the general purpose electrochemical software (GPES) version 4.9. Before potentiodynamic cyclic polarization was taken, the specimens were immersed in the electrolytes for suitable time to stabilize at the open circuit potential (OCP). Potentiodynamic polarization curves were measured at a scan rate of 2 mV/s starting from -1.0V to 1.2V. After each scan, the electrolytes were replaced with fresh electrolyte. The studied food dyes solution namely; Sunset yellow, Amaranth, Allura red, Tartrazine and fast green were replaced after each test run. All the potentials reported were plotted versus the SSE potentials. Different

electrochemical parameters such as corrosion potential (E_{corr}), corrosion current density (I_{corr}), percentage inhibition efficiency (% IE) and Tafel constant (b_a and b_c) were obtained from the cathodic and anodic curves [41, 57].

3. 6 Quantum chemical/ theoretical methods

The calculations on quantum chemical studies were done *in vacuo* and in water solution and by considering both the protonated and the non-protonated species of the inhibitors. Different quantum chemical parameters such as the dipole moment, highest occupied molecular orbital (HOMO), the lowest unoccupied molecular orbital (LUMO), partial atomic charges, etc, were calculated and use to elucidate the reactivity tendency and the reactive centers of the studies ionic liquids. All Geometry optimizations and quantum chemical calculation were performed using density functional theory (DFT) using the 6-31G (d) basis set. The Becke's Three Parameter Hybrid Functional using the Lee-Yang Parr correlation theory (B3LYP, [70]) was selected for the calculations. The DFT method is commonly used in the analysis of the characteristics of the inhibitor/metal surface mechanism and in the description of the nature of the inhibitor on the corrosion process [71]. The DFT/B3LYP combination is best known for producing good estimate of molecular properties related to molecular reactivity and selectivity, and this molecular properties include the highest occupied molecular orbital (HOMO), energy of the lowest unoccupied molecular orbital (LUMO), hardness (η) and electronegativity , electron affinity (EA), global hardness and softness and ionization potential (IP) [72].

Chapter 4

RESULTS AND DISCUSSION

4.1 Gravimetric method

The experiment on gravimetric methods was performed on mild steel metal sheets at different temperatures with and without different concentrations of inhibitors with addition of Potassium Iodide (KI). The immersion time for both experiments was 12 hours.

4.1.1 The effect of the inhibitor concentration on the inhibition efficiency for mild steel

The efficiency of an organic compound as corrosion inhibitor does not only depend on the characteristic of the environment in which it acts, the nature of the metal surface and electrochemical potential at the interface, but also on the structure of the inhibitor itself including the number of adsorption active centers in the molecule, the formation of metallic complexes and projected area of the inhibitor on the metallic surface.

Figures 4.1–4.8 shows the plots of inhibition efficiency against concentration of the inhibitors with and without KI at different temperatures. It is seen from the results that the inhibition efficiency increases as the concentration of the inhibitor increases for all the studied dyes with and without KI.

Figure 4.1 shows the plot of inhibition efficiencies against the concentrations for the four inhibitors, namely Sunset yellow (SS), Amaranth (AM), Allura red (AR), Tartrazine (TZ) and Fast green (FG) without KI (a) and with KI (b). In (a), the inhibition efficiency increased with increase in concentration of the inhibitors for all the four inhibitors. This can be explained on the basis of increased adsorption of the compound on the metal surface.

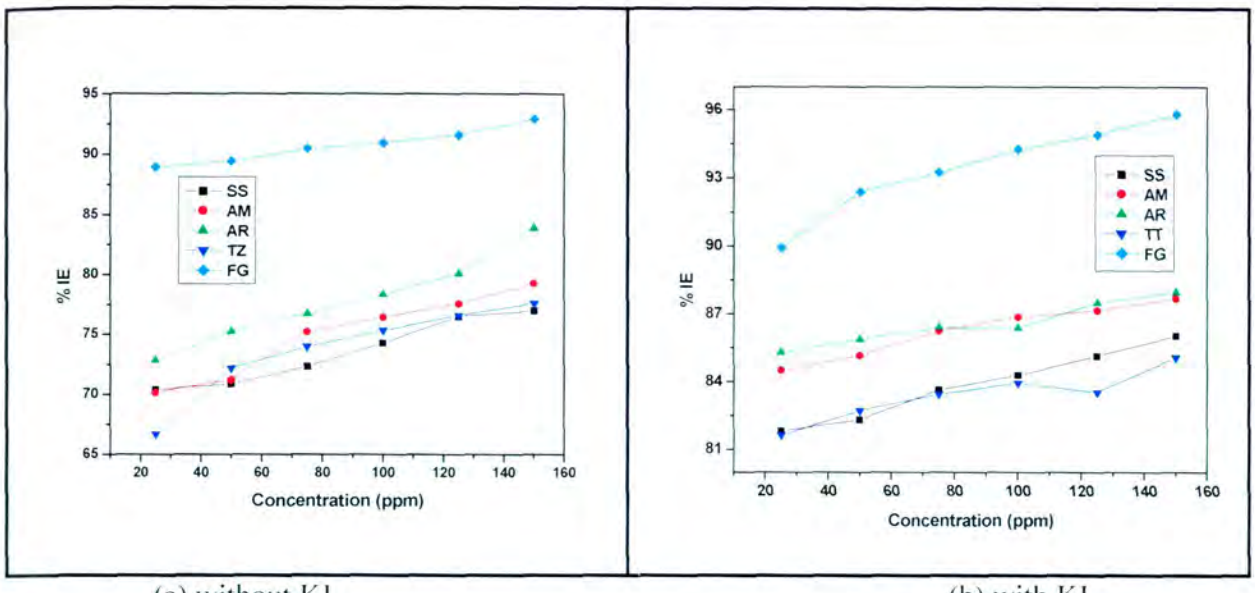

(a) without KI (b) with KI

Figure 4.1: Plot of inhibition efficiency against concentration using all five inhibitors at 30° C without (a) and with KI (b).

The results obtained from the figure 4.1 (b) also indicate that the inhibition efficiency of all the compounds studied increase with an increase with concentration on addition of KI. This is noticed in Allura red as its inhibition efficiency is increased from 85.30 % at 25 ppm to 87.94 % at 150 ppm, while Fast green increases its inhibition efficiency to 89.92 % and 95.79 % at 25 ppm and 150 ppm respectively. Studies [75] has stated that anions such Cl^-, I^-, SO_4^{2-} and S_2- have the ability of taking part in the reaction intermediates in corroding metal surface, which can either inhibit or stimulate corrosion. Halide ions have been reported to inhibit the corrosion of some metal in strong acids and the effect is said to be dependent upon the ion size, the electrostatic field set up by the charge of the ions on adsorption sites and the concentration of the halide ions.

Halides are known to have ability to replace the hydroxyl ions adsorbed on the metal surface, therefore reducing the catalytic effect of the hydroxyl ions [75]. Addition of Potassium iodide (KI) further increases the inhibition efficiency values. It has been reported in literature that the presence of the halide ion (I^-) in acidic media increases the inhibition efficiency of some organic compounds. And so the increase in inhibition efficiencies with the addition of KI is attributed to the fact that halide ion improve adsorption on the metal surface [58].

Figure 4.2 below shows the plot of the inhibition efficiencies against the concentration of the five dyes, Sunset yellow, Amaranth, Allura red, Tartrazine and Fast green without KI (a) and with KI (b) at 40° C. The inhibition efficiency increased from 42.31 % to 47.31 % using 25 ppm and 150 ppm respectively in Sunset yellow, while Amaranth increased its efficiency to 44.02 % and

47.26 % respectively. This suggest that the amount of adsorption and coverage of the inhibitor on mild steel surface increases with the inhibitor concentration.

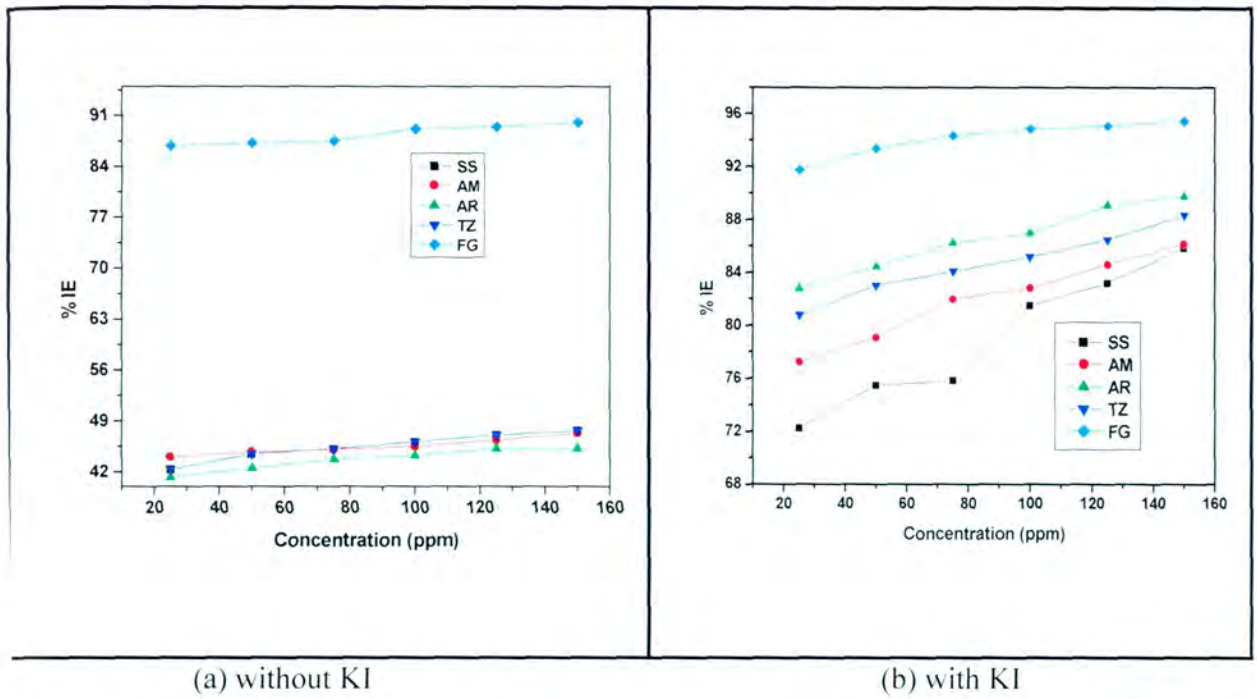

(a) without KI (b) with KI

Figure 4.2: Plot of inhibition efficiency against concentration using all five inhibitors at 40° C without (a) and with KI (b).

The results also indicate that as the temperature is increasing, the inhibition efficiency is slightly decreasing. This decrease in the inhibition efficiencies with increase in temperature may be as result of increase in the solubility of the protective film and of any reaction products precipitated on the surface of the metal that may disturb the reaction rate [75]. Fast green dye has the highest inhibition efficiency which increases from 86.83 % at 25 ppm to 90.06 % at 150 ppm.

Figure 4.2 (b) show the plot of inhibition efficiencies (%IE) and the concentration of the five studied dye compounds, namely Sunset yellow (SS), Amaranth (AM), Allura red (AR), Tartrazine (TZ) and Fast green (FG) at 40° C with addition of KI. Similar trend was obtained like in Fig. 4.1(b) for 30° C.

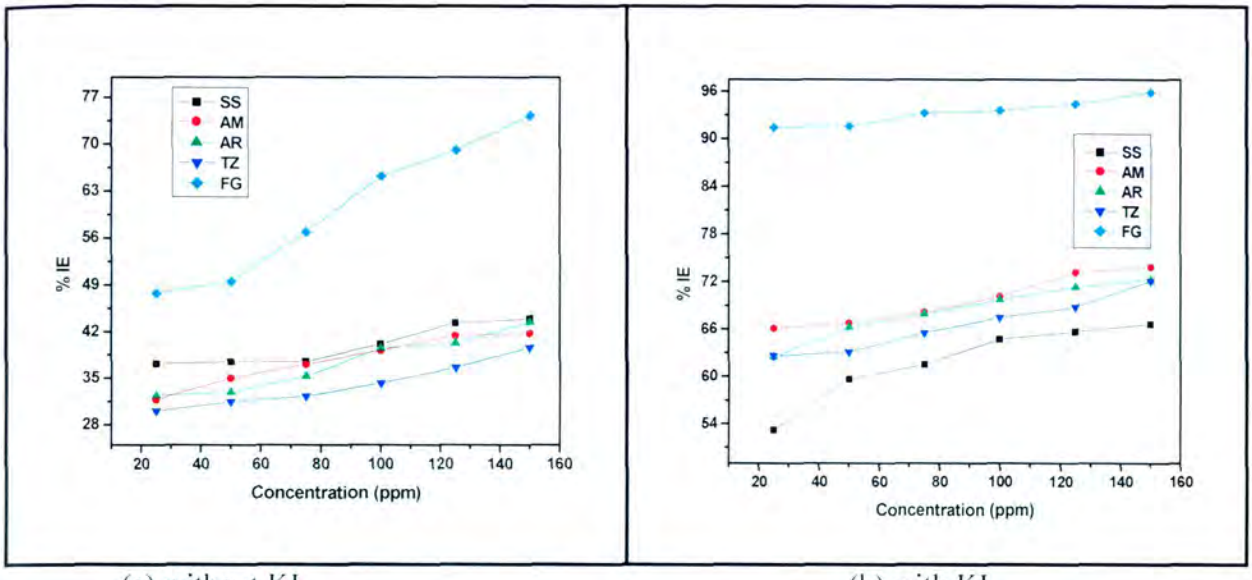

(a) without KI (b) with KI

Figure 4.3: Plot of inhibition efficiency against concentration using all five inhibitors at 50° C without (a) and with KI (b).

As the temperature increases to 50° C, the inhibition efficiencies also decreased (figure 4.3.a) but slightly increased as the concentration was increased. For example, as in the case of Tartrazine, its inhibition efficiency increases from 30.07 % at 25 ppm to 39.56 %. It is seen from the figure above that all the three compounds have decreased inhibition efficiencies, except for fast green which its inhibition efficiency increases from 47.75 % at 25 ppm to 74.19 % at 150 ppm. The plot in figure 4.3(b) shows that as the concentration of the inhibitor increases the inhibition efficiency also increases. Allura red increases its inhibition efficiency from 62.45 % to 72.17 %, whereas Fast green goes from 91.42 % to 95.83 % at 25 ppm and 150 ppm. The observed results may be due the adsorption of the dye molecules at the metal/solution interface.

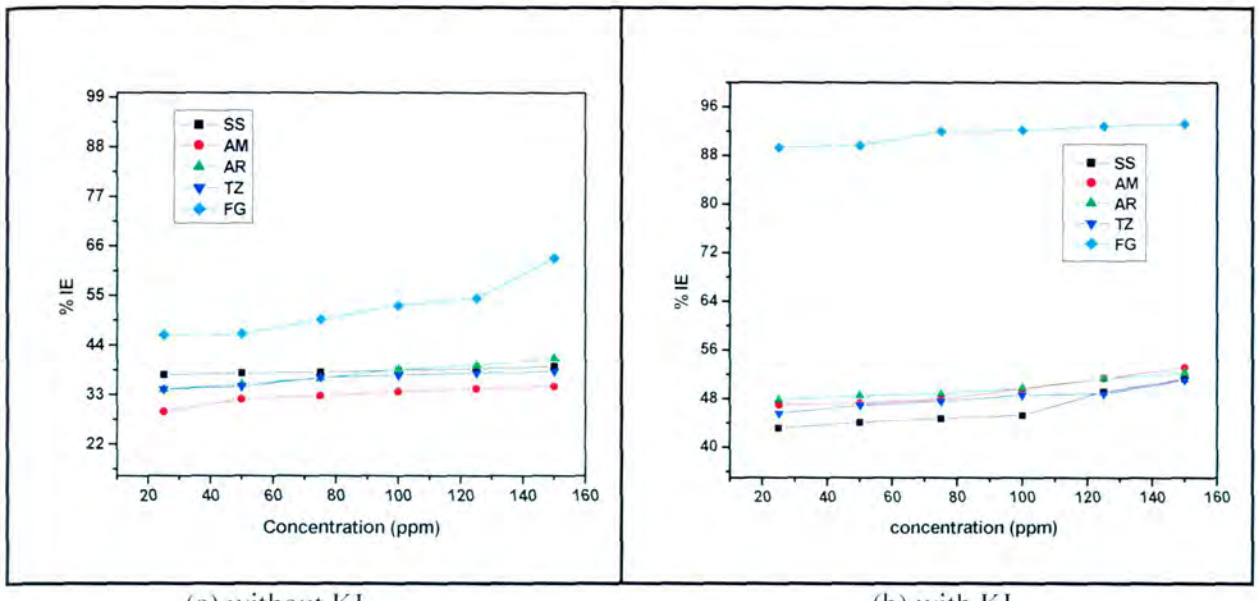

(a) without KI (b) with KI

Figure 4.4: Plot of inhibition efficiency against concentration using all five inhibitors at 60° C without (a) and with KI (b).

When the temperature is increase to 60° C (figure 4.4), the inhibition is efficiency is decreased. These results suggest a poor inhibition on mild steel implying the molecules of the inhibitor are desorbed on the metal surface at higher temperatures [58].

4.1.2 The effect of temperature on the inhibition efficiency for mild steel metal

Weight loss measurements are used in order to understand the stability of the adsorbed layer/film of inhibitor on mild steel surface as well as the activation parameters of the corrosion process of mild steel in acidic. Temperature effect on the inhibited acid-metal reaction is said to be very intricate, due to the fact that many changes occur on the metal surface like rapid etching, desorption of the inhibitor itself and possible decomposition. Corrosion rate is greatly influenced by the temperature of the environment. This effect is vital, because the mode of the inhibitor adsorption on mild steel surface can be deduced through temperature variations [58, 75, 76]. The effect of temperature on the inhibition of mild steel was investigated using the different concentration of Sunset yellow (SS), Amaranth (AM), Allura red (AR), Tartrazine (TZ), Fast green (FG) at temperatures 30° C, 40° C, 50° C and 60° C for 12 hours. Many authors have reported that corrosion rate (ρ) of mild steel in acidic medium and temperature (T) can be related using the Arrhenius equation and the transition-state equation given by the following equations [22, 75, 77–79].

$$C_R = A \exp\left(\frac{Ea}{RT}\right) \quad (23)$$

$$C_R = \left(\frac{RT}{Nh}\right) \exp\left(\frac{\Delta Sa}{R}\right) \exp\left(\frac{Ha}{RT}\right) \quad (24)$$

Where E_a is the apparent activation corrosion energy, C_R is the corrosion rate ($g.cm^{-2}\ hr^{-1}$), R is the molar gas constant ($8.314\ JK^{-1}mol^{-1}$), A is the Arrhenius pre-exponential factor, *h* is the Planck's constant, N is the Avogadro's number, ΔS_a is the entropy of activation and ΔH is the enthalpy of activation.

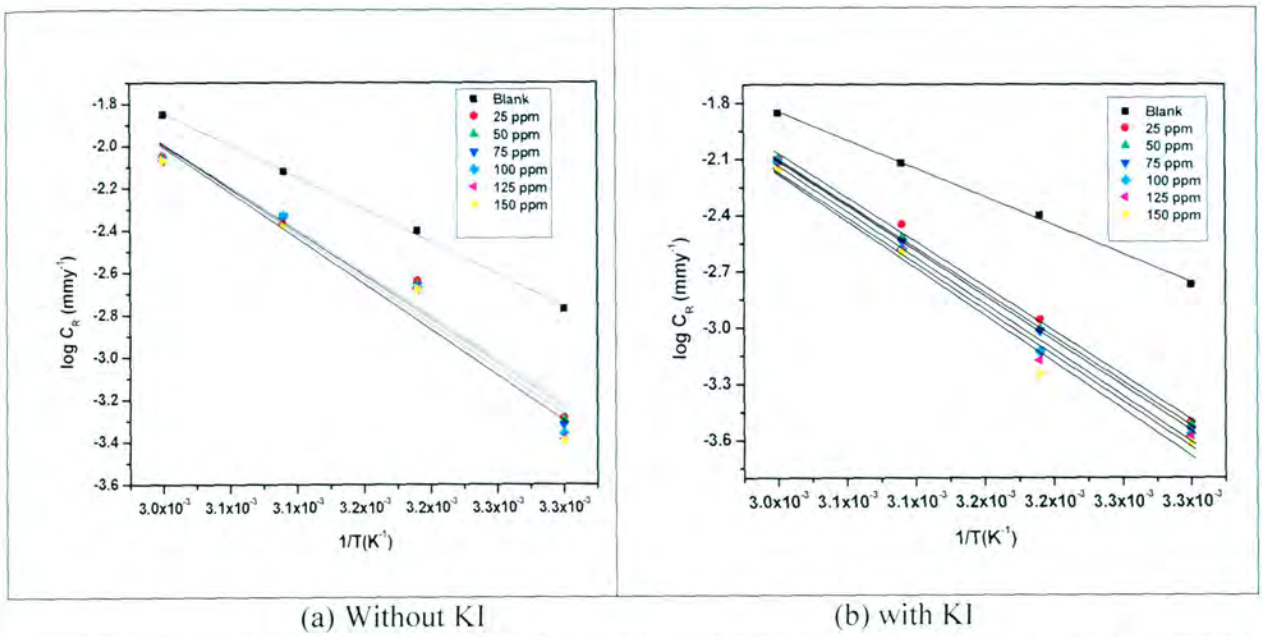

(a) Without KI (b) with KI

Figure 4.5: Arrhenius plot for mild steel corrosion in 0.5 M HCl in the absence and presence of different concentrations of Sunset yellow (SS) without KI (a) and with KI (b).

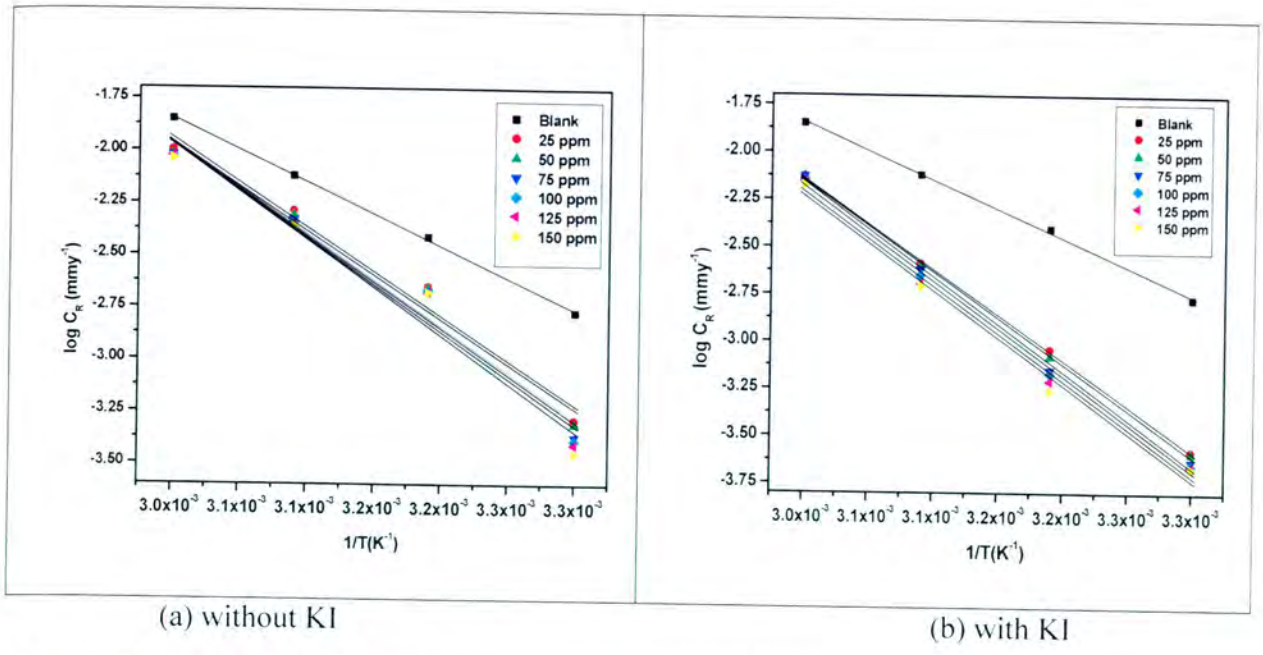

(a) without KI (b) with KI

Figure 4.6: Arrhenius plot for mild steel corrosion in 0.5 M HCl in the absence and presence of different concentrations of Amaranth (AM) without KI (a) and with KI (b).

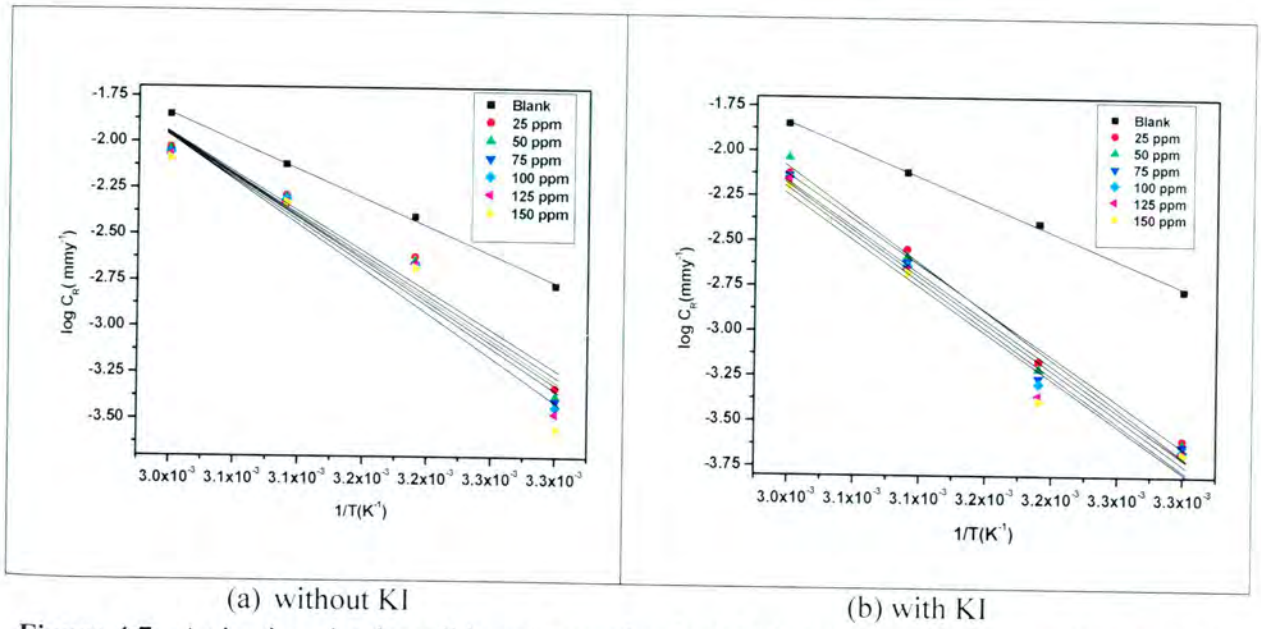

(a) without KI (b) with KI

Figure 4.7: Arrhenius plot for mild steel corrosion in 0.5 M HCl in the absence and presence of different concentrations of Allura red (AR) without KI (a) and with KI (b).

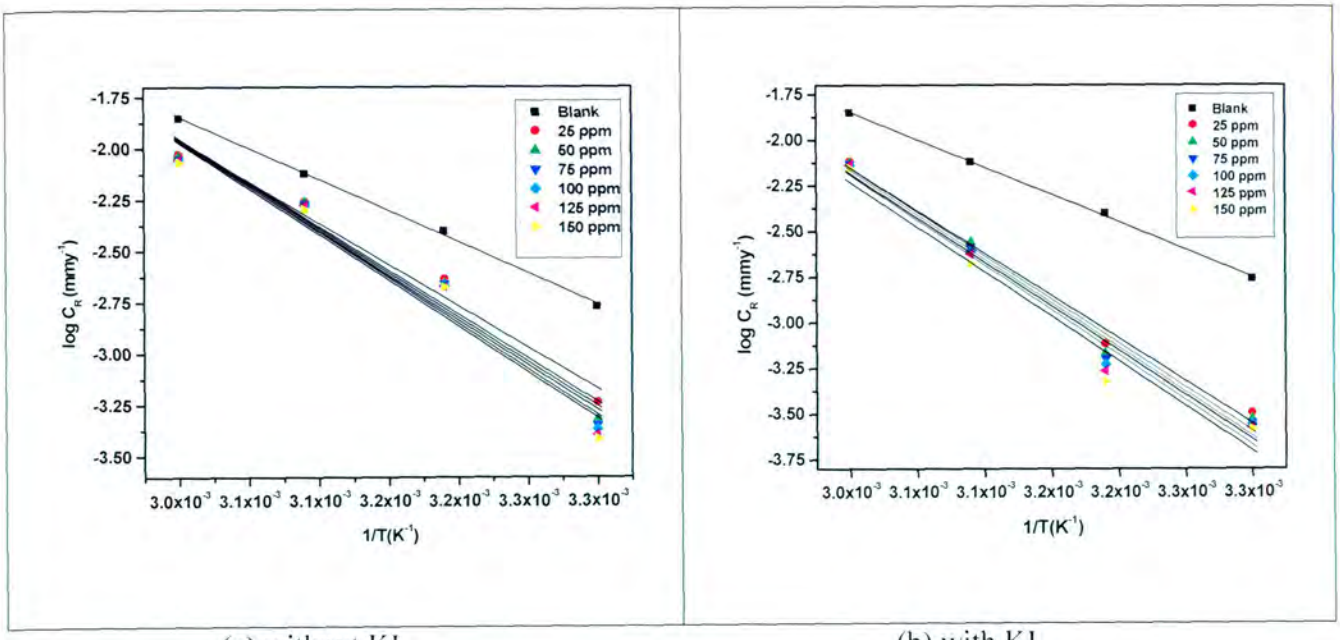

(a) without KI (b) with KI

Figure 4.8: Arrhenius plot for mild steel corrosion in 0.5 M HCl in the absence and presence of different concentrations of Tartrazine (TZ) without KI (a) and with KI (b).

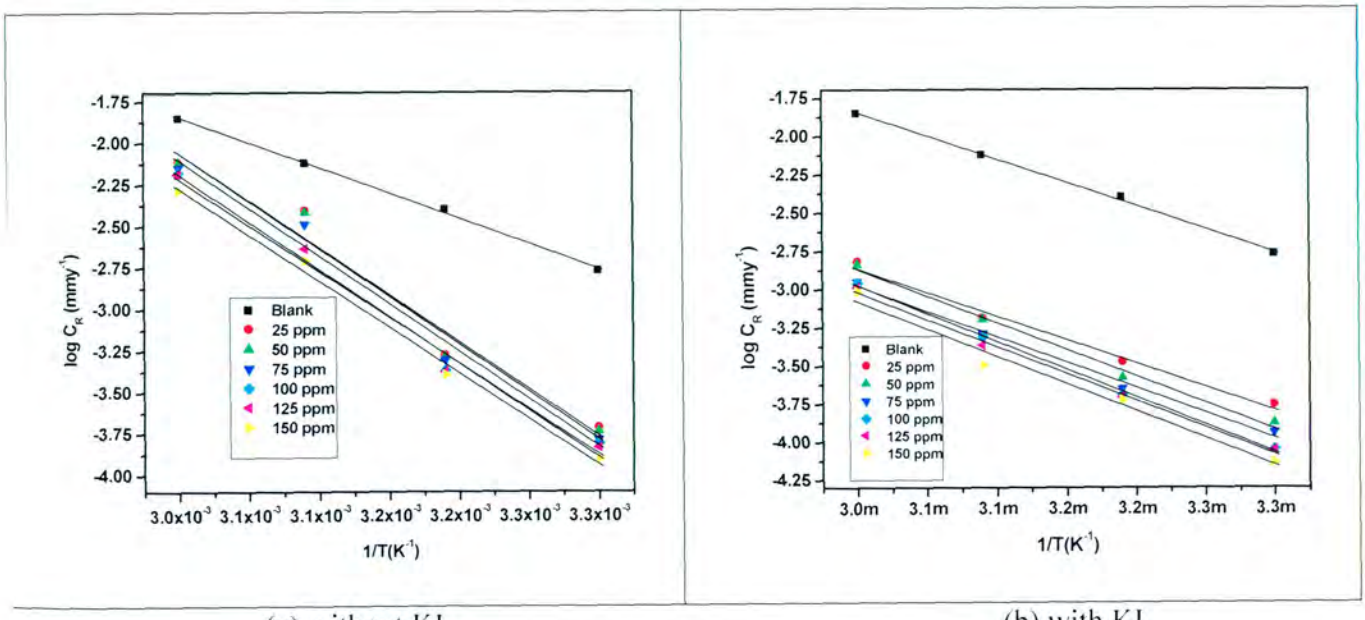

(a) without KI (b) with KI

Figure 4.9: Arrhenius plot for mild steel corrosion in 0.5 M HCl in the absence and presence of different concentrations of Fast green (FG) without KI (a) and with KI (b).

The effect of temperature in the kinetic process of corrosion in a free acidic environment and in the presence of adsorbed inhibitor leads to acquiring more information on the behavior of the materials. Corrosion reaction of mild steel in acidic medium is strongly depended upon the temperature of the reaction. The apparent activation energy (E_a) for corrosion process in the absence and presence of food dyes at different concentration were evaluated using the plots of log C_R versus 1/T (figures 4.9-4.13) and the results obtained are presented in Table 4.1 below. It can be seen from the results that the values of E_a are increasing as the concentration of the inhibitor increases. Increase in activation energy as the concentration increases, implies physical adsorption (electrostatic attraction) occurs first [78].

Other reports [79] have explained that an increase in apparent activation energy is also due to an appreciable decrease in the adsorption of the inhibitor on mild steel surface. The data obtained from the above graphs with the addition of KI indicate that the rate of mild corrosion in the absence and presence of the studied dyes increase with increase in temperature. This suggests that rise in temperature normally accelerates the corrosive process, particularly in media where H_2 gas evolution accompanies corrosion, thus giving rise to higher dissolution of rates of metal. The experimental reason that the activation energy is higher in the presence of inhibitor is discussed in different ways in literature. Some studies [77] have pointed out that the decrease in the apparent activation energy at higher inhibition are due to a shift of the net corrosion reaction, from one uncovered surface to one directly involving adsorbed sites. Studies [20–22, 60, 80] have postulated the variation of the apparent activation energy E_a in the presence of inhibitor. Higher values E_a were found in the presence of inhibitors. Some investigations [80, 81] showed that in the presence of inhibitors the apparent activation energy was lesser than that the absence of the inhibitor. Nevertheless, in this current study, E_a increased with increasing concentration of the dye inhibitor without the addition of KI in Table 4.1. The higher value of activation energies in the presence of the inhibitor suggests higher inhibition efficiency and it indicates physisorption or weak chemical bonding between the inhibitor molecules and the metal surface [20, 82, 83].

Table 4.1: Activation parameters E_a, ΔH^* and ΔS^* derived from the Arrhenius plots in the absence and presence of different concentration of the studied food dyes.

Name of inhibitor	Concentration of inhibitor (ppm)	Apparent activation energy E_a (kJ mol^{-1})	Enthalpy of activation ΔH^* (kJ mol^{-1})	Entropy of activation ΔS^* (J K^{-1} mol^{-1})
	-	58.28	55.26	-115.47
SS	25	77.72 (90.96)[a]	75.15 (88.15)[a]	-58.52 (-20.94)[a]
	50	78.09 (90.94)[a]	75.46 (88.00)[a]	-57.61 (-22.02)[a]
	75	79.28 (91.91)[a]	77.08 (89.48)[a]	-52.70 (-17.78)[a]
	100	81.27 (94.15)[a]	78.43 (91.46)[a]	-48.79 (-12.30)[a]

	125	82.38	(93.77)[a]	80.03	(91.70)[a]	-44.06	(-6.39)[a]
	150	82.76	(95.98)[a]	80.53	(93.13)[a]	-42.64	(-8.31)[a]
AM	25	81.50	(91.88)[a]	78.83	(89.40)[a]	-46.55	(-18.62)[a]
	50	81.33	(92.95)[a]	78.75	(60.60)[a]	-47.05	(-15.12)[a]
	75	84.63	(96.10)[a]	81.84	(93.17)[a]	-37.74	(-7.64)[a]
	100	85.05	(95.89)[a]	79.78	(93.30)[a]	-44.22	(-7.56)[a]
	125	85.99	(95.56)[a]	83.53	(92.60)[a]	-32.92	(-9.80)[a]
	150	87.81	(95.70)[a]	85.15	(93.21)[a]	-28.09	(-6.73)[a]
AR	25	58.28	(96.14)[a]	91.94	(87.69)[a]	-9.14	(-7.14)[a]
	50	81.69	(102.16)[a]	79.64	(89.46)[a]	-39.82	(-6.81)[a]
	75	83.64	(97.44)[a]	81.99	(89.99)[a]	-37.49	(-2.57)[a]
	100	85.20	(98.75)[a]	82.96	(87.16)[a]	-34.66	(9.40)[a]
	125	86.22	(99.58)[a]	84.59	(91.59)[a]	-29.84	(9.24)[a]
	150	87.61	(98.05)[a]	88.91	(91.20)[a]	-16.87	(-2.15)[a]
TZ	25	77.33	(89.47)[a]	74.73	(87.69)[a]	-59.19	(-23.69)[a]
	50	81.86	(85.65)[a]	107.39	(89.46)[a]	36.84	(-18.53)[a]
	75	82.88	(92.85)[a]	106.97	(89.99)[a]	34.76	(-17.37)[a]
	100	83.47	(92.85)[a]	101.74	(87.16)[a]	23.12	(-25.77)[a]
	125	85.42	(94.44)[a]	82.35	(91.59)[a]	-36.41	(-13.04)[a]
	150	85.63	(93.90)[a]	90.91	(91.20)[a]	-10.30	(-14.96)[a]
FG	25	108.63	(59.26)[a]	106.08	(57.03)[a]	33.01	(-129.52)[a]
	50	109.78	(66.77)[a]	107.39	(64.44)[a]	36.84	(-107.41)[a]
	75	109.95	(63.54)[a]	106.97	(60.95)[a]	34.76	(-119.96)[a]
	100	105.78	(69.77)[a]	105.85	(66.95)[a]	30.27	(-102.17)[a]
	125	108.75	(67.78)[a]	106.07	(64.58)[a]	30.52	(-109.99)[a]
	150	106.23	(68.47)[a]	104.38	(64.14)[a]	23.87	(-106.33)[a]

( )[a] corresponds to results with the addition of KI

Some studies [77] have pointed out that a decrease in apparent activation energy at higher inhibition are due to a shift in the net corrosion reaction, from one uncovered surface to one directly involving adsorbed sites. In the case of the addition of KI, the results shows the apparent activation energy was first decreasing then increased but not in all cases. The values of enthalpy and entropy of activation were calculated from the plots of log CR/T *vs* 1/T (Figure 4.10–4.14). The lower ΔH^* values in

the presence of the inhibitor suggests that the less energy barrier for the reaction in the presence of inhibitor is attained and hence exhibit the high inhibition efficiency at elevated temperatures.

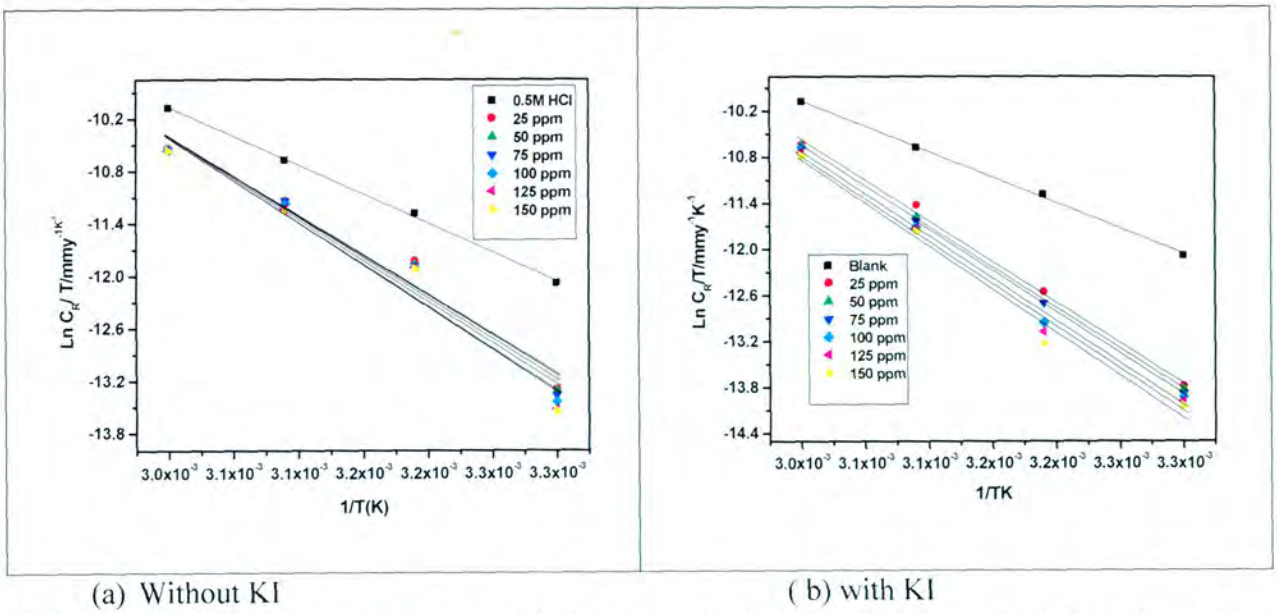

(a) Without KI (b) with KI

Figure 4.10: Transition state plots at different concentrations of Sunset yellow (SS) without KI (a) and with KI (b).

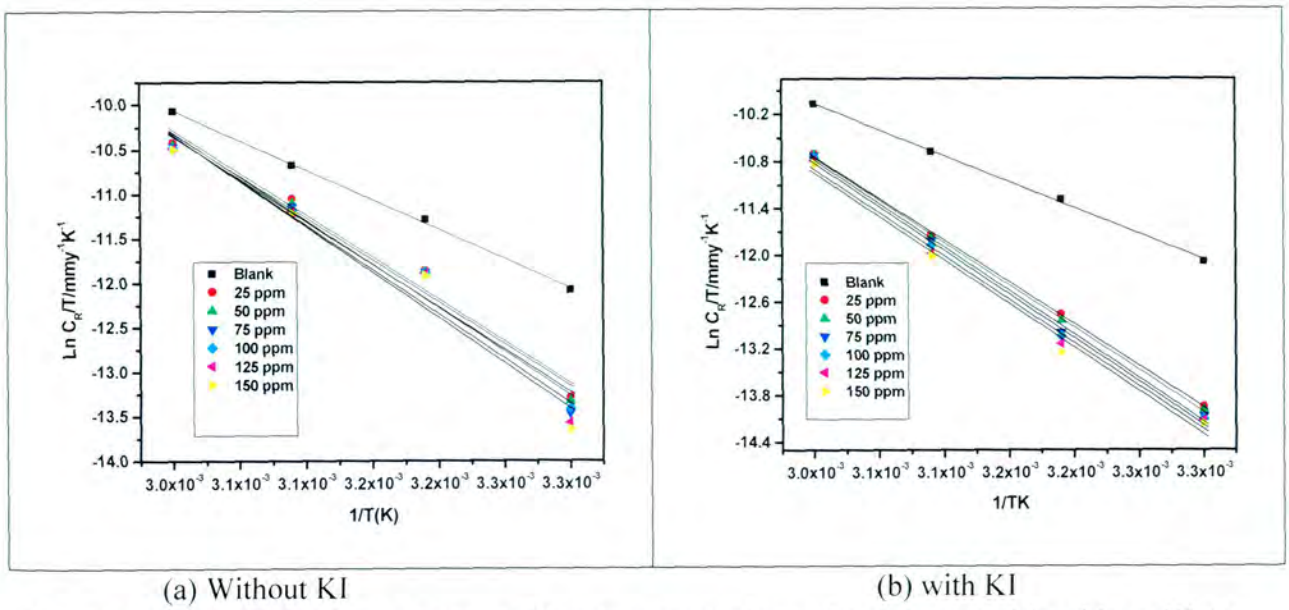

(a) Without KI (b) with KI

Figure 4.11: Transition state plots at different concentrations of Amaranth (AM) without KI (a) and with KI (b).

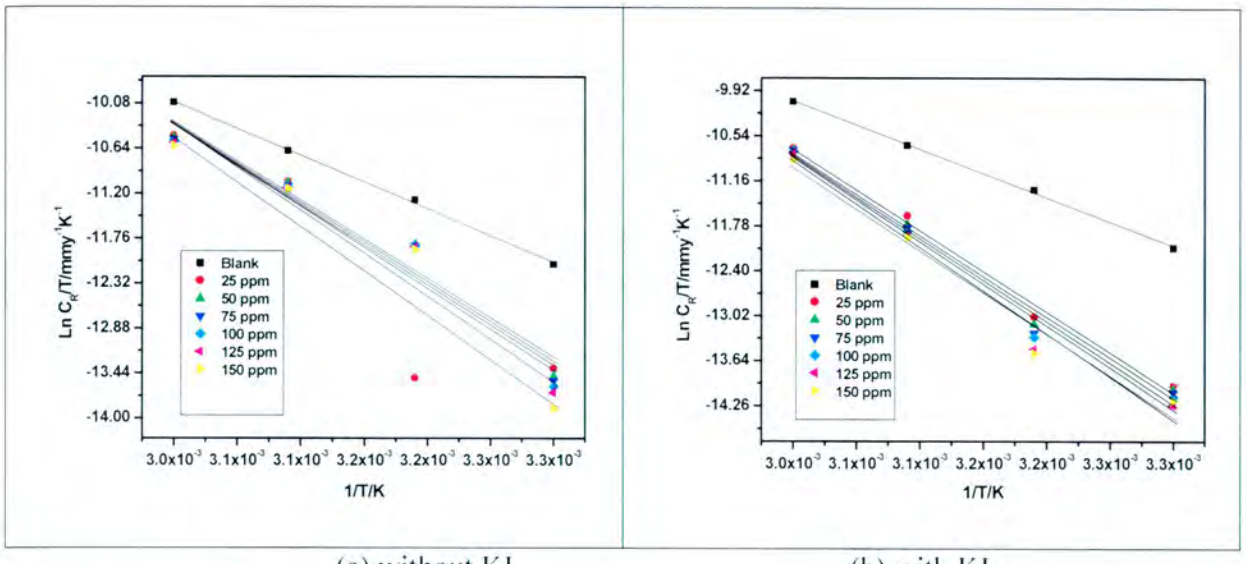

(a) without KI (b) with KI

Figure 4.12: Transition state plots at different concentrations of Allura red (AR) without KI (a) and with KI (b).

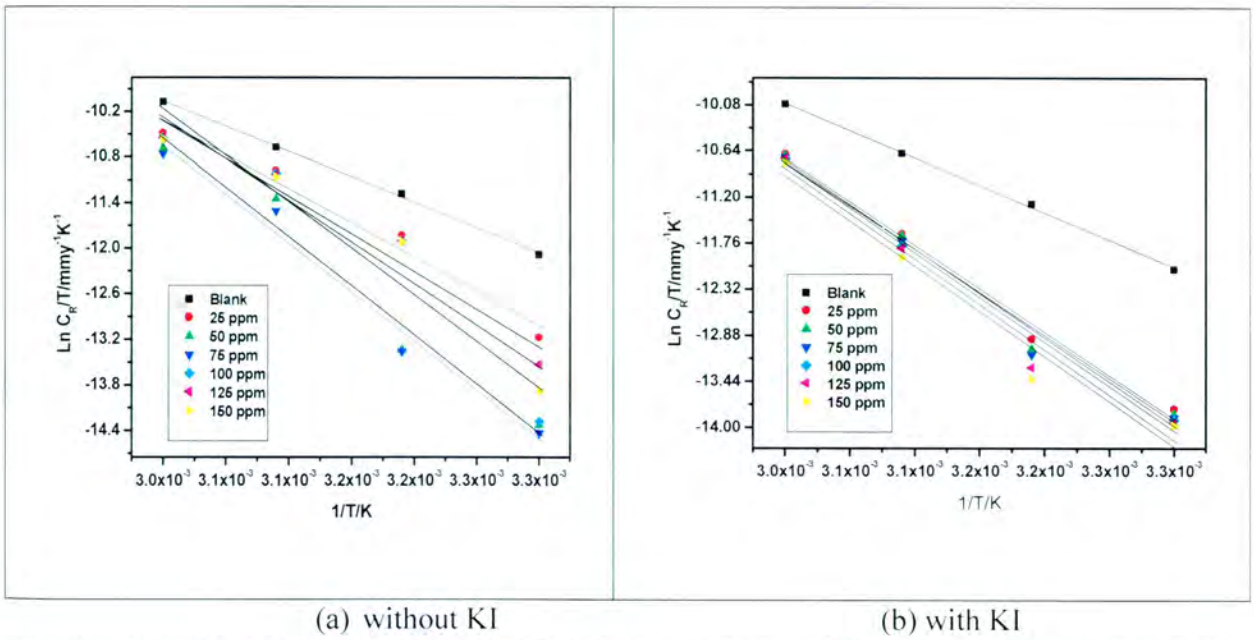

(a) without KI (b) with KI

Figure 4.13: Transition state plots at different concentrations of Tartrazine (TZ) without KI (a) and with KI (b).

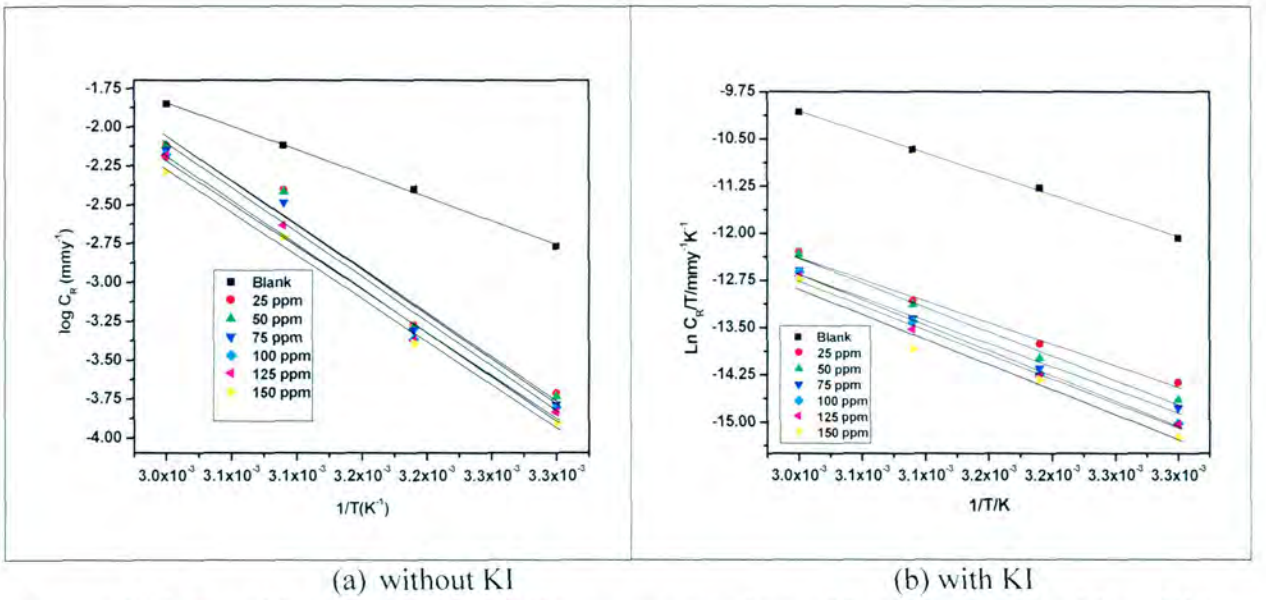

(a) without KI (b) with KI

Figure 4.14: Transition state plots at different concentrations of Fast green (FG) without KI (a) and with KI (b).

The results in Table 4.1 shows that the values of ΔH^* are positive both in the absence of the inhibitor, this implies the endothermic nature of mild steel dissolution process for both instances with and without the addition of KI. The values of ΔS^* were found to be very smaller with absence of the inhibitor and negative, but much better with the inhibitor without the addition of KI. The entropy of activation without addition of KI is higher (-38 JK^{-1}) in the presence of an inhibitor than that of (-115 JK^{-1}). This result indicate an opposite of what would be normally expected, due to the reason that the adsorption of inhibitor is an exothermic process and is always accompanied by a decrease of entropy. This mechanism could be elucidated as follows; the aqueous solution could be regarded as quasi-substitution process between the organic compound in the aqueous phase [Org $_{(sol)}$] and the water molecule at the electrode surface. The adsorption of organic inhibitor is followed by desorption of water molecules from the surface. Therefore, the adsorption process for the inhibitor is assumed to be exothermic and associated with a decrease in entropy of the solute; the opposite is believed to be true for the solvent [84, 85].

4.1.3 Adsorption isotherm and thermodynamic parameters

The adsorption isotherms are derived so as to gain more insights into the mechanism of corrosion inhibition, due the fact that it describes the molecular interaction of the inhibitor molecule with the active sites on the metal surface [85–88]. To gain more information about the mode of adsorption isotherm relating to the studied compounds, different isotherms were applied which includes the Frumkin, Flory-Huggins, Freundlich, Temkin and Langmuir adsorption isotherms. Langmuir adsorption isotherm was found to provide the best description of the behavior of the investigated food dyes. It was determined by plotting the concentration of the inhibitor/surface

coverage against the concentration of the inhibitor, which can be represented by equation (25) below. The Langmuir adsorption isotherm has an assumption which says that the solid surface contains a fixed number of adsorption sites and each site holds one adsorbed species. Figure 4.15 shows the Langmuir adsorption isotherm obtained in this study both without and with the addition of KI.

$$\frac{C_{inh}}{\theta} = \frac{1}{K_{ads}} + C_{inh} \tag{25}$$

where, θ is the degree of surface coverage, K_{ads} is the equilibrium constant of the adsorption/desorption process and C_{inh} is the concentration of the inhibitor. K_{ads} represent the degree of adsorption, i.e. the higher the value of K_{ads} implies that the inhibitor is strongly adsorbed on the metal surface [41].

Equation (26) below represents the relationship between free energy of adsorption ΔG^{o}_{ads} and the modified adsorption equilibrium constant K_{ads}. $C_{solvent}$ is known as the molar concentration of the solvent, which, normally in the case of water, is 55.5mol L^{-1}.

$$k = \frac{1}{C_{solvent}} \exp\left[\frac{-\Delta G^{o}_{ads}}{RT}\right] \tag{26}$$

The free energy of adsorption ΔG^{o}_{ads} is a very important thermodynamic parameter, because it gives information about the type of adsorption process.

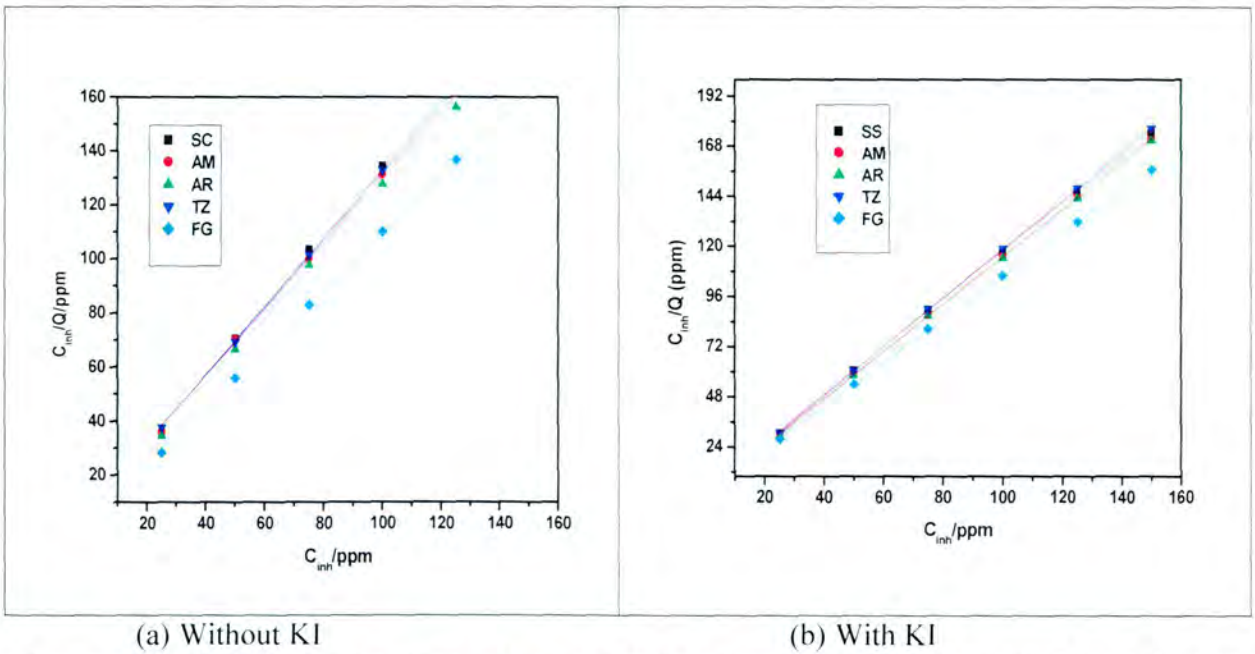

(a) Without KI (b) With KI

Figure 4.15: Langmuir adsorption isotherm plot for adsorption of all the studied food dyes at 30° C.

Generally the values for free energy of adsorption ΔG^{o}_{ads} up to −20 kJ mol^{-1}, suggest the electrostatic interaction between the charged molecules and the charged metal surface (i.e. physisorption), while those around −40 kJ mol^{-1} or higher involves charge sharing or transfer from organic molecules to the metal surface to form coordinate type of metal bond (chemisorption) [20, 84, 87–89, 92]. Other thermodynamic parameters, including the heat of adsorption (ΔH_{ads}) and the standard adsorption entropy ($\Delta S°_{ads}$), were calculated using the following equation, given by equation (27):

$$\Delta G^{o}_{ads} = \Delta H°_{ads} - T\,\Delta S°_{ads} \qquad (27)$$

A plot of ΔG^{o}_{ads} *vs* T was made with the slope equal to $-\Delta S°_{ads}$, and the value of $\Delta H°_{ads}$ was deduced from the intercept. The calculated values of free energy of adsorption, K_{ads}, enthalpy and entropy of adsorption are presented in Table 4.2 below.

Table 4.2: Thermodynamic parameters for adsorption of the studied food; Sunset yellow (SS), Amaranth (AM), Allura red (AR), Tartrazine (TZ) and fast green (FG) at different temperatures

Name of Inhibitor	Temperature/K	K_{ads} ($10^3\times$ mol^{-1})	$-\Delta G^{o}_{ads}$ (kJ mol^{-1})	ΔH^{o}_{ads} (kJ mol^{-1})	ΔS^{o}_{ads} (JK^{-1} mol^{-1})
SS	303	0.15 (0.34)[a]	-5.40 (-7.44)[a]	5.44 (7.48)[a]	0.14 (0.13)[a]
	313	0.09 (0.10)[a]	-4.40 (-4.39)[a]	4.44 (4.43)[a]	
	323	0.03 (0.08)[a]	-1.37 (-3.94)[a]	1.41 (3.98)[a]	
	333	0.05 (0.05)[a]	-2.81 (-2.81)[a]	2.85 (2.85)[a]	
AM	303	0.14 (0.55)[a]	-5.13 (-8.60)[a]	5.17 (8.63)[a]	0.15 (0.11)[a]
	313	0.09 (0.17)[a]	-4.43 (-5.89)[a]	4.42 (5.92)[a]	
	323	0.03 (0.12)[a]	-1.64 (-5.02)[a]	1.69 (5.06)[a]	
	333	0.07 (0.07)[a]	-3.79 (-3.79)[a]	3.83 (3.83)[a]	
AR	303	0.12 (0.63)[a]	-4.87 (-8.95)[a]	4.91 (8.98)[a]	0.14 (0.10)[a]
	313	0.06 (0.28)[a]	-3.07 (-7.18)[a]	3.11 (7.21)[a]	
	323	0.03 (0.12)[a]	-0.93 (-5.11)[a]	0.97 (5.14)[a]	
	333	0.11 (0.11)[a]	-4.86 (-4.86)[a]	4.91 (4.89)[a]	
TZ	303	0.14 (0.49)[a]	-5.21 (-8.32)[a]	5.25 (8.36)[a]	0.13 (0.13)[a]
	313	0.097 (0.23)[a]	-4.39 (-6.59)[a]	4.42 (6.63)[a]	
	323	0.03 (0.09)[a]	-0.93 (-4.49)[a]	0.97 (4.53)[a]	
	333	0.10 (0.10)[a]	-4.71 (-4.61)[a]	4.75 (4.65)[a]	
FG	303	0.4 (0.39)[a]	-8.04 (-7.76)[a]	8.05 (7.84)[a]	0.02 (0.27)[a]
	313	0.47 (3.57)[a]	-8.49 (-13.77)[a]	8.49 (13.85)[a]	
	323	0.0 (0.41)[a]	-1.17 (-8.37)[a]	1.17 (8.46)[a]	
	333	0.0 (0.50)[a]	-1.69 (-8.89)[a]	1.69 (8.99)[a]	

( )[a] corresponds to results with the addition of KI

The negative value of entropy, suggests the activated complex in the rate determining step represent an association rather than a dissociation step, which means that a decrease in disordering occurs on going from reactant to the activated complex [87–89]. The obtained values of ΔG^{o}_{ads} from Table 4.2 are negative suggesting the spontaneity of the adsorption process. The results also shows that the calculated values of ΔG^{o}_{ads} are range between −0.93 to −8.49 kJ mol^{-1} without KI, and this indicates that the adsorption mechanism of the studied food dyes on mild steel surface in acidic media is physisorption forming an electrostatic attraction between the charged metal surface and the charged molecule. These results suggest that the molecular structure of these dyes barely allows adsorption on the metal surface. The above data shows that in the addition of KI, the values of ΔG^{o}_{ads} showed to increase from −2.81 to −8.89 kJ mol^{-1} which is much higher as compared to the values obtained without KI. ΔG^{o}_{ads} with addition of KI increased with increasing temperature. This occurrence implies the adsorption becomes unfavorable with the increasing temperature resulting in desorption of the inhibitor from the metal surface [20]. The positive values of enthalpies indicate the endothermic nature of mild steel dissolution process, which implies the difficulty of mild steel dissolution.

On comparison between the values of the enthalpy of activation ΔH°_{ads} given in Table 4.2, it can be seen that the values of ΔH°_{ads} are positive which implies that the adsorption of the inhibitor molecules onto the mild steel surface is endothermic. The adsorption of the inhibitor molecules on mild steel surface can be explained on basis of donor-acceptor interaction between electron density of N, O and aromatic rings of the dyes and the vacant *d* orbital of iron and atoms at the surface [41, 84, 87]. The adsorption of an organic adsorbate at the metal/solution interface is known as "substitutional adsorption" phenomenon. The values of ΔS°_{ads} obtained are positive, and are related to "substitutional adsorption" and therefore the decrease in disorder takes place in going from the reactant to the activated complex [78, 90–93].

4.2 Electrochemical measurements

4.2.1 Potentiodynamic polarization (PDP)

Potentiodynamic polarization measurements were carried out in order to study the electrochemical kinetics of the reactions. The Tafel plots can be used to measure the corrosion potential (E_{corr}), corrosion current density (i_{corr}) and anodic and cathodic Tafel slopes (b_a and b_c). The linear Tafel segments of anodic and cathodic curves were deduced to obtain corrosion current densities (i_{corr}). The values i_{corr} measured are related to the inhibition efficiency through the following equation:

$$\mu_{PDP} = \frac{i^{0}_{corr} - i^{i}_{corr}}{i^{0}_{corr}} \times 100 \qquad (28)$$

where i^{0}_{corr} and i^{1}_{corr} are values of corrosion current density in absence and in presence of inhibitor, respectively, determined by extrapolation of Tafel lines to the corrosion potential. μ_{PDP} is the inhibition efficiency from the potentiodynamic polarization measurement.

Figure 4.16–4.20 represents the plots of potentiodynamic polarization curves for mild steel in 0.5 M HCl solution containing different concentrations of Sunset yellow, Amaranth, Allura red, Tartrazine and Fast green. The results show in the presence of inhibitor without the addition of KI, that the cathodic and anodic reactions were suppressed with the addition of the studied dye, which implies that the food dye molecule reduce the anodic dissolution and also impedes the hydrogen evolution reaction. In addition, hydrogen evolution is active controlled and the reduction mechanism was not affected by the presence of the inhibitor [77, 84]. With the addition of KI, the results did not show much change as compared to those without KI. It is noted that the anodic curves for mild steel in 0.5 M HCl in the presence of an inhibitor, showed that the studied dyes has no much effect at the potential higher than $E_{corr,}$ and this can be as the result of a significant mild steel dissolution which leads to a desorption of the inhibiting layer. In such case, desorption rate of the inhibitor is said to be higher than the adsorption rate, and studies [77, 96, 97, 98] has showed that the inhibitor is of mixed-type mechanism but dominantly act as a cathodic inhibitor for mild in 0.5 M HCl solution.

Electrochemical corrosion kinetic parameters, i.e. corrosion potential (E_{corr}), cathodic and anodic Tafel slopes (b_a, b_c), and corrosion current density (I_{corr}) which are obtained from extrapolation of the polarization curves, are shown in Table 4.3, with and without KI. It is clear from these data that without the addition of KI, the corrosion current density (I_{corr}) showed a decrease considerably with the increasing concentration of a dye molecule, whereas the shift in E_{corr} values did not indicate a definite trend. The obtained results also revealed that the obtained inhibition efficiency increased with increasing concentration of a studied food dye. The cathodic Tafel slope (bc) showed a slight change with the addition of an inhibitor, suggesting that the inhibiting action occurred by simply blocking of the available cathodic sites in the metal surface leading to a decrease in the exposed area required for hydrogen evolution and lowering the dissolution rate with increasing food dye concentration. Similar result was obtained by Herrag *et al* [77].

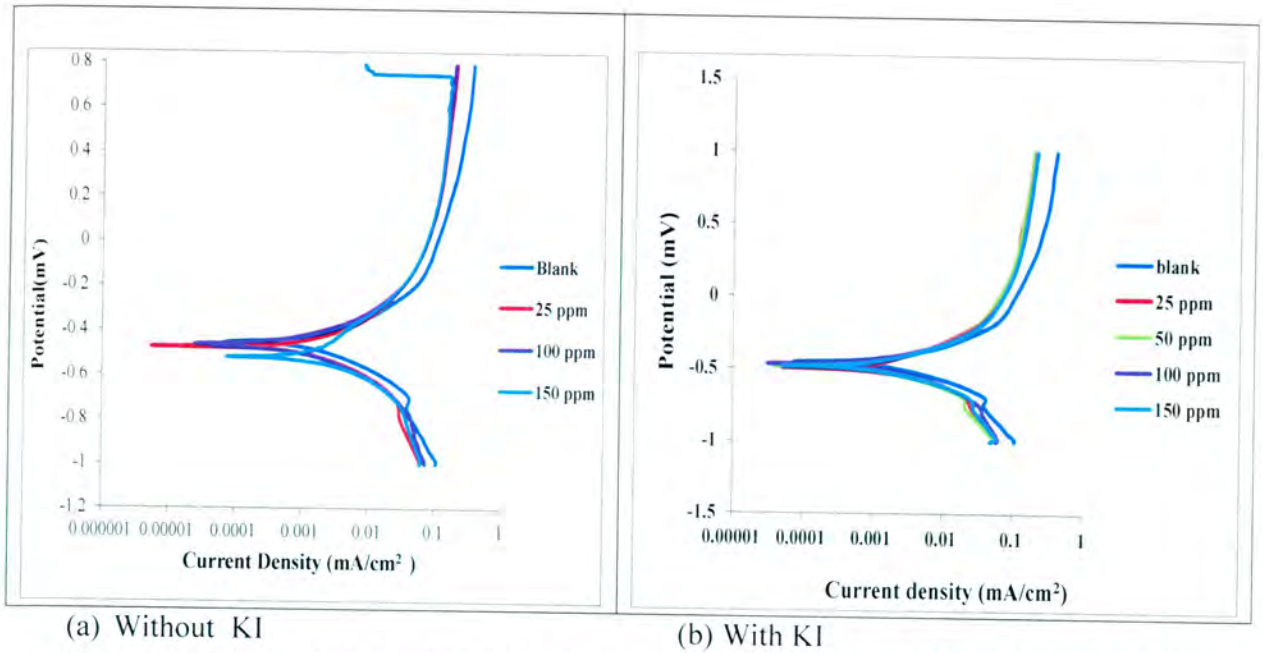

(a) Without KI (b) With KI

Figure 4.16: Potentiodynamic polarization curves for corrosion of mild steel in 0.5 M HCl in the absence and presence of different concentrations of Sunset yellow (SS).

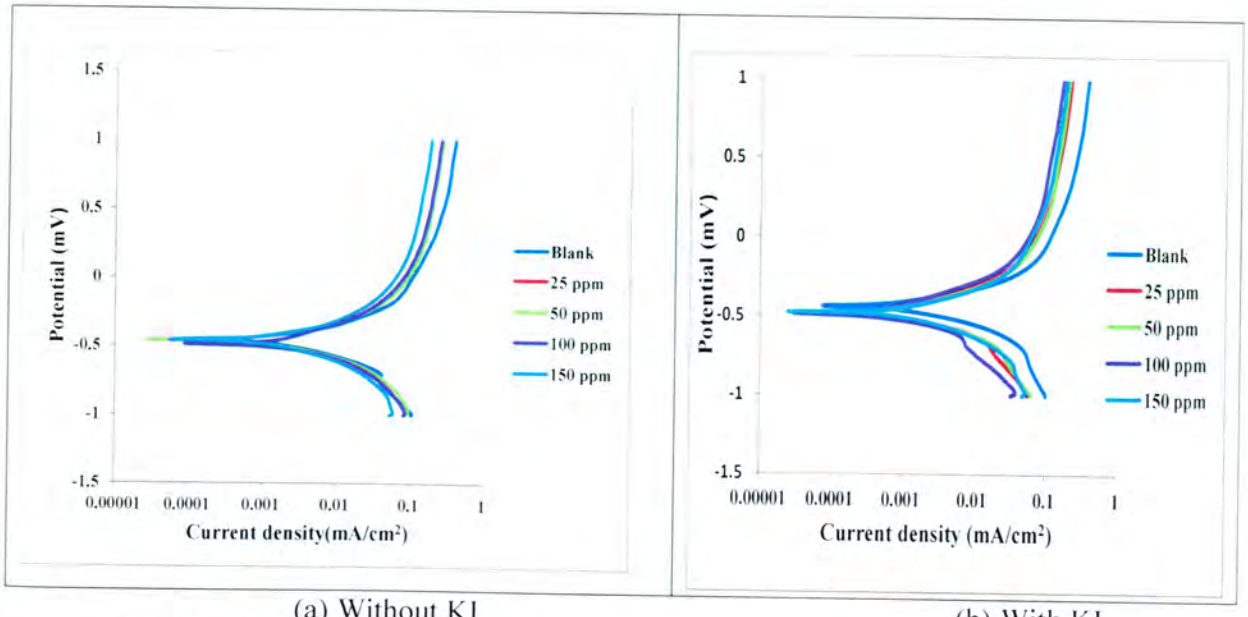

(a) Without KI (b) With KI

Figure 4.17: Potentiodynamic polarization curves for corrosion of mild steel in 0.5 M HCl in the absence and presence of different concentrations of Amaranth (AM).

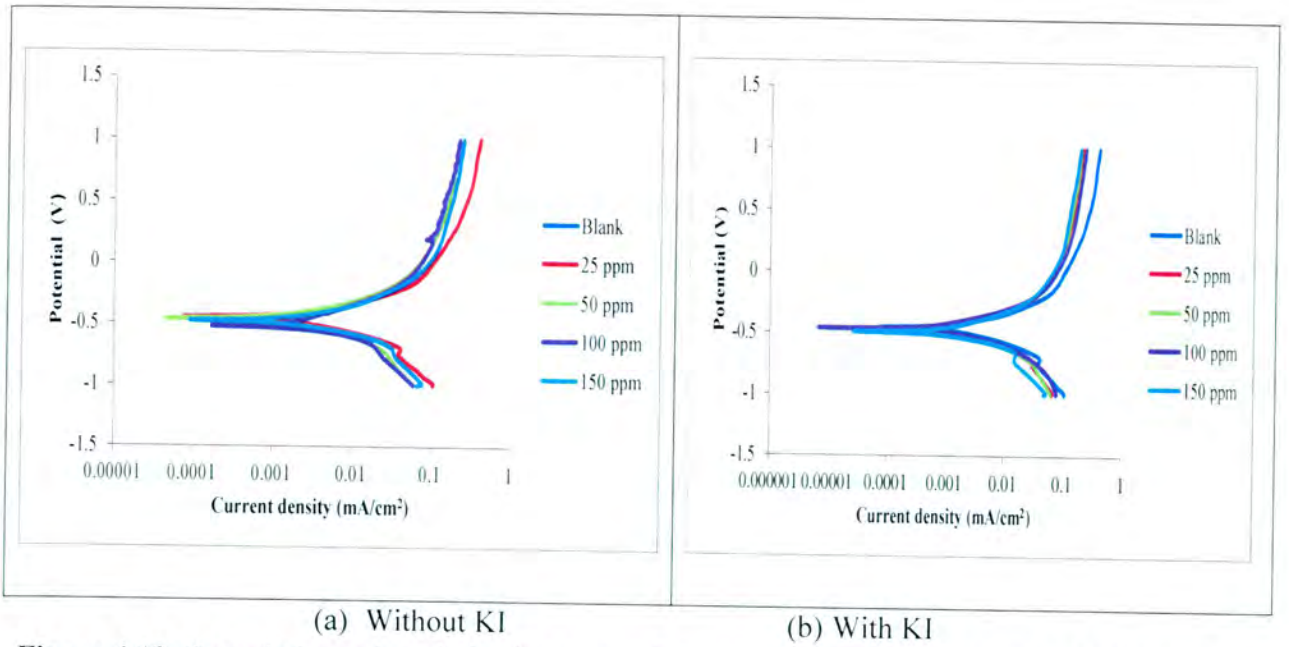

(a) Without KI (b) With KI

Figure 4.18: Potentiodynamic polarization curves for corrosion of mild steel in 0.5 M HCl in the absence and presence of different concentrations of Allura red (AR).

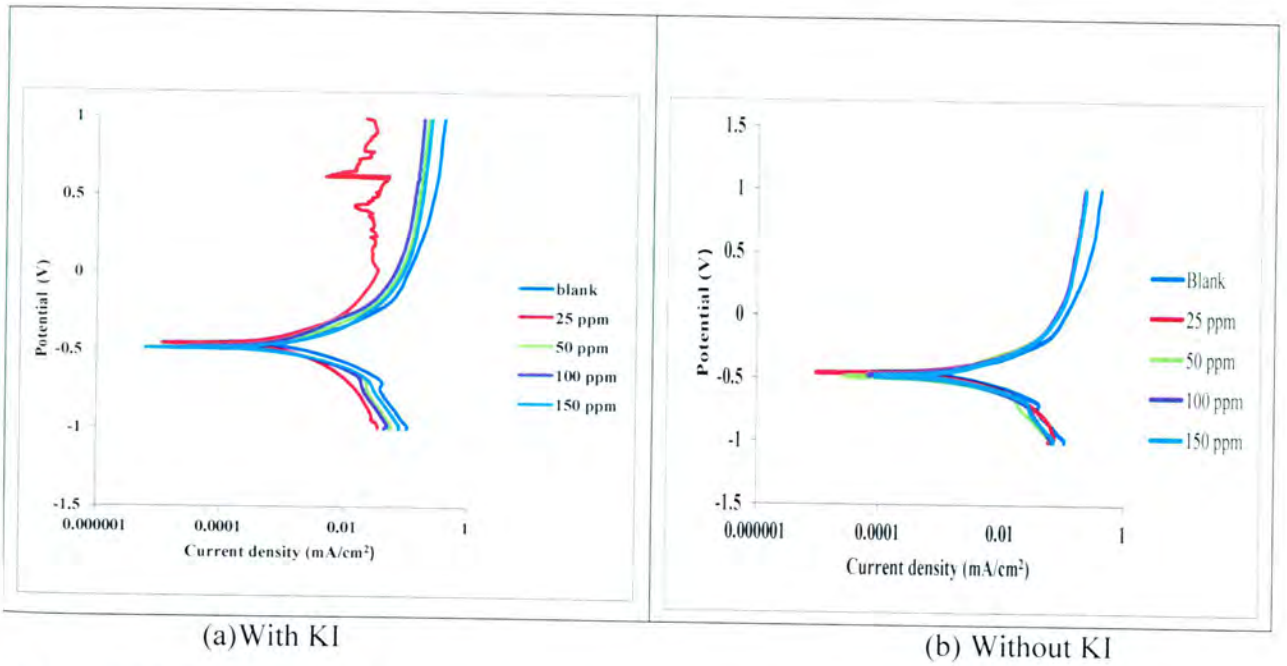

(a)With KI (b) Without KI

Figure 4.19: Potentiodynamic polarization curves for corrosion of mild steel in 0.5 M HCl in the absence and presence of different concentrations of Tartrazine (TZ).

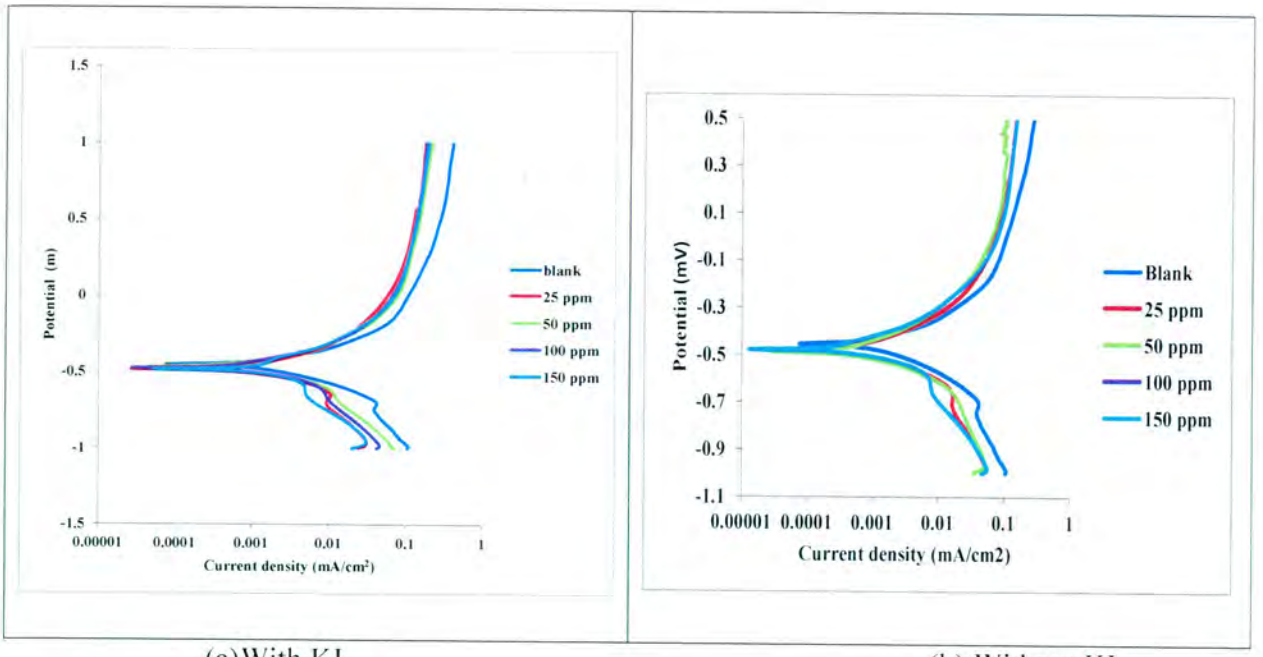

(a)With KI (b) Without KI

Figure 4.20: Potentiodynamic polarization curves for corrosion of mild steel in 0.5 M HCl in the absence and presence of different concentrations of Fast green (FG).

Table 4.3 Potentiodynamic polarization parameters such as corrosion rate, corrosion current density (i_{corr}), corrosion potential (E_{corr}), and anodic and cathodic Tafel slopes (b_a and b_c) and corrosion rate using different dye inhibitors with and without KI.

Name of Inhibitor	Conc. Of Inhibitor (ppm)	i_{corr} (A cm^{-2}) $\times 10^{-4}$	b_a ($Vdec^{-1}$)	b_c ($V\ dec^{-1}$)	Rp(Ω	$-E_{corro}$ (V)	Corrosion rate (mm/y)	μ_{PDP}%
-	-	16.86	0.148	0.147	5.598	0.459	17.320	
SS	25	8.190 (7.275)[a]	0.111 (0.080)[a]	0.101 (0.150)[a]	6.631 (7.450)[a]	0.481 (0.505)[a]	8.414 (5.181)[a]	51.42 (56.85)[a]
	100	5.588 (6.459)[a]	0.093 (6.459)[a]	0.100 (0.076)[a]	7.244 (0.099)[a]	0.478 (0.490)[a]	5.739 (4.451)[a]	66.86 (61.69)[a]
	150	4.613 (4.720)[a]	0.089 (0.076)[a]	0.075 (0.089)[a]	6.275 (9.236)[a]	0.477 (0.488)[a]	4.756 (4.851)[a]	72.94 (72.04)[a]
AM	25	5.982 (3.846)[a]	0.100 (0.067)[a]	0.093 (0.122)[a]	6.780 (9.236)[a]	0.437 (0.490)[a]	6.231 (3.557)[a]	64.52 (77.19)[a]
	50	5.122 (3.463)[a]	0.820 (0.081)[a]	0.930 (0.133)[a]	6.275 (1.325)[a]	0.458 (0.491)[a]	5.424 (3.557)[a]	27.16 (79.46)[a]
	150	4.489 (5.078)[a]	0.079 (0.087)[a]	0.081 (0.103)[a]	6.235 (7.595)[a]	0.460 (0.481)[a]	4.610 (5.215)[a]	73.37 (69.88)[a]
AR	25	7.797 (1.659)[a]	0.122 (0.168)[a]	0.109 (0.189)[a]	7.292 (8.336)[a]	0.463 (0.475)[a]	8.184 (1.704)[a]	53.75 (90.16)[a]
	100	7.425 (5.086)[a]	0.570 (0.097)[a]	0.096 (0.109)[a]	3.179 (8.994)[a]	0.524 (0.460)[a]	7.625 (5.233)[a]	55.96 (69.83)[a]
	150	7.272 (4.598)[a]	0.076 (0.080)[a]	0.095 (0.089)[a]	4.326 (6.695)[a]	0.483 (0.483)[a]	7.468 (4.721)[a]	56.86 (72.73)[a]
TT	25	4.504 (1.388)[a]	0.112 (0.154)[a]	0.125 (0.151)[a]	1.365 (7.578)[a]	0.461 (0.465)[a]	4.626 (1.374)[a]	73.29 (91.77)[a]
	100	3.554 (4.422) [a]	0.720 (0.079)[a]	0.997 (0.091)[a]	8.694 (7.045)[a]	0.481 (0.476)[a]	3.649 (4.541)[a]	78.92 (73.77)[a]
	150	2.902 (7.256)[a]	0.489 (0.091)[a]	0.610 (0.122)[a]	4.417 (6.640)[a]	0.610 (0.489)[a]	2.980 (7.451)[a]	82.79 (56.96)[a]
FG	25	9.327 (7.333)[a]	0.012 (0.101)[a]	0.144 (0.137)[a]	8.041 (8.166)[a]	0.486 (0.485)[a]	9.624 (7.530)[a]	44. 76 (56.51)[a]
	100	5.800 (3.953)[a]	0.090 (0.064)[a]	0.112 (0.116)[a]	7.520 (8.166)[a]	0.473 (0.482)[a]	5.956 (4.059)[a]	65.59 (76.55)[a]
	150	5.152 (1.763)[a]	0.069 (0.036)[a]	0.121 (0.080)[a]	7.047 (7.202)[a]	0.490 (0.480)[a]	5.291 (1.811)[a]	69.44 (89.53)a

( )[a] corresponds to results with the addition of KI

4.2.2 Summary of the electrochemical measurements findings

The values of corrosion current density (I_{corr}) obtained with addition of KI were less as compared to those without KI addition and were also found to decrease with an increasing concentration of the inhibitor. The obtained results also revealed that the studied food dyes compounds inhibit HCl corrosion of mild steel through their adsorption on both cathodic and anodic active sites without amending the mechanism of corrosion reaction [99] This is as result that the the molecules of the inhibitor adsorbed block the active sites, therefore decreasing the area available for hydrogen evolution and metal dissolution reaction. It was found in the overall studied compounds of food dyes the calculated inhibition efficiency was increasing with an increase in concentration of the inhibitor concentration.

The inhibition efficiency achieved by these compounds follows the order;

Tartrazine (TZ) < Sunset yellow (SY), Amaranth (AM) < Allura red (AR) < Fast green (FG).

4.2.3 Influence of molecular structure and the correlation of inhibition action for the studied food dyes

The results obtained from Figures (4.1–4.4) are evident that for all compounds studied, the inhibition efficiency and the surface coverage increase with an increase in inhibitor concentration and decrease with an increasing temperature. The inhibition process suggests that the type of adsorption taking place is physical adsorption. From the weight loss and electrochemical experiments it can be deduced that the inhibition efficiency follows the order Fast green (FG) > Allura red (AR) > Amaranth (AM) > Sunset yellow (SY) > Tartrazine (TZ). Report in literature [75, 84, 85, 91] showed that the adsorption process is influenced by the chemical structure of the inhibitors, the nature and the charged surface on the metal and the distribution of charge over the whole inhibitor molecule. It is normally expected that some of the organic constituents may exists in the protonated form and some on the cathodic sites of the mild steel, therefore reducing the H_2 gas evolution [94]. The highest inhibition efficiency obtained in fast green (FG) molecules is due to the aromatic rings is possess, providing more π-electrons for the interaction with metal surface, therefore causing a great electrostatic force in the surface. It has been reported that inhibition increases with high molecular masses by other authors [59, 75, 77]. Allura red (AR) also contains active centers, like N, O and S for protonation and bonding with metal surface. To understand the mechanism of inhibition it requires the full knowledge of the interaction between the protective compound and the metal surface. The increase in size of the substituent groups, results in reduced interaction between the atoms thus exposing more adsorption sites to favour attractions between the inhibitor molecules and the steel surface [59]. According to other research studies, the inhibition efficiency decreases in the order to O<N<S<P [22]. The four types of adsorption that may take place by organic molecules at the metals/surface interface are;

(i.) Electrostatic attraction between the charged molecules and charged metal
(ii.) Interaction of unshared electron pair in the molecule with the metal
(iii.) Interaction of p-electrons with the metal
(iv.) Combination of (ii) and (iii) [22]

The corrosion of iron and steel in HCl solution follows the proposed mechanism [91]. The mechanism anodic dissolution of iron follows the steps

$$Fe + Cl^- \leftrightarrow (FeCl^-)_{ads} \quad (29)$$

$$(FeCl^-)_{ads} \leftrightarrow (FeCl)_{ads} + e^- \quad (30)$$
$$(FeCl)_{ads} \rightarrow (FeCl^+)_{ads} + e^- \quad (31)$$
$$FeCl^+ \leftrightarrow Fe^+ + Cl^- \quad (32)$$

The cathodic hydrogen evolution follows;

$$Fe + H^+ \leftrightarrow (FeH^+)_{ads} \quad (33)$$
$$(FeH^+)_{ads} + e^- \rightarrow (FeH)_{ads} \quad (34)$$
$$(FeH)_{ads} + H^+ + e^- \rightarrow Fe + H_2$$

In the presence of halide ions (I^-, in this present study), the mechanism of the anodic is given by [93];

$$Fe + H_2O + I^- \leftrightarrow (FeIOH)_{ads} + H^+ + e- \quad (35)$$

$$(FeOH)^-_{ads} \xrightarrow{rds} (FeOH)^+ + e- \quad (36)$$
$$(FeIOH) + H^+ \rightarrow Fe^{2+} + I^- + H_2O \quad (37)$$

Normally a negative surface charge is favoured by a positive surface charge. Corroding mild steel specimen carries a positive charge in hydrochloric acid solution and as such, protonated species supposed to be poorly adsorbed. I^- anion is adsorbed onto the positively charged metal surface facilitating the physical adsorption of inhibitor cations. When the inhibitor molecules combine with the adsorbed intermediates form metal-inhibitor complex, the resulting complex can either be catalysed or inhibit further metal dissolution depending on its solubility [95]. In this current investigation is noted that with the addition of KI, there was a soluble complex formation occurred, thereby reducing the corrosion rate and increasing the inhibition efficiency.

4.2.4 *Synergism Consideration*

The synergism parameter, S_I, was evaluated using the relationship given by Aramaki and Hackerman and reported elsewhere [58, 64]:

$$S_I = \frac{1 - I_{1+2}}{I - I'_{1+2}} \tag{38}$$

where $I_{1+2} = I_1 + I_2$; I_1 = inhibition efficiency of the iodide ions; I_2 = inhibition efficiency of the inhibitor and I` = measured inhibition efficiency for inhibitor in combination with iodide ions. This parameter was evaluated from the inhibition efficiency values obtained from both the weight loss and potentiodynamic polarization measurements. The results obtained are presented in Table 4.2 for different concentrations of the inhibitors and are found to be greater than unity. This indicates that the improved inhibition efficiency caused by the addition of iodide ions to the inhibitors is only due to synergistic effect. Similar results have been reported [75, 95]. Strong chemisorptions of iodide ions on the metal surface are responsible for the synergistic effect of iodide ions in combination with the cation of each inhibitor. The cation is then adsorbed by columbic attraction on the metal surface where iodide ions are already adsorbed by chemisorptions. Stabilization of the adsorbed iodide ions with cations leads to a greater surface coverage and therefore greater inhibition. It could therefore be concluded that the addition of iodide ions enhances the inhibition efficiency to a considerable extent due to the increase in the surface coverage in the presence of iodide ions.

Table 4.4: Synergistic Parameters, S_I

	S_I Values at Various Concentrations of Inhibitor (ppm)					
Inhibitor	25	50	75	100	125	150
SS	1.50 (1.83)[b]	1.50	1.49	1.50 (1.94)[b]	1.52	1.50 (1.74)[b]
AM	1.45 (1.52)[b]	1.45	1.48	1.48 (1.00)[b]	1.49	1.50 (1.80)[b]
AR	1.47 (1.18)[b]	1.49	1.50	1.50 (1.55)[b]	1.52	1.55 (1.50)[b]
TZ	1.46 (1.37)[b]	1.51	1.52	1.52 (1.78)[b]	1.53	1.53 (2.39)[b]
FG	1.57 (1.72)[b]	1.54	1.53	1.52 (1.54)[b]	1.52	1.52 (1.36)[b]

( )[b] = electrochemical results

4.3 Quantum Chemical Calculations

Results of the theoretical studies on selected food dyes as potential corrosion inhibitors

4.3.1 Introduction

The interaction of corrosion inhibitors and metal surfaces depend on the molecular properties of the inhibitor. These molecular properties include the geometry of the molecule, the electronic properties such as dipole moment, partial atomic charges, frontier molecular orbitals, electronegativity and electronic energy [90, 100–107]. These molecular properties are associated with the presence of particular groups on organic molecules, including the presence of heteroatoms, π bond, aromatic systems and electron density [90, 101–103, 107–110]. It is reported that the molecules with these functional group have high tendency to act as corrosion inhibitors [100–103]. **Highest occupied molecular orbital (HOMO) and Lowest unoccupied molecular orbital (LUMO) -** The HOMO and LUMO orbitals (figure 4.21) play an important role in the reactivity of inhibitors with the metal surface. HOMO is referred to as the orbital that could act as an electron donor, because it is the outermost (highest energy) orbital with electrons, while LUMO is the orbital that could act as the electron acceptor, because it is the innermost (lowest energy) orbital having a capability to accept electrons [102, 107–109]. In the interaction between the metal surface and the corrosion inhibitor, it is considered that the corrosion inhibitor provides electrons to the vacant or partially filled d orbital of the metal surface. In this way, the corrosion inhibitors are considered to be electron donor while the metal surfaces are often considered as electron acceptors. Therefore, molecules with electron donating ability (e.g. molecules with heteroatom, π-electrons and aromatic functional groups) are preferred for interaction with metal surfaces. Also a corrosion inhibitor with high HOMO energy is preferred to a corrosion inhibitor with low HOMO energy for the interaction with the metal surface.

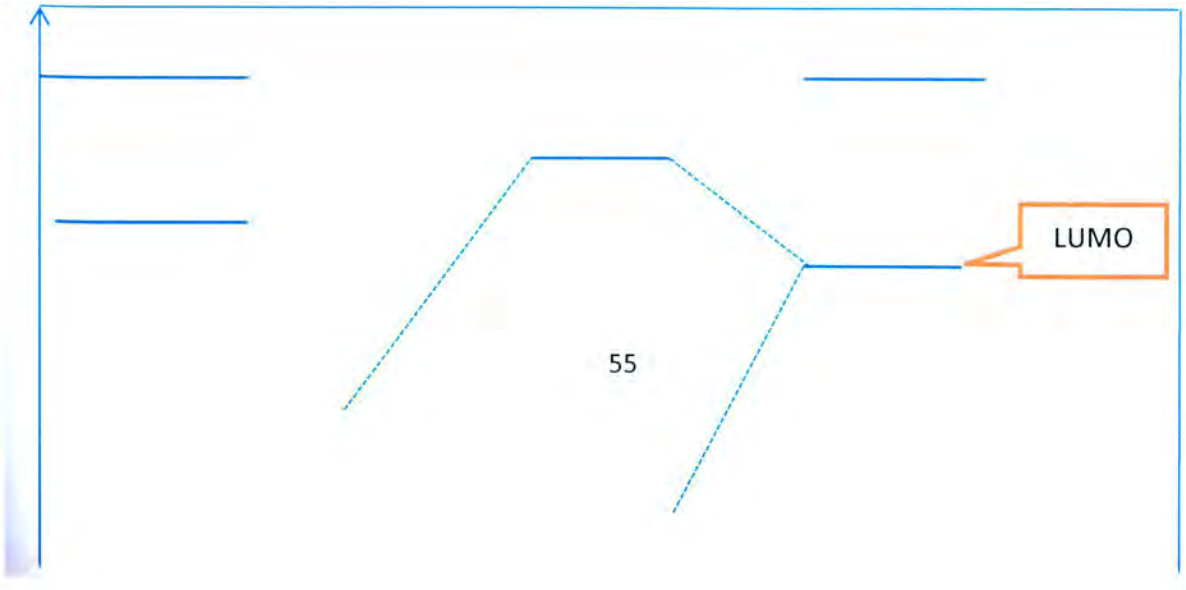

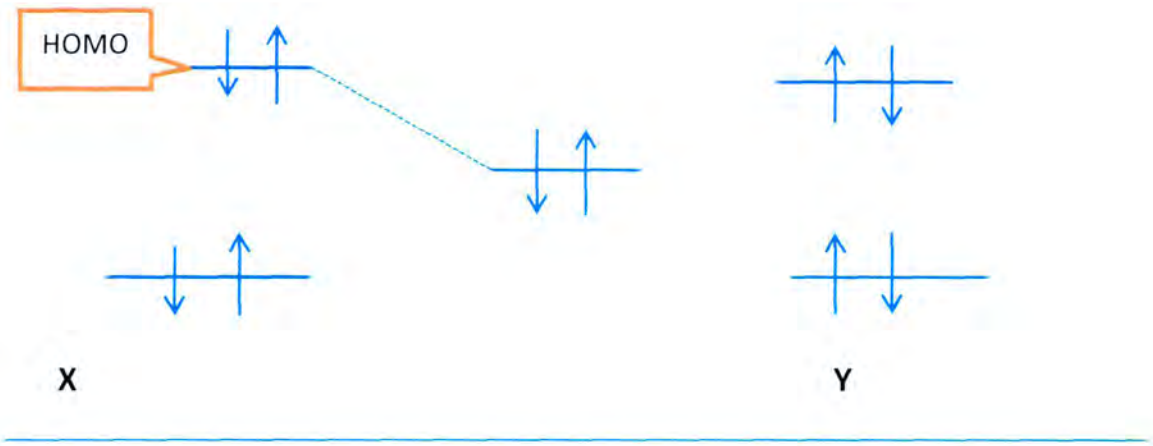

Figure 4.21: Representation of the HOMO and the LUMO orbitals for the water molecule

Dipole moment- The dipole moment measures the polarity (separation of charge in a molecule) of a covalent bond or the polarity of the molecule. The dipole moment can provide significant information on the absorption of organic molecules on the metal surface. Studies have shown that the trend in the dipole moment with adsorption on the metal surface is not univocal. This means that in some instances, it has been shown that high polarity of organic molecules results in greater corrosion inhibition [102, 110, 111], while in other instances it has been shown that a decrease in dipole moment is related to increased corrosion inhibition [109]. In other cases, the trend between corrosion inhibition and dipole moment does not exist at all [109], showing that information from dipole moment cannot be considered to provide a clear trend with respect to the corrosion inhibition trend by a set of organic molecules.

Charges on the atoms- Charges on the atoms of the molecules of corrosion inhibitors have an important role in determining selectivity. This means that the metal surface interact with specific regions on the organic inhibitors. Usually the more negative the charge on the atom, the greater the electron density and therefore the greater the tendency of that particular atom to donate electrons to the metal surface [112]. The interactions between the metal surface and the organic molecule usually occur on the regions with more negative charges. Since, heteroatoms, π bond and aromatic systems have high electron density; the metal surface is most likely to interact with these regions of organic molecules [90, 101–103, 108, 109, 112].

Chemical hardness and softness parameters- The interaction between a metal surface and an organic molecule may also be described in terms of the concepts of chemical hardness and softness. Chemical hardness (η) is the measure of resistance of an atom to charge transfer, it is estimated by the equation [113];

$$\eta \cong -1/2\ (E_{HOMO} - E_{LUMO}) \qquad (39)$$

where E_{HOMO} is the energy of the HOMO and E_{LUMO} is the energy of the LUMO
Chemical softness (σ) is the description of the capacity of an atom or group of atoms to receive electrons; it is estimated by the equation [113].

$$\sigma = 1/\eta = 2/(E_{HOMO} - E_{LUMO}) \quad (40)$$

In the interactions between a metal surface and a corrosion inhibitor molecule, the metal cations are considered as Lewis acids and the inhibitor molecules are considered as Lewis bases, as described by the hard and soft acids and bases (HSAB) theory [111]. In this way, the metal cation and inhibitor are taken as electron acceptor and donor respectively [113–116]. Softness refers to the species' electron cloud is polarizable and the electrons are mobile and easily moved. Soft species prefer to participate in covalent bonding. Hard species are comparatively rigid and non-deformable, and therefore have low polarizability, hold their electrons firmly and prefer to participate in ionic bond [114]. This information suggests that in series of compounds with potential for corrosion inhibition, the compound with smaller softness value is preferred as corrosion inhibitor.

The Fukui functions-Fukui functions also provide information on reactivity and selectivity of molecules. The Fukui functions, denoted by $f(r)$, describe the differential charge in electron density ($\rho(\mathbf{r})$) due to an infinitesimal change in the number of electrons; it is given by the equation,

$$f(\mathbf{r}) = \left(\frac{\partial \rho(\mathbf{r})}{\partial N}\right) v(r) \quad (41)$$

where $N = \int \rho(\mathbf{r})\, dr$ is the total number of electrons in the system, and $v(r)$ is the external electrostatic potential an electron at r feel due to the nuclei [114–116]. The use of Fukui functions to explain chemical reactivity of organic molecules has received a lot of attention in many studies. In the transfer of electrons in the molecules between the metal surface and the inhibitor, when a molecule accept electrons, the electrons will move to areas where $f^{+}(\boldsymbol{r})$ is much greater due to the fact that at those locations the molecule has a great ability to stabilize the addition electron. Therefore the metal surface is susceptible to nucleophilic attack (i.e., an attack by an electron-rich species) at the site where $f^{+}(\boldsymbol{r})$ is large. Likewise, if an inhibitor is susceptible to an electrophilic attack (i.e., an attack by an electron-poor species) at the site where $f^{-}(\boldsymbol{r})$ is large, since these are the regions where electrons destabilizes the molecules the least [115, 116]. The different Fukui functions (i.e., the $f^{+}(\mathbf{r})$ and the $f^{-}(\mathbf{r})$ functions) can also be defined in terms of charges on the atoms of the inhibitor. When defined in terms of the charges on the atoms the electrophilic attack and the nucleophilic attack terms could be estimated utilizing the finite difference approximation approach as follows [12]:

$$f^{+} = q_{(N+1)} - q_N \qquad \text{for a nucleophilic attack} \quad (42)$$

$f^- = q_N - q_{(N-1)}$ for an electrophilic attack (43)

where $q_{(N+1)}$, q and $q_{(N-1)}$ are the charges of the atoms on the systems with N+1, N and N–1 electrons respectively. The preferred site for nucleophilic attack is the atom or region in the molecule where the value of f^+ is the highest and the preferred site for an electrophilic attack is the atom/region in the molecule where the value of f^- is the highest. The Fukui functions for electrophilic attack is said to be related to the HOMO density for a given molecule while the Fukui function for the nucleophilic attack on the molecule is related to the LUMO density for a given molecule [115].

4.3.2 Computational methods used in corrosion inhibition studies

The use of theoretical estimated parameters possesses two main advantages, firstly being that, the compound and their various fragments and substituent can be directly characterized on the basis of their molecular structure only, and secondly, the proposed mechanism of action can be directly accounted for in term of the chemical reactivity of the compound under study [101]. Furthermore, unlike the situation with experimental results, there are no statistical errors in the results obtained using computational methods. Some molecular properties obtained using computational methods have shown to have correlation with corrosion inhibition efficiency [100–101].

There are several computational methods that are utilized in the study of the properties of molecules. These methods may be classified into molecular mechanics and quantum chemical approaches. Molecular mechanics is based on the assumption that molecules can be described by using only classical physics concepts and laws [117, 118]. The atoms making a molecule are considered as if they were spheres having a mass and connected by springs. Each spring has its own force constant and the set of force constants associated with all the springs is called the *force field* of the molecule. In the force field, one or more parameters sets are included. These parameter sets fit the equations and atom types to experimental data. The internal structure of atoms is not considered and, therefore, electrons are not considered explicitly. Individual atoms are viewed as being of different types according to their characteristics in the given molecular context. The energy of the molecule is approximated by a sum of terms describing how the potential energy of the molecule varies with the position of the particles in space [117, 119]

Without considering electrons explicitly, the computational procedures are simplified to a great extent because computations related to electronic interactions are avoided. For this reason, molecular mechanics is capable of handling large-size molecular systems, such as large organic molecules, biological macromolecules and polymers [119]. As far as the size of molecules is concerned, molecular mechanics is the only technique, available to computational chemists, that is capable of handling molecules with thousands of atoms. The molecular properties that

molecular mechanics is able to compute include: molecular geometry, rotational barriers, vibrational spectra, enthalpies of formation and the relative stability of conformers [118]. However, because of its many limitations (for example its in ability to treat conjugated π systems), quantum mechanical calculations are preferred, as long as the size of the molecule enables them. Since the molecules under investigation in the current study have a size for which quantum mechanical calculations remain affordable, they have been utilised throughout this work.

Quantum chemical methods obtain information on the molecular properties of a molecule by solving the Schrödinger equation. The Schrödinger equation for a particle of mass m moving in one dimension with energy E can be written as:

$$-\frac{\hbar^2}{2m}\frac{d^2\psi}{dx^2} + V\psi = E\psi \qquad (44)$$

where, V is the potential energy of the particle; h is a convenient modification of Planck's constant. For a three dimensional systems:

$$-\frac{\hbar^2}{2m}\nabla^2\psi + V\psi = E\psi \qquad (45)$$

where $\nabla^2 = \frac{\partial^2}{\partial x^2} + \frac{\partial^2}{\partial y^2} + \frac{\partial^2}{\partial z^2}$

All the properties of the molecules (such as the energy of the molecule, the dipole moment, electron density, etc.) can be obtained by setting up and solving the Schrödinger equation for that particular system.

Quantum chemical methods are divided into three categories; methods that solve the Schrödinger equation from first principle and methods that introduce approximations to solve the Schrödinger equation. Methods that solve the Schrödinger equation from first principle are called *ab initio* methods and methods that introduce approximation in order to solve the electron-electron integrals in the Schrödinger equation are referred to as semi-empirical methods.

Semi-empirical approaches neglect solving the electron-electron integrals and by doing so speed up the calculations. Moreover, some semi-empirical methods introduce experimental data in order to solve the Schrödinger equation. These methods serve as efficient tools which can yield fast qualitative estimates for a number of properties. However, although semi-empirical methods are fast, and therefore, would be convenient for the study of large corrosion inhibitor molecules, they are less reliable as compared to *ab initio* methods [101].

***Ab initio* methods** solve the Schrödinger equation from first principle without introducing experimental data. All *ab initio* are based on solving the time independent Schrödinger equation for the electrons of a molecular system as a function of the position of the nuclei [90,101]. The simplest type of *ab initio* electronic structure calculation method is the Hartree-Fock (HF), in which the instantaneous coulomb-electron repulsion is not specifically taken into account and only its average effect is included in the calculation [101].
The often utilized quantum chemical method in the study of corrosion inhibitor and their binding properties on the metal surface is the Density Functional Theory (DFT) method [100].
DFT can achieve accuracy similar to that of other methods in less time and with less computational expose. In DFT results, the energy of the fundamental state of poly-electronic system can be expressed as the total electronic density instead of a wave functions for calculating the energy constitute the fundamentals of DFT. One other includes semi-empirical methods. It is taken to be a very useful technique to probe the inhibitor/surface interaction as well as to analyze the experiment [90, 101].

Density functional theory expresses the energy of a system as a functional (i.e., a function of a function) of the electron density ρ.

$$E = E[\rho(r)] \tag{46}$$

The electron density is the measure of the probability of an electron being present at a specific location, and it is observable [120]. Like wave-function-based methods, DFT methods describe the electronic structure and properties of molecular systems by solving the Schrödinger equation. However, while wavefunction-based methods focus on the determination of the wavefunction, ψ, DFT methods focus on the determination of the electron density.
DFT methods are based on the proof by Kohn and Hohenberg that "There exists a universal functional of the density, $F[\rho(r)]$, independent of $v(r)$ [the external potential due to the nuclei], such that the expression

$$E = \int v(r)\,\rho(r)\,dr + F[\rho(r)] \tag{47}$$

has its minimum the correct ground state energy associated with $v(r)$" [121]. This means that the exact ground state energy of a molecular system is a functional only of the electron density and the fixed positions of the nuclei (for a given set of nuclear coordinates, the electron density uniquely determines the energy and all properties of the ground state). If the mathematical form of the universal functional were known, the exact electron density function of the ground state would provide a reference for the utilization of the variational principle [122]. Regrettably, this form it is not known, nor it can be precisely determined or systematically improved. Therefore, approximate functionals have been proposed, often built in such a way as to fit the correct results

for certain well characterised systems. To achieve this, their mathematical form contains parameters, what makes DFT a basically semi-empirical method [123, 124].

4.3.3 Discussion of the results

The Optimized structures of the dyes

The molecular structures of the studied food dyes (i.e. Sunset Yellow (SY), Amaranth (AM), Allura Red (AR) and Tartrazine (TZ)) and the corresponding atom numbering are shown in Figure 4.22 for the studies only (4) of the dyes studied. The optimized structures are shown in Figure 4.23. Since the adsorption on the metal surface depend on the functional groups present on the inhibitor molecules, it is interesting to mention here, for each molecule, the type of functional groups present. Sunset yellow has two sulphonic acid groups, one linked to the naphthalene groups at C5 and the other linked to the benzene ring at C21. The molecule also has the aza (N=N) group and the hydroxyl group attached at C15 atom on the naphthalene unit.

Like, sunset yellow, Allura red has the naphthalene and the benzene rings held together by an aza group. The naphthalene group also has two substituents, the sulphonic acid group and the hydroxyl group, in similar positions as in Sunset yellow. The benzene ring has two substituents, the sulphonic group in para position to the C atom linked to the aza group and the methoxy group in *ortho* position to the C atom linked to the aza group. Therefore, the difference in the functional groups between sunset yellow and Allura red is the presence of the methoxy group in Allura red. It will be interesting to investigate how this difference in structural functional groups affects their role as metal corrosion inhibitors.

Amaranth molecule consists of two naphthalene units linked together by the aza group. On each naphthalene unit, there is a sulphonic acid groups; on one naphthalene group it is in meta position to the C atom attached to the aza group and on the other naphthalene unit it is in *para* position to the C atom attached to the aza group. One of the naphthalene unit (to which the sulphonic group is in *meta* position with respect to the C atom attached to the aza group) also has the keto group (C=O) in ortho position to the C atom attached to the aza group.

Tartrazine molecule possesses has three rings, two of which are benzene rings; it has two sulphonic acid groups, an hydroxyl group, a carboxylic acid group and an aza group.

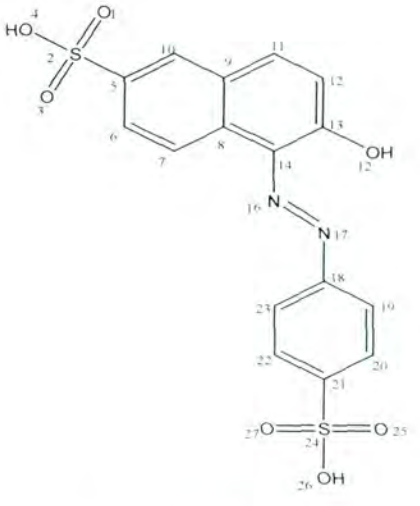

Sunset yellow (SS)

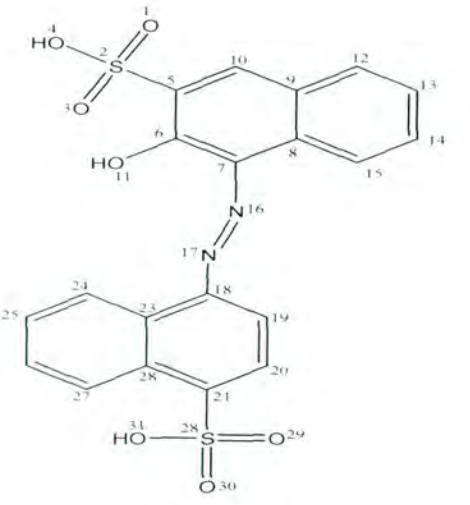

Amaranth (AM)

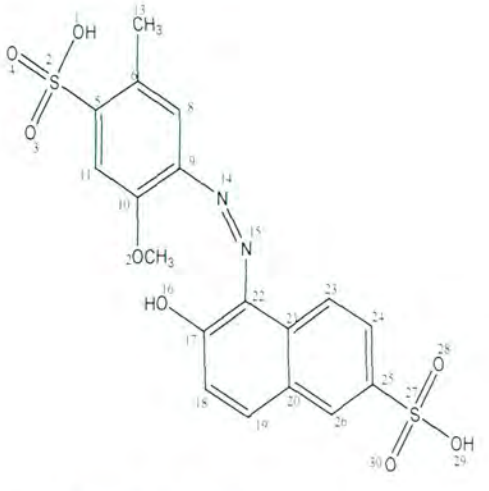

Allura Red (AR)

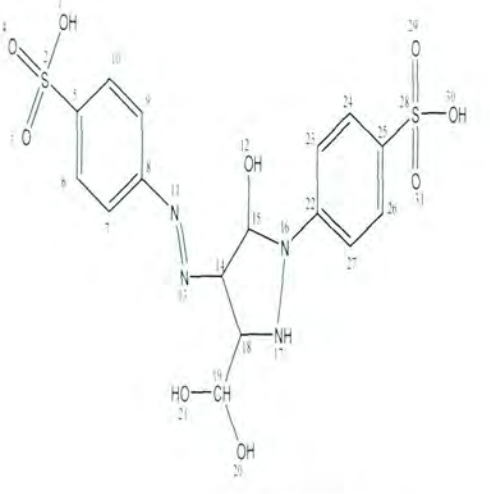

Tartrazine (TZ)

Figure 4.22 Schematic representation and atom numbering for the studied food dyes

Sunset Yellow (SS)

Amaranth (AM)

Allura Red (AR)

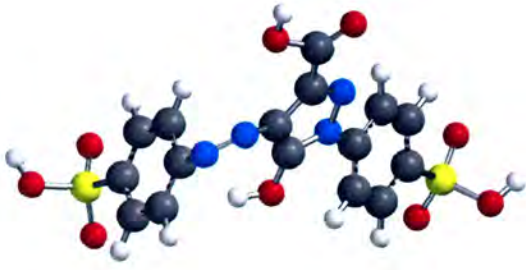

Tartrazine (TZ)

Figure 4.23 Optimized geometries for the structures of the studied food dyes. Only the lowest energy conformer of each structure is shown. The blue colour represent the N atoms, the red colour represent O atoms, the grey colour represent C atoms, the yellow colour represent S atoms and the while color represent H atoms.

4.3.4 The molecular properties related to the reactivity of food dyes

The highest occupied molecular orbitals

The study of molecular properties related to the reactivity of molecules is important in the fact that it may provide information on the sites on which the reaction with the metal surface occurs and may also provide information on the kind of interactions that take place. For instance, the interaction between a metal surface and the organic molecule may be regarded as physisoption or chemisorption. In a physisorption mechanism, the metal surface and the inhibitor molecule interact by weak attractions while in chemisorption, the interactions are stronger involving the donation of electrons by the inhibitor molecule to the metal surface resulting in coordination bond. The reactivity parameters obtained from quantum chemical results often are related to the description of chemisorption type of mechanism. Some of the most interesting quantities to consider is the location of the highest occupied molecular orbital and the lowest unoccupied molecular orbital (LUMO) for the inhibitor molecule. In the current study, the HOMO is shown

in figure 4.24. In sunset yellow, the HOMO is largely distributed above and below (C13=C14, C9=C11, C7=C6, C10=C5) of the naphthalene ring attached at N16. This HOMO is due to the presence of the π electrons of the aromatic rings. The HOMO is also distributed on N17, C18=C19 &C18=C23 and C21 attached to the sulphonic group. In Amaranth, the HOMO is distributed above and below the naphthalene ring attached at N17. This HOMO is due to the π electrons of the aromatic ring. The HOMO is also distributed on N17, C6=C7, C12=C13 and C8=C15. Therefore, in Amaranth, much of the HOMO is due to the π electrons of the aromatic rings. In Allura Red, the HOMO is distributed largely on the C17=C22, C19=C20, C23=C24 and C25=C26 double bonds of the naphthalene ring, on the aza group (N14=N15), on O16 and on O12. This HOMO indicates that the naphthalene ring with S, N atoms possess large electron density. The HOMO is also distributed on C10=C9=C8, C5 on the benzene ring attached at N14. The benzene ring with N, S atoms are suitable for adsorption onto the metal surface due to the presence of the lone pair of electrons. In Tartrazine the HOMO is mainly distributed on C5, C7, C9, C8 on the benzene ring linked at N11. The HOMO is also distributed on N11, N13 and the group attached at N13.

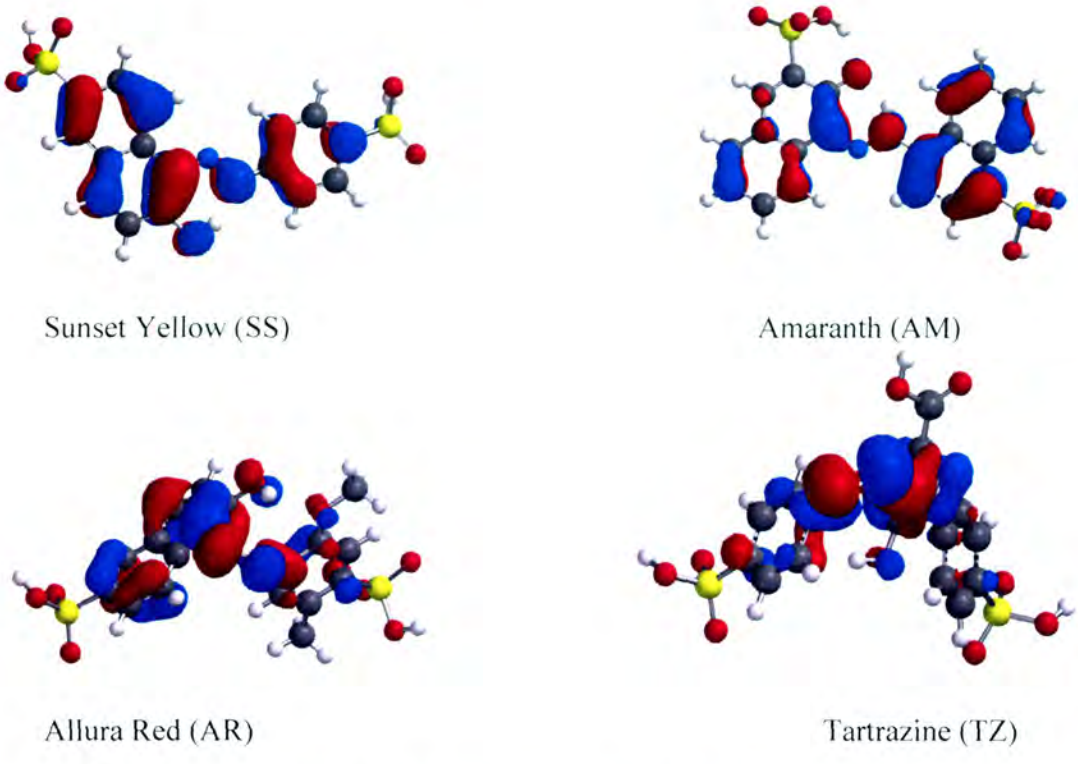

Figure 4.24 The highest occupied molecular orbital (HOMO) for the studied food dyes. The blue colour represent the N atoms, the red colour represent O atoms, the grey colour represent C atoms, the yellow colour represent S atoms and the while colour represent H atoms.

The lowest unoccupied molecular orbitals

The LUMO provides information about the region in a molecule having the highest tendency to accept electrons from an electron rich species. The information from the LUMO is crucial in identifying regions, on the molecule, which can easily accept electrons from the *d* orbitals of the metal. The lowest unoccupied molecular orbital for the studied compounds are shown in figure 4.25. In sunset yellow; the LUMO is mainly distributed on C13=C12, C11, N16, N17≡C18, C19, C20, C23 and C21. In Amaranth the LUMO is mostly distributed on C5=C6, C6=C7, C7=C8, C10=C9 of the naphthalene ring attached at N16. The LUMO is also distributed on N16, N17≡C18, C19 and C21. This suggests that these regions have high tendency to accept the electrons.

In Allura Red the LUMO is mainly distributed on C8, C5, C9, C10 on the benzene ring attached at N14. The LUMO is also distributed on N15, C17=C18, C19 and C21. The LUMO indicates the greater capacity to accept free electrons from the metal using the anti-bond orbitals therefore forming stable chelate. In Sunset yellow the LUMO is distributed on C11, C8, C12=C13 on the naphthalene ring. Some regions also showing possibilities of LUMO are O11, C20, C23, C19 on the benzene ring. In Tartrazine the LUMO is largely distributed at C5, C9, C6=C7, C8≡N11 on the benzene ring attached at N11. Due to presence of double aza group, too much electrons are being poor pulled away from two benzene rings suggesting more electrons to be donate from the metal surface. Therefore these regions have high tendency to accept the electrons. The LUMO is also distributed at N13, C15, C18, O11 and N17.

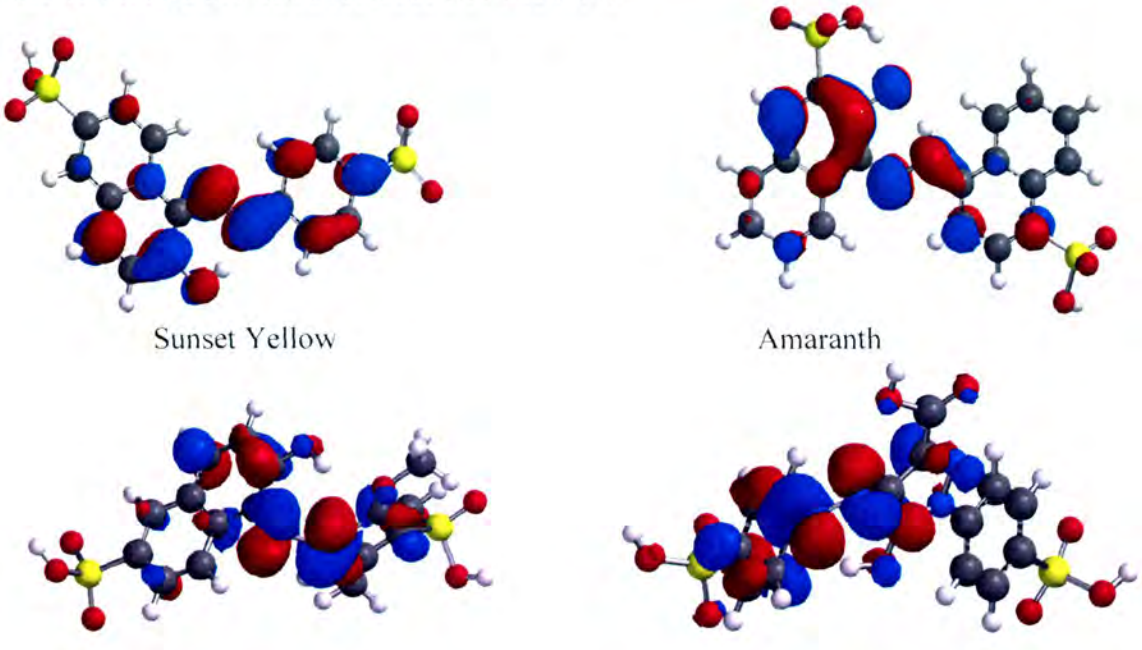

Sunset Yellow Amaranth

Allura Red Tartrazine

Figure 4.25 The lowest unoccupied molecular orbital (LUMO) for the studied food dyes. The blue colour represent the N atoms, the red colour represent O atoms, the grey colour represent C atoms, the yellow colour represent S atoms and the while colour represent H atoms.

The energies of the HOMO (E_{HOMO}) and the LUMO (E_{LUMO})

E_{HOMO} gives information about the tendency of the molecule to donate electrons to an electron poor species. In a set of homologous series of molecules, the molecule with the highest E_{HOMO} is considered to have the highest tendency to donate electrons to an electron poor species. E_{LUMO} on the other hand shows the tendency of a molecule to accept electrons and the lower the E_{LUMO} value, the greater the tendency of that particular system to accept electrons. The E_{HOMO} and the E_{LUMO} for the studies compounds are reported in Table 4.5. The results suggest that E_{HOMO} is highest for Allura Red and lowest for Tartrazine. This indicates that Tartrazine has lesser tendency to donate electrons to the metal surfaces and thus has minimal binding tendency on the metal surface. The overall trend is such that Tartrazine (TZ) < Sunset yellow (SS) < Amaranth (AM) < Allura Red (AR). Allura Red on the other hand has the greatest tendency to donate its electrons to the metal surface and would have the strong binding effect on the metal surface. The sites on the Allura Red molecule that have greater tendency to donate electrons have already been discussed in the section on optimized structures of the dyes.

The trend in the calculated values of E_{LUMO} shows that Amaranth has the lowest E_{LUMO} while Allura Red has the highest of E_{LUMO} This results suggest that if at all there is a possibility of a metal surface to donate electrons from its *d*-orbitals, the preferred molecule, among the studied compounds, to a accept the electrons would be Amaranth. In such a case the type of interaction involved is termed back-donation (i.e. the electrons are donated by the metal surface to the inhibitor molecule [27].

The energy difference between the HOMO and the LUMO (denoted as of ΔE) provides important information on the reactivity of inhibitor molecules; the smaller value of ΔE, the greater the reactivity of a molecule. High reactivity means that the molecule has greater change to interact with the metal surface. The ΔE values, reported in table 4.5 suggest that Allura red has the lowest value and Tartrazine has the highest value. These results suggest that Allura red is the most reactive compound while Tartrazine is the least reactive compound. Therefore on the interaction with the metal surface, Allura Red is most likely to adsorb strongly than Tartrazine. The trend in the ΔE is in agreement with the trend observed with experimental inhibition efficiencies (FZ > AR > AM > SS > TZ).

Table 4.5 Calculated quantum chemical parameters for the studied food dyes.

Calculated Molecular properties	AR	AM	SS	TZ
E_{HOMO}, (eV)	−6.15	−6.35	−6.46	−6.62
E_{LUMO}, (eV)	−2.62	−3.63	−3.27	−2.87
ΔE, (eV)	3.53	2.72	3.19	3.75
Hardness (η) (eV)	1.77	1.36	1.60	1.88
Softness (σ)	0.57	0.74	0.63	0.53
Fraction of electron transferred ΔN (*e*)	−0.74	−0.74	−0.67	−0.60

ω	5.45	9.15	7.42	6.00
μ (Debye)	6.14	6.73	3.74	5.28
IE (%)	87.94	87.65	86.03	85.06

η is Hardness, σ is Softness, ΔN is Fraction of electrons transferred, ω is Electrophilicity, μ is dipole moment

The global softness and hardness parameters

Global hardness and softness parameters indicate the description of the hard and soft acid/base through the acid-base theory. The values of softness and hardness parameters are also shown in Table 4.5. The order of hardness AM > SS > AR > TZ, while the order of softness TZ > AR > SS > AM. From the results, Tartrazine (TZ) is the least reactive compound while Amaranth is the most reactive. The trend in the results obtained here are slightly in agreement with the results of the experimental inhibition efficiencies (FZ > AR > AM > SS > TZ).

Fraction of electron transferred (ΔN)

The number of fraction of electrons transferred (ΔN) gives information about the tendency of a molecule to donate electrons. Higher values ΔN, implies the greater tendency of a molecule to donate electrons to an electron poor species. In relation to corrosion inhibitors, the higher the higher value of ΔN implies a greater tendency to interact with the metal surface (i.e. a greater tendency to adsorb on the metal surface). According to results calculated, Tartrazine has less value of ΔN, while Allura Red and Amaranth both has the highest values.

Electrophilicity parameter (ω)

The electrophilicity values provide the information on the nucleophilic or electrophilic nature of the molecules. A higher value of electrophilicity show that the molecules has a higher tendency to act as an electrophile while a low value electrophilic value indicates that molecule has high tendency to act a nucleophile. From the studied compounds, the order of electrophilicity value ω shows that Allura red has lowest value of ω while Amaranth has the highest.

The dipole moment

The calculated values of dipole moment are shown in Table 4.5. Dipole moment is the product of the charge atoms and the distance between the bonded atoms. As already stated in theory that dipole moment in corrosion studies, does not show univocal trends within the inhibition of the inhibitors [105, 110, 113, 114]. From this current study the trends in dipole moment is in the order of Sunset yellow < Tartrazine < Allura Red < Amaranth. These results suggest that sunset yellow has the lowest dipole moment and Amaranth has the greatest dipole moment. Some studies have reported that an increase in dipole moment is an increase in inhibition efficiency, while others reports that the dipole moment increases with a decrease in inhibition efficiency. In this current study, it can be seen that dipole moment does not show any correlation with the dipole moment (i.e. the dipole moment increase when the experimental inhibition efficiencies decreases and also decreases when the experimental inhibition effiencies increases).

The Mulliken atomic charges-Charges on the atoms provide information on the electron distribution in the molecule and therefore the reactivity of a molecule. It also indicates the selectivity of the molecule, i.e. the specific centers on the molecule for which a certain type of reaction can occur. Atoms with highest negative charge in the molecule are often susceptible to an electron electrophilic attack. In Sunset yellow; the atoms which the highest negative charge are O1, O3, O4, O5, O15, O25 and O27 .This results that these atoms have a greater capacity to interact more with the metal surface, and also to attract the electrons to itself. Other atoms in this molecule include N16, N17, and C10. However in the results obtained, oxygen atoms have more electronegative charge than nitrogen indicating the ability to take part in an electrophilic attack in case oxygen which readily donate electron to the electrophilic species. In Amaranth atoms showing highest negative charges are O1, O3, O4, O11, O29, O30 and O31. These atoms possess greater tendency for better interaction with the metal surface and donating more electrons. Some atoms also having the highest negative charge are N16, N17, C5, and C7. These results suggest that these atoms are possible sites for adsorption by the inhibitor on the metal surface. In Allura red the atoms with highest negative charges are on O1, O3, O4, C5, C7, C11, O12, C15 O16, O28, O29, and O30.

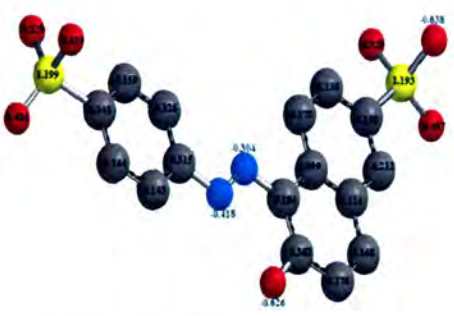

Sunset Yellow FCF

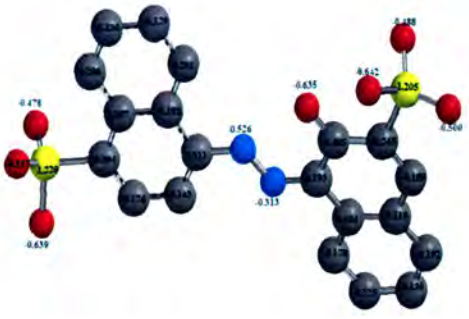

Amaranth

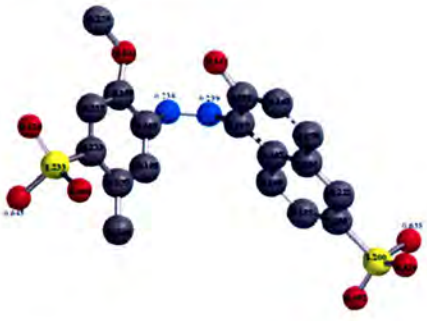

Allura Red

Tartrazine

Figure 4.26 Mulliken atomic charges for the studied food dyes.

These results suggest that those regions are likely to be part in an electrophilic attack where they will readily donate electron to the electrophilic species (i.e. electron poor species). When the donated electrons metal surface is an electrophilic species, which are accepted in the partially filled or vacant *d* orbital of the metal, they allows molecules to be adsorbed on the metal surface in a chemisorption process [110]. Other atoms having highest negative charges are N14, N15 and C26. In Tartrazine, the atoms having the highest negative charge are O1, O3, O4, O12, O21, O20, O29, O30 and O30. These are atoms with which are possible for adsorption by inhibitor on the metal surface. Other atoms also with highest negative charges include N11, N13, N16 and N17. These also atoms which are expected to interact with metal surface by donating some electrons. However Nitrogen atoms in this molecule are sterically hindered or saturated (i.e. possess more one single bond), therefore the negative charge is not high as in other molecules.

The Fukui functions

The Fukui functions provide information about the centers in a molecule in which nucleophilic and electrophilic reactions mostly likely to occur. Table 4.6 reports the estimated condensed Fukui functions for the non-hydrogen atoms for the studied compounds; Table 4.6a reports the results for sunset yellow, Table 4.6b reports the results for Amaranth, Table 4.6c reports the results for Allura Red and Table 4.6d reports the results for Tartrazine. In all the tables $q_{(N+1)}$ represent the anion, q_N is the neutral ion and f^+ represent the difference in charges for the nucleophilic attack, while $q_{(N-1)}$ represent the cation, q_N is neutral ion, f^- represent the different in charges for the electrophilic attack. The preferred site for nucleophilic attack (shown by the highest value of f^+) is on N16 and N17 in sunset yellow, O11 and N16 in Amaranth, C17 and N14 in Allura Red and N11 and N13 on Tartrazine. The results obtained from these regions are in agreement with analysis from HOMO because the same predictions from the site with most electron deficient. The highest values of f^- are on C14 and O15 in sunset yellow, C7 and C21 Amaranth, N14 and N15 in Allura red and on C8 and N11 in Tartrazine. The site for atoms with nucleophilic attack in Sunset yellow does not correlates with those atoms that are obtained in HOMO for this molecule. In Amaranth the atoms with nucleophilic attack also does show any correlation with those obtained for HOMO, however there is a correlation for atoms with electrophilic attack with those obtained in LUMO (i.e. C7, C21). In Allura Red, the results obtained for these regions in nucleophilic attack agrees with the analysis in HOMO (i.e. C17, N14), and no correlation with the LUMO and the electrophilic attack regions obtained. In Tartrazine the regions for the nucleophilic attack corresponds to the analysis of HOMO for Tartrazine.

Table 4.6 Estimation of the Fukui functions on the studied food dyes.

a) Estimation of the Fukui functions on the atoms for the Sunset yellow (SS) molecule.

Atom of interest	Site for nucleophilic attack			Site for electrophilic attack		
	$q_{(N+1)}$		diff (f^+)		$q_{(N-1)}$	diff (f^-)
O1	−0.506	−0.487	−0.019	−0.487	−0.460	−0.027
S2	1.171	1.193	−0.022	1.193	1.218	−0.025
O3	−0.641	−0.638	−0.003	−0.638	−0.631	−0.007
O4	−0.545	−0.528	−0.017	−0.528	−0.501	−0.027
C5	−0.167	−0.158	−0.009	−0.158	−0.132	−0.026
C6	−0.157	−0.138	−0.019	−0.138	−0.121	−0.017
C7	−0.176	−0.173	−0.003	−0.173	−0.140	−0.033
C8	0.076	0.099	−0.023	0.099	0.095	0.004
C9	0.136	0.124	0.012	0.124	0.125	−0.001
C10	−0.228	−0.212	−0.016	−0.212	−0.189	−0.023
C11	−0.210	−0.168	−0.042	−0.168	−0.137	−0.031
C12	−0.182	−0.176	−0.006	−0.176	−0.165	−0.011
C13	0.340	0.383	−0.043	0.383	0.412	−0.029
C14	0.183	0.184	−0.001	0.184	0.248	−0.064
O15	−0.671	−0.626	−0.045	−0.626	−0.567	−0.059
N16	−0.384	−0.304	−0.080	−0.304	−0.297	−0.007
N17	−0.471	−0.418	−0.053	−0.418	−0.382	−0.036
C18	0.313	0.315	−0.002	0.315	0.317	−0.002
C19	−0.158	−0.143	−0.015	−0.143	−0.122	−0.021
C20	−0.157	−0.144	−0.013	-0.144	−0.137	−0.007
C21	−0.170	−0.143	−0.027	−0.143	−0.117	−0.026
C22	−0.165	−0.159	−0.006	−0.159	−0.151	−0.008
C23	−0.154	−0.126	−0.028	−0.126	−0.103	−0.023
S24	1.163	1.199	−0.036	1.199	1.222	−0.023
O25	−0.513	−0.486	−0.027	−0.486	−0.459	−0.027
O26	−0.642	−0.643	0.001	−0.643	−0.622	−0.021
O27	−0.553	−0.528	−0.025	−0.528	−0.505	−0.023

b) Estimation of the Fukui functions on the atoms for the Amaranth (AM) molecule.

Amarath	Site for nucleophilic attack			Site for electrophilic attack		
	$q_{(N+1)}$	q_N	diff (f^+)	q_N	$q_{(N-1)}$	diff (f^-)
O1	−0.527	−0.500	−0.027	−0.500	−0.477	−0.023
S2	1.178	1.205	−0.027	1.205	1.233	−0.028
O3	−0.661	−0.642	−0.019	−0.642	−0.627	−0.015
O4	−0.512	−0.488	−0.024	−0.488	−0.471	−0.017
C5	−0.225	−0.245	0.020	−0.245	−0.238	−0.007
C6	0.438	0.485	−0.047	0.485	0.502	−0.017
C7	0.178	0.193	−0.015	0.193	0.238	−0.045
C8	0.085	0.104	−0.019	0.104	0.101	0.003
C9	0.131	0.118	0.013	0.118	0.123	−0.005
C10	−0.239	−0.189	−0.050	−0.189	−0.169	−0.020
O11	−0.695	−0.635	−0.060	−0.635	−0.600	−0.035
C12	−0.204	−0.192	−0.012	−0.192	−0.177	−0.015
C13	−0.141	−0.130	−0.011	−0.130	−0.107	−0.023
C14	−0.140	−0.125	−0.015	−0.125	−0.121	−0.004
C15	−0.186	−0.178	−0.008	−0.178	−0.152	−0.026
N16	−0.388	−0.313	−0.075	−0.313	−0.315	0.002
N17	−0.545	−0.526	−0.019	−0.526	−0.493	−0.033
C18	0.312	0.311	0.001	0.311	0.327	−0.016
C19	−0.169	−0.143	−0.026	−0.143	−0.108	−0.035
C20	−0.176	−0.176	0.000	−0.176	−0.169	−0.007
C21	−0.233	−0.204	−0.029	−0.204	−0.167	−0.037
C22	0.111	0.107	0.004	0.107	0.103	0.004
C23	0.088	0.103	−0.015	0.103	0.116	−0.013
C24	−0.203	−0.201	−0.002	−0.201	−0.183	−0.018
C25	−0.139	−0.129	−0.010	−0.129	−0.112	−0.017
C26	−0.136	−0.130	−0.006	−0.130	−0.118	−0.012
C27	−0.210	−0.200	−0.010	−0.200	−0.179	−0.021
S28	1.191	1.220	−0.029	1.220	1.246	−0.026
O29	−0.645	−0.639	−0.006	−0.639	−0.629	−0.010
O30	−0.557	−0.537	−0.020	−0.537	−0.507	−0.030
O31	−0.499	−0.478	−0.021	−0.478	−0.446	−0.032

c) Estimation of the Fukui functions on the atoms for the Allura Red (AR) molecule.

Atoms of interest	Site for nucleophilic attack			Site for electrophilic attack		
	$q_{(N+1)}$	q_N	diff (f^+)	q_N	$q_{(N-1)}$	diff (f^-)
O1	−0.553	−0.528	−0.025	−0.528	−0.506	−0.022
S2	1.197	1.233	−0.036	1.233	1.254	−0.021
O3	−0.516	−0.494	−0.022	−0.494	−0.472	−0.022
O4	−0.654	−0.645	−0.009	−0.645	−0.635	−0.010
C5	−0.258	−0.233	−0.025	−0.233	−0.211	−0.022
C6	0.176	0.177	−0.001	0.177	0.177	0.000
C7	−0.543	−0.548	0.005	−0.548	−0.552	0.004
C8	−0.213	−0.195	−0.018	−0.195	−0.185	−0.010
C9	0.180	0.163	0.017	0.163	0.142	0.021
C10	0.365	0.398	−0.033	0.398	0.425	−0.027
C11	−0.238	−0.227	−0.011	−0.227	0.218	−0.445
O12	−0.525	−0.533	0.008	−0.533	−0.522	−0.011
C13	−0.207	−0.229	0.022	−0.229	−0.253	0.024
N14	−0.354	−0.238	−0.116	−0.238	−0.163	−0.075
N15	−0.370	−0.259	−0.111	−0.259	−0.204	−0.055
O16	−0.682	−0.651	−0.031	−0.651	−0.601	−0.050
C17	−0.327	0.352	−0.679	0.352	0.382	−0.030
C18	−0.171	−0.163	−0.008	−0.163	−0.157	−0.006
C19	−0.215	−0.178	−0.037	−0.178	−0.142	−0.036
C20	0.146	0.134	0.012	0.134	0.130	0.004
C21	0.007	0.102	−0.095	0.102	0.106	−0.004
C22	0.129	0.117	0.012	0.117	0.161	−0.044
C23	−0.186	−0.190	0.004	−0.190	−0.168	−0.022
C24	−0.156	−0.137	−0.019	−0.137	−0.119	−0.018
C25	−0.165	-0.159	−0.006	−0.159	−0.141	−0.018
C26	−0.240	−0.222	−0.018	−0.222	−0.201	−0.021
S27	1.176	1.200	−0.024	1.200	1.222	−0.022
O28	−0.643	−0.635	−0.008	−0.635	−0.623	−0.012
O29	−0.546	−0.529	−0.017	−0.529	−0.506	−0.023
O30	−0.510	−0.492	−0.018	−0.492	−0.466	−0.026

d) Estimation of the Fukui functions on the atoms for the Tartrazine (TZ) molecule.

Atoms of interest	Site for nucleophilic attack (f^+)			Site for electrophilic attack (f^-)		
	$q_{(N+1)}$ anion	q_N neutral	diff (f^+)	q_N neutral	$q_{(N-1)}$ cation	diff (f^-)
O1	−0.513	−0.484	−0.029	−0.484	−0.461	−0.023
S2	1.164	1.204	−0.040	1.204	1.224	−0.020
O3	−0.550	−0.523	−0.027	−0.523	−0.503	−0.020
O4	−0.643	−0.632	−0.011	−0.632	−0.620	−0.012
C5	−0.177	−0.149	−0.028	−0.149	−0.129	−0.020
C6	−0.161	−0.147	−0.014	−0.147	−0.140	−0.007
C7	−0.129	−0.114	−0.015	−0.114	−0.102	−0.012
C8	0.146	0.147	−0.001	0.147	−0.124	0.271
C9	−0.192	−0.175	−0.017	−0.175	−0.159	−0.016
C10	−0.138	−0.127	−0.011	−0.127	−0.120	−0.007
N11	−0.339	−0.241	−0.098	−0.241	−0.141	−0.100
O12	−0.666	−0.634	−0.032	−0.634	−0.606	−0.028
N13	−0.368	−0.254	−0.114	−0.254	−0.176	−0.078
C14	0.098	0.063	0.035	0.063	0.099	−0.036
C15	0.543	0.600	`−0.057	0.600	0.642	−0.042
N16	−0.423	−0.427	0.004	−0.427	−0.416	−0.011
N17	−0.385	−0.342	−0.043	−0.342	−0.294	−0.048
C18	0.272	0.303	−0.031	0.303	0.332	−0.029
C19	0.529	0.556	−0.027	0.556	0.582	−0.026
O20	−0.484	−0.447	−0.037	−0.447	−0.405	−0.042
O21	−0.550	−0.565	0.015	−0.565	−0.572	0.007
C22	0.312	0.313	−0.001	0.313	0.316	−0.003
C23	−0.147	−0.145	−0.002	−0.145	−0.134	−0.011
C24	−0.155	−0.150	−0.005	−0.150	0.141	−0.291
C25	−0.154	−0.141	−0.013	−0.141	−0.121	−0.020
C26	−0.164	−0.157	−0.007	−0.157	−0.149	−0.008
C27	−0.142	−0.140	−0.002	−0.140	−0.127	−0.013
S28	1.181	1.201	−0.020	1.201	1.221	−0.020
O29	−0.512	−0.488	−0.024	−0.488	−0.464	−0.024
O30	−0.639	−0.633	−0.006	−0.633	−0.621	−0.012
O31	−0.542	−0.526	−0.016	−0.526	−0.504	−0.022

4.3.5 Summary

The results of the computational study on four of the food dyes (SS, AR, AM, TZ) have been presented. The calculations were performed using the density functional theory (DFT) with the objective of obtaining molecular reactivity parameters that provide information on the reactivity of these compounds. A comparison of such reactivity parameters provide information on the tendency of these compounds to interact with the metal surface.

In this study, the HOMO and the LUMO regions of the molecules have been identified and explained in terms of their possible interaction with the metal surface. The charges on the atoms and the Fukui functions were utilized to identify the possible sites on the molecule on which such interactions could occur. The outcome shows that that there is a good correlation for the site of nucleophilic attack (as identified by the Fukui function) and the HOMO regions. The correlation between and the site for the electrophilic attack and LUMO regions is however very limited. Most importantly some of the quantum chemical parameters have been found to correlate well with the experimental determined inhibition efficiency. These results therefore emphasize the importance of using both experimental and theoretical approaches in the study of corrosion inhibitors.

Chapter 5

CONCLUSIONS

e following are the conclusions drawn from the results of this present study;

i.) Weight loss experiments were performed which showed that the inhibition efficiency was found to increase with the concentration of the inhibitor (from 25 ppm to 150 ppm) for all the studied food dyes, but decrease with an increase in temperature

ii.) The thermodynamic and kinetic parameters (Gibbs free energy of adsorption ΔG_{ads}, entropy of activation, ΔS_{ads}, apparent enthalpy of activation, ΔH_{ads} and apparent energy of activation E_a) were deduced from the thermodynamics studies. From the obtained values of these parameters, a conclusion can be made that the reaction between mild steel and the food dye corrosion inhibitor was found to be spontaneous due the negative values of Gibbs free energy of adsorption, and the values of free energy were less than -40 kJ mol^{-1} indicating the spontaneous physical adsorption of the inhibitors on metal surface. From the thermodynamic values obtained, the apparent activation energy E_a was also found to be increase with increase in concentration of the inhibitor in the without the addition of KI.

ii.) The addition of potassium iodide (KI) enhances the inhibition efficiencies and the obtained thermodynamics parameters such as ΔG_{ads}, ΔS_{ads}, ΔH_{ads} and the apparent activation energy of adsorption E_a. Synergism parameters evaluated was found to be greater than unity for all the concentration of dyes studied suggesting that the increase in inhibition efficiency of inhibitors by addition of KI is only due to synergism

v.) The results based on potentiometric polarization for both cases with and without the addition of KI, indicated that the mechanism of adsorption is of mixed-type inhibitor but dominantly act a cathodic inhibitor towards mild steel. Potential of mild steel was shifted slightly towards negative the potential and cathodic Tafel changed with an increase in concentration.

v.) The adsorption of the studied food dyes on mild steel surface in 0.5 M HCl with and without KI obeys the Langmuir adsorption isotherm.

i.) The Density Functional Theory method was utilized in quantum chemical studies. The E_{HOMO} results revealed that Allura red has the highest tendency of donating electrons to the metal surface while Tartrazine has the least tendency thus showing minimal binding tendency on the metal surface. The obtained values of E_{LUMO} indicated that Tartrazine molecule has the tendency to accept electrons, where Allura red showed the least tendency to accept the electrons. The data attained from Fukui functions showed that the preferred sites for nucleophillic attack were on N14 and C17 in the cations while the site

preferred for electrophilic attack was on the C7, and C17 atoms of the anion. The results were true for protonated and the non-protonated species and in both media, *in vacuo* and solution. The increase in inhibition efficiency of Allura red is attributed to high aromaticity as compared to other compounds. Unlike Amaranth and sunset yellow which also possesses two naphthalene groups, it has a methoxy group attached to it on the ring, implying that the molecule has less tendency to remain in the solution. The protonated species are said to have poor electron donor character and higher electron accepting ability. In comparing the non-protonated species, the protonated species have less tendency to chemically adsorb onto the metal surface.

References

1. Ahamad Z. Principles of corrosion engineering and corrosion control. *Butterworth-Heinemann*. ISBN 9780750659246, **2006**, pp. 1–10.
2. Tomashaw T.D. Theory of corrosion and protection of metal: The science of corrosion. *The Macmillan Company, New York*, **1996**, pp. 5–25.
3. Syed S. Atmospheric corrosion of material. *Emirates Journal of engineering research* 11 (1), **2006**, pp. 1–26.
4. Fontana F.G. Corrosion Engineering. *McGraw Hill, New York*, **1986**, pp.1–75.
5. Singh A.K, Quraishai M.A. The effect of some bis-thiadiazole derivates on the corrosion of mild steel in hydrochloric acid. *Corrosion Science* 52(4), **2010**, pp. 1373–1385.
6. Raja P.B, Sethuraman M.G. Natural products as corrosion inhibitors for metals in corrosive media-A review. *Materials Letters* 62(1), **2008**, pp. 113–116.
7. Roberge P.R. Corrosion basic: An introduction, 2nd Ed, *NACE Press book*, **2006**, 1-57590–198-0, pp 12–50.
8. Uhlig's Corrosion Handbook, 2nd Ed, R.W Winston Revie, Editor. *John Wiley & Sons, New York*, **2000,** pp. 23–123.
9. Shreir L.L. Basic concepts of corrosion, 3rd Ed *Elsevier B.V* 1, **2010**, pp. 89–95
10. Bogaerts W (ed), NACE. Basic Corrosion course, *NACE international, Houston*, **1999**, pp. 14–52.
11. Bushman J.B. Corrosion and Cathodic Protection Theory. *Bushman & Associates, Inc. (Medina), Ohio USA. Corrosion Consultants*, **2000**, pp. 2–5.
12. Davis J.R. Corrosion: Understanding the basics. ASM International. *The Material Information Society*, **2000**, pp. 10–13.
13. Solomon M. M, Umoren S.A, Udousoro I.I, Udoh A.P. Inhibitive and adsorption behavior of carboxymethyl cellulose on mild steel corrosion in sulphuric acid solution. *Corrosion Science* 52(4), **2010**, pp. 1317–1325.
14. Solmaz R, Altunbas E, Kardas G. Adsorption and corrosion inhibition effect of 2-((5-Mercapto-1, 3, 4–thidiazol-2-ylimino)methyl)phenol Schiff base mild steel. *Materials Chemistry and Physics* 125(3), **2011**, pp.796–801.
15. Carino N.J. Nondestructive techniques to investigate corrosion status in concrete structures. *Journal of Performance of Constructive Facilities* 13(3), **1999**, pp. 96–106.
16. Ebenso E.E, Obot I.B and Murulana L.C. Quinoline and its derivatives as effective corrosion inhibitors for mild steel in acidic media. *International Journal of Electrochemical Science* 5, **2010**, pp. 1574–1586.

17. Mora N, Cano E, Mora E.M, Bastidas J.M. Influence of pH and oxygen on copper corrosion in simulated urine fluid. *Bio Materials* 23(3), **2002**, pp. 667–671.
18. Bardal E. Corrosion and Protection. *Springer- Verlag London limited*, **2004**, ISBN 1-85233-785-3. pp. 27–35.
19. Zarrouk A, Warad I, Hammouti B, Dafali A, Al-Deyab S.S, Benchat N. The effect of temperature on the corrosion of Cu/HNO_3 in the presence of organic inhibitor: Part -2, *International Journal Electrochemical Science* 5, **2010**, pp. 1516–1526.
20. Fuchs-Godec R, Pavlovic M.G, Tomic M.V. Effect of temperature on the corrosion inhibition of Nonionic surfactant TRITON-X-405 on Ferric stainless steel in 1.0 M H_2SO_4. *Industrial and Engineering Chemistry Research 51* (1), **2012**, pp. 274–284.
21. Noor E.A, Al-Moubaraki A.H. Thermodynamic study of metal corrosion and inhibitor adsorption process in mild steel/1–Methyl–4[4′(-X)-Styrylpyridnium iodides/hydrochloric acid systems. *Materials Chemistry and Physics* 110 (1), **2008**, pp. 145–154.
22. Singh A.K, Quraishi M.A. Effect of Cefazolin on the corrosion of mild steel in HCl solution. *Corrosion Science* 52(1), **2010**, pp. 152–160.
23. Quraishi M.A, Ahamad I, Singh A.K, Shukla S.K. N- (Piperidinomethyl)-3-[(pyridylidene)amino] isatin: A new and effective acid corrosion inhibitor for mild steel. *Materials Chemistry and Physics* 112(3), **2008**, pp. 1035–1039.
24. Burns R.M. The corrosion of metals-I. Mechanism of corrosion process. *Bell system Technical Journal* 15, **1936**, pp. 20–36.
25. Charng T, Lansig F. Review of corrosion causes and corrosion control in a technical facility. DSN Engineering section, TDA progress report, **1982**, pp. 144–156.
26. Abd El-Rehim S.S, Madgy Ibrahim A.M and Khaled K.F. 4-Aminoantipyrine as an inhibitor of mild steel corrosion in HCl solution. *Journal of Applied Electrochemistry* 29(5), **1999**, pp. 593–599.
27. Ashassi-sorkhabi H, Es'haghi M. Corrosion inhibition potential of mild steel in acidic media by [BMIm]Br Ionic liquid. *Materials Chemistry and Physics* 114(1), **2009**, pp. 267–271.
28. Selvi S.T, Raman V, Rajendran N. Corrosion inhibition of mild steel by benzotriazole derivatives in acidic medium. *Journal of Applied Electrochemistry* 33 (12), **2003**, pp. 1175–1182.
29. Achary G, Sachin H.P, Arthoba Naik Y, Venkatasha T. The corrosion inhibition of mild steel by 3-Formyl-8-hdroxyl quinoline in hydrochloric acid. *Materials Chemistry and Physics* 107(1), **2008**, pp. 44–50.
30. Abd El-Rehim S.S, Ibrahim M.A.M, Khaled K.F .4- Aminoantipyrine as an inhibitor of mild steel corrosion in HCl solution. *Journal of Applied Electrochemistry* 29(5), **1999**, pp.593–599.
31. Virmani P.Y. Cost of and preventive strategies in the United States .FHWA-RD-01-156, **2002**, pp. 2–10.

32. Koch G.H, Brongers M.P, Thompson N.G, Virmani Y.P and Payer J.H. Corrosion cost and strategies in the United States, Supplement to Material Performance, Report No. FHWA-RD-01-156-Federal Highway Administration, Mclean, **2002**, pp. 4–7.
33. Kruger J. Cost of metallic corrosion, in Uhling's corrosion Handbook, 2nd Edition. R.W. Review editor, *Wiley, New York*, **2002**, pp.3–10.
34. Schmitt G, Schute M, Hays G.F, Burns W, Han E, Pourbaix A, Jacobson G. *World Corrosion Organization*, **2009**, pp. 3–5.
35. Bentiss F, Lebrini M, Lagrenée M. Thermodynamic characterization of metal dissolution and inhibition adsorption process in mild steel/ 2, 5-bis (n-thienyl)-1, 3, 4-thiadizoles/ hydrochloric acid system. *Corrosion Science* 47(12), **2005**, pp. 2915–2931.
36. Nathan C. C. Corrosion inhibitors, National Association of corrosion Engineers (NACE), **1973**, pp. 278–279.
37. Amita Rani B.E, Bharathi Bai B.J. Green inhibitors for corrosion protection of metals and Alloys: An overview. *International Journal of Corrosion* 2012, **2011**, pp. 1–15.
38. Uhlig H.H. Corrosion and corrosion control, 2nd ed. *John Wiley York*. **1971**.
39. Ebenso E.E, Oguzie E.E. Corrosion inhibition of mild steel in acidic media by some organic dyes. *Materials Letters* 59(17), **2005**, pp. 2163–2165.
40. Zhang Q, Hua Y. Corrosion inhibition of aluminium in hydrochloric acid solution by alkyimidazolium ionic liquids. *Materials Chemistry and Physics* 119(1–2), **2010**, pp.57–64.
41. Ahamad I, Quraishi M.A. Bis (benzimidazol-2-yl) disulphide: An efficient water soluble inhibitors for corrosion of mild steel in acidic media. *Corrosion Science* 51(9), **2009**, pp. 2006–2013.
42. Ahamad I, Prasad R, Quraishi M.A. Inhibition of mild steel corrosion in acidic by Pheniramine drug: Experimental and theoretical study. *Corrosion Science* 52(9), **2010**, pp. 3033–3041.
43. Economic Effects of Metallic Corrosion in the United States, National Bureau of Standards, *NBS Special Publication* 511-1, U. S. Dept. of Commerce, **1978**. pp. 5–9.
44. Epp D.N. The Chemistry of Food dyes (Palette of color monograph series) .*Terrific Science Press*, **1995**, ISBN: 1-883822-07-6, pp. 1–9.
45. Zollinger H. Color chemistry, syntheses, properties and applications of organic dyes and pigment. Wiley *VCH. New York*, **1987**, pp. 80–92
46. Jacobson M.F, Kobylewski S. Rainbow of Risks. *Centre for Science in the public interest*, **2010**, 1875 Connecticut Avenue, NM, Suite 300, Washington, DC 20009-5728 available at www.cspinet.org.

47. Venkataraman K. The chemistry of synthetic dyes, *Academic Press, New York* 7, **1970**, pp. 31–35, 311.
48. Hoffmann J, Puszynski A. Pigments and dyestuff. *Chemical engineering and chemical process technology* 5, Encyclopedia of Life Support Systems(EOLSS), pp.2–5.
49. Singh. R. Synthetic dyes 1st edition. *Mittal publications*, **2002**, ISBN: 81-7099-832-8, pp. 1–3.
50. Abrahart E.N. Dyes and their Intermediates. *New York: Chemical Publishing*, **1977**, pp.1–12.
51. Oguzie E.E, Unaegbu C, Ogukwe C.N, Okolue B.N, Onuchukwu A.L. Inhibition of mild steel corrosion in sulphuric acid using Indigo dye and synergistic halide additives. *Materials Chemistry and Physics* 84 (2–3), **2004**, pp. 363–368.
52. Christie R. M. Colour chemistry. *Royal society of chemistry: Cambridge*, **2001**, pp. 5–20.
53. Ensminger A.H, Ensminger M.E, Kolande J.E, Robson J.R.K. Colouring of food: In foods and Nutrition encyclopaedia. *BotaRato, CRC Press* 1, **1994**, pp. 458–461.
54. Kirk-Othmer. Encyclopedia of chemical technology 9, 5th Ed. *John Wiley & Sons*, **2005,** pp. 12–18.
55. Shore J. Colorants and auxiliaries. Organic chemistry and application properties 1, 2nd Ed. *Society of dyers and colourists*, **2002**, pp. 12–89.
56. Sabins. R.W. Handbook of biological dyes and stains: Synthesis and industrial application. *John Wiley& Sons. Inc.* **2010**, ISBN 9 780470586242, pp. 8–15.
57. Abdeli M, Ahmadi N.P, Khosroshahi R.A. Nile blue and Indigo Carmine organic dyes as corrosion inhibitor of mild steel in hydrochloric acid. *Journal of solid electrochemistry* 14(7), **2010**, pp. 1317–1324.
58. Ebenso E.E, Alemu H, Umoren S.A, Obot I.B. Inhibition of mild steel corrosion in sulphuric acid using Alizarin yellow GG dye and Synergistic Iodide addictive. *International Journal of Electrochemical Science* 3, **2008**, pp. 1325–1339.
59. Onen A.I, Maitera O.N, Joseph J, Ebenso E.E. Corrosion inhibition potential and adsorption of Bromophenol blue and Thymol blue on mild steel in acidic medium .*International Journal of Electrochemical Sci*ence 6, **2011**, pp. 2884–2897.
60. Zarrouk A, Warad I, Hammouti B, Dafali A, Al-Deyab S.S, Benchat N. The effect of temperature on the corrosion of Cu/HNO_3 in the presence of organic inhibitor: Part -2. *International Journal Electrochemical Science* 5, **2010**, pp. 1516–1526.
61. Prabhu R.A, Venkatesha T.V, Shanbhag A.V. Carmine and Fast Green as corrosion inhibitors of mild steel in Hydrochloric acid solution. *Journal Iranian Chemical Society* 6(2), **2009**, pp. 353–363.
62. Oguzie E.E. Corrosion inhibition of mild steel in hydrochloric acid solution by methylene blue. *Materials letters* 59(8–9), **2005**, pp. 1076–1079.

63. Ashassi-Sorkhabi H, Masoumi B, Ejbari P, Asghari E. Corrosion inhibition of mild steel in acidic media by Basic yellow dye 13. *Journal of Applied Electrochemistry* 39(9), **2009**, pp. 1497–1501.
64. Oguzie E.E, Unaegbu C, Ogukwe C.N, Okolue B.N, Onuchukwu A.I. Inhibition of mild steel corrosion in sulphuric acid using dye and synergistic halide additives. *Materials Chemistry and Physics* 84(2–3), **2004**, pp. 363–368.
65. Abboud Y, Abourriche A, Saffaj T, Berrada M, Charrouf M, Bennamara A, Hannache H. A novel azo, 8-quinolinol-5-azoantipyrine as corrosion inhibitor for mild steel in acidic medium. *Desalination* 237(1–3), **2009**, pp. 175–189.
66. El-Haddad N.M, Fouda A.S, Mostafa H.A. Corrosion inhibition of carbon steel by new thiophene derivatives in acidic solution. *Journal of Materials Engineering and Performance* 22(8), **2013.** pp. 2277–2287.
67. Amin K.A, Abdel Hameid II H, Abd Elsttar A.H. Effect of food azo dyes Tartrazine and carmoisine on biochemical parameters related to renal, heptic function and oxidatives stress biomarkers in young male rats. *Food and Chemical Toxicology* 48 (10), **2010**, pp. 2994–2999.
68. Alexandro M.M. Vargas, André L. Cazetta. L, Martins A.C, Juliana C.G Moraes, Garcia E.E, Gauze G.F, Costa W.F, Almeida V.C. Kinetic and equilibrium studies: Adsorption of food dyes Acid Yellow 6, Acid Yellow23, and Acid red 18 on activated carbon from flamboyant pods. *Chemical Engineering Journal* 181–182, **200**2, pp. 243–250.
69. Obi-Egbedi N.O, Obot I.B, Umoren S.A. *Spondious Mombin L.* as green corrosion inhibitor for aluminum in sulphuric acid: Correlation between inhibitive effect and electronic properties of extracts of major constituents using functional theory. *Arabian Journal of Chemistry* 5(3), **2012**, pp. 361–373.
70. Becke A. D, Density-functional thermochemistry. III. The role of exact exchange. *Journal of Chemical Physics* 98(7), **1993**. pp. 5648–5652.
71. Ebenso E. E., Arslan T, Kandemirli F, Caner N, Love I. Quantum chemical studies of some rhodanine azosulpha drugs as corrosion inhibitors for mild steel in acidic medium, *International Journal of Quantum Chemistry* 110(5), **2010**, pp. 1003–1018.
72. Kabanda M.M, Murulana L.C Ebenso E.E. Theoretical studies on Phenazine and related compounds as corrosion inhibitors for mild steel in Sulphuric acid medium. *International Journal of Electrochemical Science* 7, **2012**, pp. 7179–7205.
73. Barner B.J, M.J Green, E.I Sáez, Corn R.M. Polarization modulation Fourier transform Infrared reflectance measurement of thin films and monolayers at metal surface utilizing Real-time sampling electronics. *Analytical chemistry* 63(1), **1991**, pp. 55–60.
74. Kolb D.M. UV-Visible reflectance spectroscopy in the study of the metal-electrode interface. *Trends in Interfacial Electrochemistry*, **1986**, pp. 301–330.

75. Umoren S.A, Ebenso E.E. The synergistic effect of polyacrylamide and iodide on the corrosion inhibition of mild steel in H_2SO_4 *Materials Chemistry and Physics* 106(2–3), **2007**, pp. 387–393.
76. Oguzie E.E. Influence of halide ions on the inhibitive effect of the Congo red on the corrosion of mild steel in sulphuric acid solution. Material Chemistry and Physics 84(1), **2004**, pp. 212–217.
77. Herrag L, Hammouti B, Elkadiri S, Aouniti A, Jama C, Vezin H, Bentiss F. Adsorption properties and inhibition of mild steel corrosion in hydrochloric solution by some newly synthesized diamine derivatives: Experimental and theoretical investigations. *Corrosion Science* 52(9), **2010**, pp. 3042–3051.
78. Obot. I.B, Ebenso E.E, Obi-Egbedi N.O, Afolabi A.S, Gasem Z.M. Experimental and theoretical investigations of adsorption characteristics of itraconazole as green corrosion inhibitor at a mild steel/ hydrochloric acid interface. Res*earch on Chemicals Intermedi*ates 38(8), **2012**, pp. 1761–1779.
79. Singh A.K, Quraishi M.A. Effect of 2,2-benzothiazolyl disulfide on the corrosion of mild steel in acidic medium, *Corrosion Science* 51(11), **2009**, pp. 2752–2760.
80. Fernander M.G, Latanision R.M, Searson P.C, Morphological aspects of anodic dissolution, *Physical Review B* 47, **1993**, pp. 11749–11756.
81. Hai Q.H, Shan Y.K, Lu B, Yaun X.H. Inhibitive behavior of cadmiun sulfate on corrosion of Aluminum in hydrochloric acid. *Corrosion. The Journal of Science and Engineering* 49(6), **1993**, pp. 486–490.
82. Bentiss F, Traisnel M, Gengembre, Lagrenée M. A new triazole derivative as inhibitor of the acid corrosion of mild steel: Electrochemical studies, weight loss determination, SEM and XPS. *Applied Surface Science* 152(3–4), **1999**, pp 237–249.
83. Kertit, S.; Hammouti, B. Corrosion inhibition of iron in 1 M HCl by 1-phenyl-5-mercapto-1,2,3,4-tetrazole. *Applied Surface Science*, **1996**, 93(1), pp. 59–66.
84. Ahamad I, Prasad R, Quaraishi M.A Experimental and theoretical investigation of adsorption of fexofenadine at mild steel/hydrochloric acid interface as corrosion. *Journal of Solid State Electrochemistry* 14(11), **2010**, pp.2095–2105.
85. Ateya B, El-Anadauli B. E, El-Nizamy F.M. The adsorption of thiourea on mild steel. *Corrosion Science* 24(6), **1984**, pp. 509–515.
86. Emregül K.C, Hayvalì M. Studies on the effect of a newly synthesized Schiff base compound from phenazone and vanillin on the corrosion of steel in 2M HCl. *Corrosion Science* 48(4), **2006**, pp. 797–812.
87. Mohammed K.Z Hamdy A, Abdel-wahab A, Farid N.A. Temperature effect on corrosion inhibition of carbon steel in formation water by Non-ionic synergistic influence of halide ions. *Life Science Journal* 9(2), **2012**, pp. 424–434.
88. Behpour M. Ghoreishi S.M. Soltani N, Salavati-Niasari, Hamadanian M, Gandomi A. Electrochemical and theoretical investigation on the corrosion of mild steel by

thiosalicylaldehyde derivatives in hydrochloric acid. *Corrosion Science* 50(8), **2008**, pp. 2172–2181.

89. Zarrouk A, Hammouti B, Zarrok. Al-Deyab S.S. Messali M. Temperature effect, activation energies and the thermodynamic adsorption studies of L-Cysteine methyl ester Hydrochloride as copper corrosion inhibitor in nitric acid 2M. *International Journal of Electrochemical Science* 6, **2011**, pp. 6261–6274.
90. Bentiss F, Mernari B, Traisnel M, Vezin H, Lagrenée M. On the relationship between corrosion inhibiting effect and molecular structure of 2, 5-bis (n-pyridyl)-1, 3, 4-thiodiazole derivatives in acidic media. Ac impedance and DFT studies. *Corrosion Science*. 53(1), **2011**, pp. 487–495.
91. Obot I.B, Obi-Egbedi N.O. Fluconazole as an inhibitor for aluminium corrosion in 0.1 M HCl. *Colloids and Surfaces A: Physicochemical and engineering aspects* 330(2–3), **2008**, pp. 207–212.
92. Fouda A.S, El-Aal A. A. Kandil A.B. The effect of some phthalimide derivatives on corrosion behavior of copper in nitric acid. *Desalination* 201(1–3), **2006**, pp. 216–223.
93. Nagvi I, Saleemi A.R, Naveed S. Cefixime: A drug as efficient corrosion inhibitor for mild steel in acidic media. Electrochemical and thermodynamic studies. *International Journal of Electrochemical Science* 6, **2011**, pp. 146–161.
94. Oguzie E. E. Studies on the inhibitive effect of *Occimum viridis* extract on the acid corrosion of mild steel. *Material Chemistry and Physics* 99(2–3), **2006**, pp. 441–446.
95. Umoren S.A, Solomon M.M, Udosoro I.I, Udon A.P. Synergistic and antagonistic effects between halide ions and carboxymethyl cellulose for the corrosion inhibition of mild steel in sulphuric acid solution. *Cellulose* 17(3), **2010**, pp.635–648.
96. Benabdellah M, Aouniti A, Dafali A, Hammouti B, Benkaddour M, Yahyi A, Ettouhami A. Investigation of the inhibitive effect of triphenyltin 2-thiophene carboxylate on corrosion of steel in 2 M H_3PO_4 solutions. *Applied Surface Science* 252 (23), **2006**, pp.8341–8347.
97. Mengoli G, Musiani, Pagura C, Paolucci. The inhibition of the corrosion of mild steel in aqueous acid by situ polymerization of unsaturated compounds. *Corrosion Science* 32 (7), **1991**, 743–753.
98. Szauer T, Brandt A. On the role of fatty acid in adsorption and corrosion inhibition of iron by amine-fatty acid in acidic solution. *Electrochimica Acta* 26(9), **1981**, pp. 1257–1260.
99. El Mehdi B, Mernari B, Trainei M, Lagrenée M. Synthesis and comparative study of the inhibitive effect of some new triazole derivatives towards corrosion of mild steel in hydrochloric acid solution. *Materials Chemistry and Physics* 77(2), **2003**, pp. 489–496.

100. Kosari M, Momeni M, Parvizi R, Zakeri, Moayed M.H, Davoodi A, Eshghi H. Theoretical and electrochemical assessment of inhibitive of behavior of some thiophenol derivatives on mild steel in HCL. *Corrosion Science* 53(10), **2011**, pp. 3058–3067.

101. Gece G. The use of quantum chemical methods in corrosion inhibitor studies. *Corrosion Science* 50(11), **2008**, pp. 2981–2992.

102. Mistry B.M, Patel N.S, Sahoo S, Jauhari S. Experimental and quantum chemical studies on corrosion inhibition performance of quinolone derivatives for MS in 1N HCl. *Bulletin of Material Sci*ence 35(3), **2012**, pp. 459–469.

103. Musa N.Y, Mohamad A.B, Kadhum A. A.H, Takriff M.S, Ahmonda. Quantum chemical studies on corrosion inhibition for series of thio compound on mild steel in hydrochloric acid. *Journal of Industrial and Engineering Chemistry* 18(1), **2012**, pp. 551–555.

104. Yousif Q.A. Studying of correlation between the molecular structure and the corrosion inhibiting effect of some pyrimide compound. *Journal of Al- Nahrain University*, 13(3), **2010**, pp. 14–23.

105. M.M Kabanda, L.C Murulana, M. Ozcan, Karadag F, Dehri I, Obot I.B, Ebenso E.E. Quantum chemical studies on the corrosion inhibition of mild steel by some Triazoles and Benzimidazole derivatives in acidic medium. *International Journal of Electrochemical Sci*ence 7, **2012**, pp. 5035–5056.

106. J. Fang, J. Li. Quantum chemistry study on the relationship between molecular structure and corrosion inhibition efficiency of amides. *Journal of molecular Structure (THEOCHEM)* 593(1–3), **2002**, pp. 179–185.

107. Kabanda M.M, Sudhish K.S, A.K Singh, L.C Murulana, E.E Ebenso. Electrochemical and quantum chemical studies in Calmagite and Fast sulphone Black F dyes as corrosion inhibitors for mild steel in hydrochloric medium. *International Journal of Electrochemical Scienc*e 7, **2012**, pp. 8813–8831.

108. Khaled K.F. Molecular simulation, quantum chemical calculation and electrochemical studies for inhibition of mild steel by triazoles. *Electrochimica Acta* 53(9), **2008**, pp. 3484–3492.

109. Laarej K, Bouachrine, Radi S, Kertit S, Hammouti B. Quantum chemical studies on the inhibiting effect of Bipyrazoles on steel corrosion in HCl. *E-Journal of Chemistry* 7(2), **2010**, pp. 419–424.

110. Ebenso E.E, Isabirye D.A, Eddy N.O. Adsorption and quantum chemical studies on the inhibition potentials of some Thiosemicarbazide for the mild steel in acidic medium. *International Journal of Molecular Science* 11(6), **2010**, pp. 24730–2498.

111. Kikuchi O. Systematic QSAR procedures with quantum chemical descriptors. *Quantitative Structure-Activity Relationship* 6(4), **1987**, pp. 179–184.

112. Udhayakala P, Rajendiran T.V, Gunasekaran S. Theoretical approach to the corrosion inhibition efficiency some pyrimidine derivatives using DFT method. *Journal of Computational Methods in Molecular Design* 2(1), **2012**, pp. 1–15.
113. Parr R.G, Pearson R.G. Absolute Hardness: companion parameters to absolute electronegativity. *Journal of American Chemical Society* 105(26), **1983**, pp. 7512–7516.
114. Allison T.C, Tong Y.J. Evaluation of methods to predict the reactivity of Gold nanoparticles. *Journal of Physical Chemistry Chemical Physics* 13(28), **2011**, pp. 12858–12864.
115. Yang W, Parri R.G. Hardness and softness and the Fukui function in the electronic theory of metals and catalysis. *Proceedings of the National Academy of science of the United States of America* 82(20), **1985**, pp. 6723–6726.
116. Fuentealba, P. Perez, R. Contreras, On the condensed Fukui function. *Journal of Chemistry and Physics* 113(7), **2000**, pp. 2544–2552.
117. Burkert U., Allinger N. L. Molecular Mechanics, ACS Monograph, *American Chemical Society*, Washington, DC, **1982**.
118. Richon A. B. An Introduction to Molecular Modelling. http://www.netsci.org/Science/Compchem/feature01.html, **2001**.
119. Atkins P. W., Friedman R. S. Molecular Quantum Mechanics, *Oxford University Press Inc., New York*, **1997**.
120. Gaussian 03 User's Reference Manual Version 7, Gaussian Inc, **2003**.
121. Hohenberg P., Kohn W. Inhomogeneous Electron Gas, *Physical Reviews* B, 136 (3B), **1964**, pp. 864–871.
122. Head-Gordon M. Quantum Chemistry and Molecular Processes. *Journal of Physical Chemistry*. 100 (31), **1996**, pp. 13213–13225.
123. Naomi L. H. Quantum chemical Studies of Thermochemistry, Kinetics and Molecular Structure. Doctoral Thesis at the University of Sydney, **2003.**
124. Jensen F, Introduction to Computational Chemistry; John Wiley & Sons: Chichester, UK, **2007**, pp. 104.

Appendix 1

Tables

Table 1 Calculated values of corrosion rate (g.c.m^{-2} hr^{-1}), and inhibition Efficiency (IE %) for mild steel in HCl using Sunset yellow dye with and without KI

Temp	**30°C**		**40°C**		**50°C**		**60°C**	
Inh.Conc. (ppm)	CR	IE%	CR	IE%	CR	IE%	CR	IE%
Blank	**0.00343**	-	**0.00792**	-	**0.0150**	-	0.02186	
25	0.000508	70.40	0.002285	42.31	0.004712	37.18	0.008816	37.44
+ 0.125g KI	0.000312	81.82	0.001100	72.23	0.003509	53.21	0.008001	43.17
50	0.000500	70.85	0.002200	44.45	0.004689	37.48	0.008753	37.83
+ 0.125g KI	0.000303	82.31	0.000970	75.50	0.003024	59.68	0.007867	44.13
75	0.000474	72.34	0.002172	45.15	0.004685	37.52	0.008731	37.99
+ 0.125g KI	0.000281	83.64	0.000956	75.85	0.002885	61.53	0.007779	44.75
100	0.000441	74.29	0.002134	46.12	0.004490	40.14	0.008601	38.41
+ 0.125g KI	0.000269	84.29	0.0007332	81.52	0.002645	64.73	0.007702	45.29
125	0.000403	76.52	0.002096	47.08	0.004238	43.30	0.008543	38.83
+0.125g KI	0.000255	85.14	0.000655	83.22	0.002573	65.69	0.007153	49.20
150	0.000394	77.00	0.002074	47.64	0.004207	43.91	0.008543	39.31
+0.125g KI	0.000240	86.03	0.000560	85.85	0.002502	66.64	0.006859	51.29

Table 2 Calculated values of corrosion rate (g.c.m^{-2} hr^{-1}), and inhibition Efficiency (IE %) for mild steel in HCl using Amaranth dye with and without KI

Temp	**30°C**		**40°C**		**50°C**		**60°C**	
Inh.Conc. (ppm)	CR	IE%	CR	IE%	CR	IE%	CR	IE%
Blank	**0.00343**	-	**0.00792**	-	**0.0150**	-	0.02186	
25	0.000513	70.12	0.002210	44.02	0.005122	31.70	0.009983	29.09
+ 0.125g KI	0.000266	84.49	0.000903	77.19	0.002550	66.00	0.007483	46.86
50	0.000494	71.21	0.002190	44.69	0.004883	34.89	0.009597	31.85
+ 0.125g KI	0.000255	85.14	0.000829	79.06	0.002501	66.66	0.007444	47.13
75	0.000426	75.18	0.002198	45.03	0.004728	36.95	0.009501	32.52
+ 0.125g KI	0.000236	86.23	0.000715	81.96	0.002396	68.06	0.007356	47.76
100	0.000405	76.39	0.002160	45.46	0.004569	39.07	0.009353	33.57
+ 0.125g KI	0.000226	86.84	0.000682	82.78	0.002249	70.02	0.007107	49.53
125	0.000385	77.53	0.002127	46.29	0.004403	41.28	0.009265	34.20
+0.125g KI	0.000221	87.13	0.000612	84.55	0.002017	73.10	0.006860	51.28
150	0.000356	79.23	0.002089	47.26	0.004379	41.61	0.009194	34.70
+0.125g KI	0.000212	87.65	0.000551	86.09	0.001969	73.74	0.006620	52.98

Table 3 Calculated values of corrosion rate (g.c.m^{-2} hr^{-1}), and inhibition Efficiency (IE %) for mild steel in HCl using Allura Red with and without KI

Temp	**30°C**		**40°C**		**50°C**		**60°C**	
Inh.Conc. (ppm)	CR	IE%	CR	IE%	CR	IE%	CR	IE%
Blank	**0.00343**	-	**0.00792**	-	**0.0150**	-	0.02186	
25	0.000466	72.83	0.002399	41.79	0.005071	32.39	0.009274	34.13
+ 0.125g KI	0.000252	85.30	0.000683	82.75	0.002816	62.45	0.007353	47.78
50	0.000425	75.22	0.002278	42.49	0.005035	32.87	0.009099	35.38
+ 0.125g KI	0.000242	85.87	0.000616	84.45	0.002532	66.24	0.007249	48.52
75	0.000399	76.72	0.002228	43.75	0.004853	35.28	0.008929	36.59
+ 0.125g KI	0.000233	86.39	0.000544	86.25	0.002408	67.89	0.007208	48.81
100	0.000372	78.34	0.002208	44.26	0.004720	39.49	0.008644	38.61
+ 0.125g KI	0.000217	87.37	0.000516	86.96	0.002274	69.69	0.007081	49.71
125	0.000342	80.08	0.002170	45.20	0.004689	40.26	0.008507	39.58
+0.125g KI	0.000215	87.49	0.000433	86.06	0.002154	71.28	0.006861	51.27
150	0.000280	83.8787	0.002111	46.69	0.004654	43.37	0.008127	41.05
+0.125g KI	0.000207	.94	0.000408	89.71	0.002088	72.17	0.006278	52.22

Table 4 Calculated values of corrosion rate (g.c.m^{-2} hr^{-1}), and inhibition Efficiency (IE %) for mild steel in HCl using Tartrazine with and without KI

Temp	**30°C**		**40°C**		**50°C**		**60°C**	
Inh.Conc. (ppm)	CR	IE%	CR	IE%	CR	IE%	CR	IE%
Blank	**0.00343**	-	**0.00792**	-	**0.0150**	-	0.02186	
25	0.000572	66.66	0.002285	42.31	0.005522	30.07	0.009278	34.11
+ 0.125g KI	0.000315	81.62	0.000761	80.78	0.002807	62.57	0.007670	45.53
50	0.000477	72.18	0.002200	44.45	0.005465	31.41	0.009187	34.76
+ 0.125g KI	0.000297	82.71	0.000673	83.01	0.002772	63.04	0.007473	46.93
75	0.000447	73.96	0.002172	45.15	0.005365	32.26	0.008904	36.76
+ 0.125g KI	0.000284	83.44	0.000630	84.09	0.002588	65.50	0.007385	47.56
100	0.000423	75.34	0.0002134	46.11	0.005295	34.21	0.008754	37.33
+ 0.125g KI	0.000276	83.93	0.000587	85.46	0.002443	67.43	0.007240	48.58
125	0.000401	76.59	0.002096	47.08	0.005197	36.56	0.008660	37.75
+0.125g KI	0.000265	84.53	0.000536	86.46	0.002344	68.75	0.007211	48.78
150	0.000384	77.61	0.002074	47.64	0.005019	39.56	0.008576	37.18
+0.125g KI	0.000256	85.06	0.000463	88.30	0.002099	72.02	0.006892	51.05

Table 5 Calculated values of corrosion rate (g.c.m^{-2} hr^{-1}), and inhibition Efficiency (IE %) for mild steel in HCl using Fast green dye with and without KI

Temp	**30°C**		**40°C**		**50°C**		**60°C**	
Inh.Conc. (ppm)	CR	IE%	CR	IE%	CR	IE%	CR	IE%
Blank	**0.00343**	-	**0.00792**	-	**0.0150**	-	0.02186	
25	0.000190	88.91	0.000522	86.83	0.003921	47.72	0.007571	46.23
+ 0.125g KI	0.000173	89.92	0.000328	91.72	0.000644	91.42	0.001505	89.31
50	0.000182	89.39	0.000506	87.21	0.003789	49.48	0.007550	46.38
+ 0.125g KI	0.000131	92.39	0.000262	93.39	0.000635	91.54	0.001460	89.69
75	0.000164	90.45	0.000495	87.49	0.003234	56.88	0.007092	49.63
+ 0.125g KI	0.000116	93.24	0.000224	94.34	0.000509	93.21	0.001130	91.98
100	0.000156	90.93	0.000429	89.16	0.002610	65.19	0.006649	52.78
+ 0.125g KI	0.00009	94.25	0.000205	94.34	0.000485	93.54	0.001106	92.14
125	0.000144	91.5894	0.000418	89.44	0.002317	69.10	0.006425	54.36
+0.125g KI	0.000088	.89	0.000196	94.83	0.000424	94.34	0.001019	92.76
150	0.000122	92.91	0.000394	90.06	0.001936	74.19	0.005175	63.27
+0.125g KI	0.000072	95.79	0.000186	95.06	0.000313	95.83	0.000963	93.16

Appendix 2:

Formulas used

1. **Weight loss (W)** : $W = w_1 - w_2$
2. **The corrosion rate:** $C_{(R)} = \frac{W_b - W_a}{At}$
3. **Degree of surface coverage** : $\theta = (\rho_1 - \rho_2 / \rho_2)$
4. **Inhibition efficiency (% IE)** : $\% IE = (\rho_1 - \rho_2 / \rho_2) \times 100$
5. **Langmuir plot:** $\frac{\theta}{1-\theta} = KC$
6. **Arrhenius equation:**

$$k = Ae^{-E_a / RT}$$

7. **Arrhenius equation (another form):**

$$\log \rho = \log A - \frac{E_a}{2.303RT}$$

8. **Heat of adsorption (Q_{ads}):**

$$Q_{ads} = 2.303R\left[\log\left(\frac{\theta_2}{1-\theta_2}\right) - \log\left(\frac{\theta_1}{1-\theta_1}\right)\right] x \left(\frac{T_1 T_2}{T_2 - T_1}\right) kJmol^{-1}$$

9. **Transition-state equation:**

$$C_R = \frac{RT}{Nh}\exp\left(\frac{\Delta S^*}{R}\right)\exp\left(-\frac{\Delta H^*}{RT}\right)$$

10. **Surface coverage (with thermodynamic parameters):**

$$\theta = \frac{K_{ads} C_{inh}}{1 + K_{ads} C_{inh}}$$

11. **Surface coverage (with thermodynamic parameters) rearranged:**

$$\frac{C_{inh}}{\theta} = \frac{1}{K_{ads}} + C_{inh}$$

12. Gibbs free energy of adsorption:

$$k = \frac{1}{55.5}\exp\left[\frac{-\Delta G^{o}_{ads}}{RT}\right]$$

13. Entropy and Enthalpy relationship:

$$\Delta G^{0}{}_{ads} = \Delta H^{0}{}_{ads} - T\Delta S^{0}{}_{ads}$$

14. Van't Hoff equation:

$$\ln K = -\frac{\Delta H^{0}{}_{ads}}{RT} + Cons\tan t$$

15. Gibbs-Helmholtz equation:

$$\left[\frac{\partial\left(\Delta G^{0}{}_{ads}/T\right)}{\partial T}\right]_{P} = -\frac{\Delta H^{0}{}_{ads}}{T^{2}}$$

16. Equilibrium constant (K_{eq}):

$$RT\ln K_{eq} = -\Delta G^{0} = nF\Delta E^{0}$$

17.Potentiodynamic polarization inhibition efficiency:

$$\mu_{PDP} = \frac{i^{0}_{corr} - i^{i}_{corr}}{i^{0}_{corr}} \times 100$$

18. Electronegativity:

$$\chi \cong -\tfrac{1}{2}\,(E_{HOMO} + E_{LUMO})$$

19. Global hardness:

$$\eta \cong -\tfrac{1}{2}\,(E_{HOMO} - E_{LUMO})$$

20. Global softness:

$$\sigma = 1/\eta \cong -2/(E_{HOMO} - E_{LUMO})$$

21. Electron affinity related to E_{HOMO} :

$$I \cong - E_{HOMO}$$

22. Electron affinity related to E_{LUMO} :

$$A \cong - E_{LUMO}$$

23. Global electrophilicity index:

$$\omega = \chi^2/2\eta$$

24. Nucleophilic Fukui function:

$$f^+ = q_{(N+1)} - q_N$$

25. Electrophilic Fukui function:

$$f^- = q_N - q_{(N-1)}$$